VOLUMETRIC PROPERTIES AND VIRIAL COEFFICIENTS OF THE METHANE-ETHYLENE SYSTEM, USING THE TECHNIQUE OF ISOCHORIC CHANGES OF PRESSURE WITH TEMPERATURE

By

HENRY GRADY MCMATH, JR.

Bachelor of Science
Louisiana Polytechnic Institute
Ruston, Louisiana
January, 1961

Master of Science
Louisiana Polytechnic Institute
Ruston, Louisiana
June, 1962

Submitted to the Faculty of the Graduate School of
the Oklahoma State University
in partial fulfillment of the requirements
for the degree of
DOCTOR OF PHILOSOPHY
May, 1967

VOLUMETRIC PROPERTIES AND VIRIAL COEFFICIENTS

OF THE METHANE-ETHYLENE SYSTEM, USING

THE TECHNIQUE OF ISOCHORIC CHANGES

OF PRESSURE WITH TEMPERATURE

Thesis Approved:

Wayne C. Edmister

Thesis Adviser

Robert D. Freeman

Kenneth J. Bell

Robert L. Robinson, Jr.

A. O. Durham

Dean of the Graduate School

PREFACE

An isochoric PVT apparatus was developed for the determination of precise volumetric data. Compressibility factor data was taken for methane, ethylene, and four intermediate mixtures; and virial coefficients were derived from the data. By comparing the results of the above determinations with empirical equations of state, improvements to the equations were indicated.

Appreciation is expressed for the advice and direction of the members of the Doctoral Committee, Professors K. J. Bell, W. C. Edmister, J. H. Erbar, and R. D. Freeman. The guidance of Professor W. C. Edmister, the author's major adviser, has been especially helpful.

The financial support of the National Science Foundation and the Petroleum Research Fund of the American Chemical Society is acknowledged.

The author is particularly grateful to his wife, Sara, and to his parents in Arkansas for their understanding and encouragement throughout the duration of this work.

TABLE OF CONTENTS

LIST OF TABLES

LIST OF FIGURES

LIST OF PLATES

CHAPTER I

INTRODUCTION

This investigation was undertaken with a two-fold objective: 1) the design and construction of an experimental facility for the determination of precise Pressure-Volume-Temperature (PVT) data for a fluid, and the subsequent operation of the facility to obtain such data for a selected binary mixture; 2) a comparison of the resultant data with existing virial coefficient data and with equations of state. The purpose of the comparison was to emphasize the need for further equation of state improvements and to recommend future methods for such improvements.

Volumetric data are of industrial interest in process design calculations. The data are also of value in the calculation of derived properties such as the thermodynamic quantities enthalpy and entropy, and in the further development of generalized methods for estimating thermodynamic properties from a minimum of direct data.

In the experimental determination of PVT (or compressibility factor) data it is generally necessary to have a simultaneous knowledge of the following five quantities: pressure, temperature, composition, mass, and volume. Of these five quantities, the latter two are generally the most troublesome to measure; and their resultant measurement is frequently the least accurate. This characteristic led to the design and operation of a PVT apparatus that requires no direct experimental

measurement of either of the two quantities mass or volume. The apparatus is of the isochoric (constant volume-constant mass) type, and was operated at temperatures from 77 to 20°F, with pressures from 260 to 2400 psia. The apparatus is described herein.

In the study of compressibility factor data from the virial coefficient and equation of state approach, it was desirable to select for study a system whose pure component properties have been previously reported in the literature. It was further desirable to make a practical contribution by reporting mixture data on a system that has not been previously studied. This led to the selection of the methane-ethylene binary system. Methane and ethylene and their mixtures are of industrial importance and are encountered frequently in the petrochemical industry. Although both methane and ethylene have been widely studied, no experimental investigation of the methane-ethylene binary system has been reported in the literature.

CHAPTER II

PREVIOUS PVT INVESTIGATIONS

In this chapter various types of PVT investigations, past and present, are discussed. These involve experimental measurements on apparatus classified as follows:

1) constant volume-variable mass
2) constant mass-variable volume
3) variable volume-variable mass
4) constant volume-constant mass

These types of apparatus will be discussed in this order. The constant volume-constant mass apparatus of Michels (37, 47) is quite similar to the isochoric apparatus reported in this thesis; thus special emphasis is placed on this apparatus.

For each type of apparatus, the operating conditions, accuracies, and specific applications are stated. Lastly, a survey is given of PVT determinations for methane and for ethylene.

A. General Comments Regarding PVT Determinations

The early studies of the effects of pressure and temperature on the volume of a confined gas were made at pressures and temperatures not greatly removed from ambient conditions.

One of the earlier investigations of PVT behavior of a confined fluid at extreme conditions of pressure and temperature was reported by

Amagat (1) in 1893. Amagat made accurate determinations of the isotherms of carbon dioxide over the temperature range 0 to 250°C, with pressures as high as 3000 atmospheres. The importance of PVT data was emphasized by this work, and the field has progressed rapidly throughout the present century.

As stated above, the variables associated with the experimental determination of PVT data are pressure, volume, mass, temperature, and composition. Before discussing in detail the various types of PVT apparatus, several introductory comments regarding the determination of these five quantities are in order.

Measurement of Pressure

The pressure is determined precisely by means of the pressure balance, or dead weight piston gage. The dead weight gage principle is simple, consisting of a cylinder with an accurately fitted piston which is loaded by weights. Oil is injected into the cylinder beneath the piston until the load is balanced. The mass of the loading weights and the known piston area are sufficient to determine the pressure, making the necessary corrections.

Gages of this general nature may be calibrated quite accurately over wide ranges of pressure; instruments having an absolute accuracy of one part in 10,000 parts are commercially available.

Dead weight gages have been discussed adequately in the literature. In particular, gages and their characteristics have been discussed by Keyes (28), Bridgman (8), and Johnson et al (27).

Determination of Volume

The determination of volume and mass is done separately in some cases. In others only the ratio, mass/volume, is determined.

If the volume of an apparatus is to be separately determined, this is commonly done in two ways. The first method involves the direct weighing of the volumetric portion of the apparatus when filled with a fluid of precisely known density, such as water or triple-distilled mercury. The second method involves the charging of the apparatus to a high pressure with a known mass of gas whose PVT properties have previously been established, and measuring the pressure and temperature. The density of the gas is determined from the known PVT properties of the gas and is then combined with the mass to determine the volume.

Determination of Mass

The mass of sample may similarly be determined in one of two ways. The first method involves the direct determination by weighing. If the sample is a gas, the weighing must usually be done in a light-weight thin-walled glass pipet if high accuracy is to be obtained. This necessitates the pressure of the gas being approximately one atmosphere; thus a relatively large volume is required. The second method assumes that the PVT properties of the sample are established along some reference isotherm (frequently near ambient conditions). Further, the volume of the apparatus must be accurately known. The sample is then charged to the apparatus at high pressure and allowed to come to equilibrium at the temperature of the reference isotherm, whereupon the pressure of the sample is measured. The pressure and temperature of the sample are then combined with the known volume and

the properties of the reference isotherm to yield the mass.

Measurement of Temperature

The primary standard for temperature measurement is the platinum resistance thermometer. Such instruments may be calibrated with a precision of 0.001 degree, and the platinum metal has a high order of stability for several years. Thermometers are calibrated by the National Bureau of Standards (NBS) at several fixed temperatures, and a resulting practical working scale, known as the International Practical Centigrade Scale (65) is established.

Composition Determinations

For most investigations the composition is varied only in the sense that samples of different fixed composition are studied in a similar manner. In this manner the composition parameter becomes established. Composition determinations are commonly carried out by chromatographic or mass spectrometry methods, with compositions being frequently reported to 0.1%. The accuracy is dependent upon the number and type of components present. For binary mixtures higher accuracies may be obtained with very careful work. In the experimental determinations reported in this thesis, the samples were blended and were analyzed by mass spectrometry before being received.

The four types of apparatus will be considered in more detail in the following.

B. Constant Volume-Variable Mass Apparatus

The Bean Apparatus

An apparatus of the constant volume-variable mass type was reported by Bean (3) in 1930. An unknown mass of gas was expanded in successive increments from a high pressure bomb of known volume into a calibrated buret at roughly atmospheric pressure, where the volumetric properties of the gas were presumed known. The mass of gas at each step of the procedure was determined by summing the increments of mass.

The compressibility of the gas in the high pressure bomb was determined at each step of the procedure by measuring the pressure and temperature and from a knowledge of the bomb volume and the calculated sample mass. The mass of the gas in the buret was determined from the known volume of the buret, the pressure of the gas in the buret (near atmospheric), and the known low pressure compressibility of the gas.

A series of runs consisted of charging the bomb initially to a high pressure and measuring the pressure and temperature. A small increment of the gas was then expanded into the calibrated buret and its pressure and temperature measured to determine the mass of the increment. Then the pressure and temperature of the sample in the bomb were again measured, and the second increment was expanded into the pipet. In this manner the compressibilities were determined along an isotherm.

It would have been equally feasible, at each successive increment, to determine the pressure and temperature inside the high pressure bomb at several different levels of temperature, thus determining the data at constant densities as well as along an isotherm. This was not

done in the original Bean apparatus as the apparatus operated in a water bath, and only temperatures near ambient were maintained.

There was no provision in this apparatus to make an independent check of the mass. The accuracy of the mass determination obviously depends upon the knowledge of the compressibility near atmospheric pressure. All errors made in this step will be reflected, since the incremental masses are directly summed to obtain the total mass. This factor is one of the disadvantages of the apparatus.

Bloomer (7) reports data on natural gases accurate to 0.1% at pressures up to 1000 psi and temperatures near ambient for an apparatus of this type.

The Solbrig-Ellington Apparatus

A similar apparatus was reported by Solbrig and Ellington (64) at the Institute of Gas Technology. This apparatus further permitted the independent check on the sample mass, as the mass was determined both before it was charged into the high pressure vessel and as it was released from it. Data was taken at constant density at several different temperatures before expanding a portion of the sample into the measuring buret. This reduced the effort for a given amount of data. This apparatus has been applied to hydrogen-methane and hydrogen-ethane mixtures, and the data have a reported accuracy of 0.1%. The apparatus is applicable for the temperature range -300 to +300 °F, for pressures up to 3000 psi.

C. Constant Mass-Variable Volume Apparatus

Since the early work of Amagat (1) with a constant mass-variable

volume apparatus, several apparatus of this type have been reported.

The Michels Original Cryostat

The original Michels cryostat was described by Michels and Gibson (40) in 1928. The gas under investigation was contained within a glass piezometer, the piezometer being contained within a steel pressure vessel. The glass piezometer consisted of a large reservoir and several small reservoirs connected by narrow capillaries. A platinum wire was sealed through each of these capillaries, and all capillaries made contact with a second platinum wire wound around the outside of the capillary and connected to leads. The piezometer volumes above each of these contacts were calibrated by weighing with mercury. The steel vessel contained mercury for compressing the gas in the piezometer, the remainder of the fluid being oil. Pressure was applied to the oil, forcing the mercury up inside the piezometer and compressing the gas until the mercury surface made contact with the platinum wires. Contact was indicated by a drop in the electrical resistance of the platinum wire wound around the capillary.

The fixed mass of gas was determined separately by expanding the entire sample into a large piezometer and measuring the normal volume of the gas at 25°C and a pressure of one atmosphere.

A series of runs consisted of charging the apparatus to the desired density and measuring the pressure and temperature at a known volume. The density of the sample was then varied by injecting or withdrawing oil from the system until the next selected volume was arrived at, whereupon the pressure and temperature were again

measured. In this manner isothermal data for a fixed amount of mass were taken. After an isotherm had been established, the above series of measurements could be repeated at other temperatures.

This apparatus was operational over the temperature range 0 to 150°C and at densities as high as 200 Amagat.[1/]

The above apparatus was limited in range of application, however. For higher densities the apparatus had the disadvantage that either the final volumes of the sample must be very small or the initial volume must be very large. The first disadvantage would cause inaccurate density measurements, the second would necessitate a large bulky apparatus for withstanding high pressures.

The Michels Improved Cryostat

The above disadvantages led to the alteration of the apparatus so that it could operate as high as 3000 atmospheres. The improved apparatus was described by Michels, Michels, and Wouters (43). In this design the piezometer was filled to an initial pressure of 20 to 50 atmospheres, and the amount of gas was determined under pressure. This assumed that data were available from a previous source for the pressure range 20 to 50 atmospheres.

The top portion of the piezometer containing the electrical contacts was similar to the original cryostat. The bottom half was altered to allow the piezometer to be filled under pressure and to

---

[1/] Characteristically, the Dutch and German workers express volumetric properties in Amagat units. The Amagat volume of a given amount of sample is obtained by dividing the actual volume of sample by the corresponding volume at 0°C and one atmosphere. The Amagat density is defined as the reciprocal of the Amagat volume.

provide a contact for the determination of the normal volume. Other general features of the original cryostat were preserved.

This apparatus was applicable in the pressure range 70 to 3000 atmospheres and at temperatures from 0 to 150°C. The apparatus was claimed by the authors to have an accuracy of one part in 2000 parts at 3000 atmospheres, with higher accuracy at pressures lower than 3000 atmospheres.

In both the original and later Michels piezometers the sample mass was ultimately determined by measuring the pressure and temperature of the sample in a known volume and by combining the measurements with the known PVT relations of the gas under those conditions. In the technique described below the sample mass is determined by direct weighing in a glass pipet.

The Beattie Apparatus

In the constant mass-variable volume apparatus used by Beattie (4) in 1934 a known amount of sample (determined by direct weighing) was placed within a glass liner or pipet of accurately known volume. The glass pipet was inverted and placed within a pressure vessel, which was so constructed as to allow a space between the pipet and the pressure vessel. The pipet was provided with a thin glass tip which confined the sample to the known volume. At the beginning of a series of runs the space between the pressure vessel and pipet was filled with mercury, and the tip of the inverted pipet was snapped off. During the course of a series of runs more mercury was injected into the inverted pipet via a volumetrically calibrated spoke device. The decrease in the original pipet volume was given by the amount of mercury

displaced through the spoke device, the necessary corrections to the density of mercury being made.

A "blank run" (using a gas with known compressibility factors) was first made for a series of pressures at each bomb temperature to determine the effect of pressure and temperature on the apparent volume of the pressure vessel, including the confining mercury. This was one advantage of the method. The apparatus operated in the temperature range 0 to 325 °C and at pressures from 10 to 500 atmospheres. Compressibilities of a substance could be determined along isochors as well as isotherms. The overall uncertainty in the compressibility data ranged from 0.3% at the lower pressures and temperatures to 0.1 to 0.2% at the higher pressures and temperatures.

An apparatus after the design of Beattie has been in recent use by Douslin et al (17) on fluorocarbons, hydrocarbons, and their binary mixtures. This apparatus has a temperature range of from 0 to 350°C and an operating pressure as high as 400 atmospheres. The overall accuracy in the compressibility measurements is reported to be 0.03% at the lowest temperature and pressure and 0.3% at the highest temperature and pressure.

Also, a Beattie type apparatus has been constructed at the University of Texas (25). The operating temperature range is reported as 35 to 225°C, with pressures from 6 to 310 atmospheres. An accuracy of 0.1 to 0.3% in the compressibility measurements is realized.

Other accurate versions of constant mass-variable volume type apparatus have been reported by Doolittle, Simon, and Cornish (15) and by Connolly and Kandalic (13).

D. Variable Volume-Variable Mass (The Burnett Apparatus)

The Burnett (9) apparatus was introduced in 1936, and is a variable volume-variable mass apparatus. This apparatus provides an accurate means of determining the volumetric properties of a gas without making volume or mass measurements; only the measurement of pressure and temperature is required. The apparatus is equally applicable to pure components or to mixtures.

As will be discussed below, the Burnett apparatus is interrelated with the isochoric apparatus of this work, as the densities for the isochoric runs are calculated from the experimental data from the Burnett apparatus.

General Principles of the Burnett Apparatus

Essentially the apparatus consists of two high pressure chambers, connected through an expansion valve. The volumes may be referred to as V_I and V_{II}, respectively. The bombs are enclosed in a constant temperature medium. Chamber I is initially filled to a pressure p_o, with the expansion valve being closed and chamber II evacuated. The pressure p_o is determined; then the expansion valve is opened and the gas allowed to expand into chamber II. After the attainment of thermal equilibrium the expansion valve is closed, chamber II is evacuated, and the new pressure p_1 in chamber I is determined. The pressure measurement, expansion, and evacuation are repeated, the result after r expansions being p_o, p_1, p_2, . . . , p_{r-1}, p_r, along an isotherm.

By making a simple material balance it may be shown that the ratio p_o/Z_o may be determined from

$$\lim_{p_r \to 0} \; p_r N^r = \frac{p_o}{Z_o} \qquad \text{(II-1)}$$

Here Z_o is the compressibility factor of the gas at p_o, and N is an apparatus constant, determined experimentally, and defined as $N = (V_I + V_{II})/V_I$. Once p_o/Z_o has been determined for a particular run the compressibility factor Z_r may be calculated from

$$p_r N^r = \frac{p_o}{Z_o} Z_r \qquad \text{(II-2)}$$

Here Z_r is the compressibility factor at the pressure p_r.

No correction for the effect of temperature on the bomb volumes is required, as the expansions are made isothermally. The apparatus constant N is slightly temperature dependent, and must be determined at each isotherm of the pressure expansions. Thus the accuracy of the Burnett apparatus depends primarily upon the measurement of two quantities--pressure and temperature. The apparatus is potentially most applicable to gases having a linear compressibility isotherm; however, it may be applied to any gas. Measurements with a calculated maximum error of 0.15% over a wide range of temperature and pressure have been reported by Canfield et al (10).

The Burnett apparatus has come into prominence within the last 10-15 years (7, 48, 53, 62, 63). Miller et al (48) determined compressibilities near room temperature at pressures up to 4000 psia for helium-nitrogen mixtures. Pfefferle, Goff, and Miller (53) applied a Burnett apparatus at 30°C, at pressures up to 120 atmospheres, to the

determination of compressibilities of helium, nitrogen, and carbon dioxide. Silberberg, Kobe, and McKetta (63) reported compressibility factor isotherms of isopentane from 50 to 200°C at pressures up to 65 atmospheres. Bloomer (7) reported compressibility isotherms, near ambient temperature, of two natural gases at pressures up to 1000 psia using a Burnett apparatus. Canfield et al (10) studied the helium-nitrogen system at temperatures from 0 to -140° C and at pressures ranging up to 10,000 psi.

The OSU Burnett Apparatus

The Burnett apparatus at Oklahoma State University consists of two stainless steel bombs, of approximately the same volume (85 cc's each), located in a constant temperature air bath. The bombs are of the same design as the jacketed bomb used for the isochoric apparatus of this work. The bombs are separated from the pressure measuring device by a differential pressure indicator (DPI) cell.

The apparatus is designed for use at room temperature and above. Since no low temperatures are involved, no limitations arise due to the DPI cell. The DPI cell is thus situated directly alongside the high pressure bombs in the air bath. The bomb volumes are maintained constant by filling the jackets with high-pressure oil. The apparatus was used for studies of the methane-ethylene system and for establishing the reference isotherm for the isochoric apparatus reported herein.

The pressure measuring equipment is connected between the Burnett apparatus and the isochoric apparatus so as to serve for either apparatus by the proper valving arrangement.

E. Constant Volume-Constant Mass Apparatus

The Apparatus of Goodwin

A modified Reichsanstalt apparatus[2/] has been described by Goodwin (22) for the determination of PVT and specific heat data of hydrogen. This constant volume-constant mass apparatus consists of a heavy-walled copper pipet situated in a cryostat and connected through stainless steel capillary tubing to a null pressure detector (or DPI cell). The null pressure detector, connecting valves, and tubing are at room temperature. No temperature control arrangement is provided for the null pressure detector and connecting valves, and their volumes are calibrated independently.

An experimental run consists of the measurement of a sequence of pressure versus temperature points beginning at the lowest temperature. The total mass of sample is determined by releasing the total quantity of confined fluid into a calibrated volumetric system and measuring P, V, and T at about normal conditions. Finally, the copper pipet volume must be known in order to compute the density of the gas. The normal (25°C) pipet volume is first determined by expanding a gas with known PVT properties (in this case, hydrogen) into the calibrated volumetric system, the necessary corrections being made. The pressure and temperature dependence of the pipet volume is then calculated by conventional equations.

[2/] The term Reichsanstalt apparatus is derived from PVT work done by Holborn et al (24) at the Physikalische Technische Reichsanstalt, Berlin, around 1920.

The copper pipet is situated inside an evacuable copper can, the copper can being inside of and soldered to a protected refrigeration tank containing liquid hydrogen refrigerant. The PVT data taken with this apparatus was for parahydrogen from 16 to 100°K and at pressures from 2 to 350 atmospheres.

The Isochoric Apparatus of Michels

The constant mass-variable volume cryostats of the design of Michels have been previously discussed in this chapter. Although suitable to the measurement of properties of fluids to high densities, this equipment was applicable only at temperatures of 0°C and above largely due to the freezing of the mercury or oil which confined the sample.

To allow operation at lower temperatures, a new type apparatus was constructed (37, 47). In this case the sample (at high pressure and low temperature) was separated from the oil of the pressure measuring device by a DPI cell, connected through a fine capillary and placed in a thermostat outside the low temperature cryostat. The DPI cell contained a thin diaphragm whose null or zero position was detected electronically. As the DPI cell was always operated in its null position the DPI cell volume, and thus the total volume of the sample, remained constant.

A series of runs consisted of charging the system to a high density and observing the pressures corresponding to a series of selected temperature levels. The density of the sample remained constant since the sample mass and volume remained unchanged. In order to

uniquely determine the volumetric properties of the sample along the isochoric path it was sufficient to know values of three quantities--pressure, temperature, and density. The pressure and temperature of the sample were directly measured during the course of the experiment; the density, however, was determined indirectly as follows.

The volumetric properties of the sample were presumed known from an independent source at some reference temperature level. Reference temperatures of 25 and 0°C were used by Michels. The cryostat was initially charged and allowed to equilibrate at the reference temperature, whereupon the exact values of temperature and pressure were measured. From the reference temperature and pressure, and from a knowledge of the volumetric properties along the reference isotherm, the density of the sample was determined.

After all desired points were taken along an isochor the cryostat was brought back to the reference temperature level, and a small amount of sample mass was vented from the system, thus lowering the density. After equilibrium was achieved, the temperature and pressure were again measured, and the new lower value of density was computed from the known volumetric properties along the reference isotherm. The above procedure was repeated.

In this manner, volumetric properties along a series of isochoric paths were determined. For many applications it is convenient if the data are available along an isotherm; for this reason the same series of temperature levels was selected along each isochor so that the final results could be presented in both isothermal as well as isochoric form.

In principle there are three corrections which must be made to the experimental data. These are: 1) the change in volume of the bomb with internal pressure, 2) the change in volume of the bomb due to temperature changes, and 3) the mass correction for the small amount of sample trapped in the DPI cell outside the low temperature cryostat.

The volume change due to internal pressure was determined experimentally. The method (36) involved calculating the change in inside volume from the measured change in external volume. The effect of temperature on the bomb volume was calculated from the dimensions of the bomb and the experimentally determined linear temperature coefficient of the material.

The DPI cell was located outside the cryostat, because the oil from the pressure balance would freeze if subjected to the low temperatures. Thus, corrections must be made for the amount of gas sample in the DPI cell and interconnecting capillaries. As the volumetric properties of the sample were presumed known at the reference temperature, it was convenient to maintain the DPI cell thermostat at or near the reference temperature. A simple mass balance shows that the correction may be made from two quantities--1) the volumetric properties of the sample confined in the DPI cell, and 2) the ratio of the volume of the DPI cell to the volume of the bomb.

To facilitate determining the volume ratio between the cells, Michels placed a valve between the DPI cell and the bomb. The cryostat was brought to the reference temperature, the connecting valve opened, and the system charged to about one atmosphere with a sample of known volumetric properties. The exact pressure and

temperature of the bomb were noted, and the valve was closed. The DPI cell only was then charged to a high pressure, and its pressure and temperature carefully noted. The interconnecting valve was then opened, allowing the gas to expand into the bomb, and the final pressure was noted. The knowledge of the two different pressures before the expansion and after the expansion, combined with the known volumetric properties of the gas, are sufficient to calculate the required ratio from a mass balance.

The correction for the amount of gas in the capillary was determined from scale drawings of the apparatus.

An apparatus of this design has the advantage that no direct determination of either mass or volume of the sample is necessary. The accuracy of the technique is ultimately limited only by the accuracy of measurement of temperature and pressure, and by the accuracy of the volumetric data of the sample along the reference isotherm. The temperature and pressure may be accurately determined without undue difficulty. The dependence of this technique on the reference isotherm, measured by an independent method, dictates that the technique can, in the limiting case, never be made more accurate than is the related independent method of obtaining the reference isotherm.

Depending upon the design of the cryostat, the characteristic that only one data point is taken at each temperature level can cause the data taking to proceed at a slow rate. It is mandatory that the cryostat be completely lined out at the next temperature level before the data point is taken. Types of apparatus that operate along an isotherm (such as those of Beattie and of Burnett) do not have this objectionable feature.

The apparatus was operational over the temperature range 25 to -180°C and at pressures from five to 1000 atmospheres. The reported accuracy of the determinations was given as one part in 10,000 parts.

This apparatus has been further discussed by Levelt (32) in an investigation of the volumetric properties of argon in the gaseous and liquid phases at temperatures from -25 to -155°C, pressures from five to 1000 atmospheres. This work is reported by Michels, Levelt, and De Graaff (41). The compressibility isotherms of air were determined with this apparatus at -25 to -155°C at pressures up to 1000 atmospheres (densities up to 560 Amagat units) and were reported by Michels, Wassenaar, Levelt, and De Graaff (46).

F. Existing PVT Data for Methane and Ethylene

Experimental Data for Methane

The volumetric properties of the methane system have been extensively reported. The system has been studied from -170°C (-274°F) to +350°C (+650°F) and at pressures as high as 1000 atmospheres.

Most experimental data is reported above the critical temperature (-115.8°F); the work of Mueller et al (49, 50), Vennix (67), and Pavlovich and Timrot (52) extends below the critical temperature. A summary of volumetric data for methane is given in Table I.

Experimental Data for Ethylene

The ethylene system has not been as widely studied as has methane, one reason being that its critical temperature (+49.8°F) is not far removed from ambient conditions. An extensive source of

data is that of Michels (39), extending from 32 to 302°F with pressures as high as 45,000 psi.

No significant amount of data, except at or near atmospheric pressure, has been taken for this system at temperatures below 32°F. A summary of available data from the literature is given in Table II.

Experimental Data for the Methane-Ethylene Mixture

There are no vapor phase PVT data for the methane-ethylene system reported in the literature.

TABLE I

SUMMARY OF LITERATURE VOLUMETRIC DATA FOR METHANE

Temperature Range °F	Pressure Range psia	Investigator	Reference
57 to 212	575 - 4,400	Amagat	(2)
32 to 650	220 - 5,900	Douslin	(16)
36 to 68	250 - 3,150	Freeth and Verschoyle	(21)
32 to 392	470 - 3,700	Keyes and Burks	(29)
-94 to 392	300 - 15,000	Kvalnes and Gaddy	(30)
77 to 167	30 - 12,000	Lee	(31)
-260 to 500	10 - 1,500	Matthews and Hurd	(34)
32 to 302	295 - 1,175	Michels et al	(44)
32 to 302	270 - 5,600	Michels et al	(45)
-200 to 50	40 - 7,000	Mueller et al	(49, 50)
100 to 460	200 - 10,000	Olds, Reamer, Sage and Lacey	(51)
-274 to 140	150 - 2,800	Pavlovich and Timrot	(52)
32 to 302	295 - 3,400	Schamp, Mason, Richardson, and Altman	(61)
-226 to 32	- 10,000	Vennix	(67)

TABLE II

SUMMARY OF LITERATURE VOLUMETRIC DATA FOR ETHYLENE

Temperature Range °F	Pressure Range psia	Investigator	Reference
32 to 70	20 - 60	Cawood and Patterson	(11)
77 to 167	30 - 12,000	Lee	(31)
77	75 - 1,850	Masson and Dolley	(33)
32 to 302	295 - 4,000	Michels et al	(38)
32 to 302	240 - 45,000	Michels et al	(39)
90 to 150	0 - 30	Pfennig and McKetta	(54)
40 to 100	50 - 600	Walters et al	(68)
-140 to 500	15 - 4,400	York and White	(69)

CHAPTER III

THEORETICAL CONSIDERATIONS

In this chapter all theoretical relationships underlying the treatment of the experimental data (Chapter VI) are presented.

As stated in Chapter I, one of the goals of this thesis is to emphasize the need for further development of an equation of state. This is done by comparing experimental virial coefficients and compressibility factors versus empirical equations of state. For this reason primary emphasis in this chapter is given to the virial equation of state and to empirical equations of state. These equations are discussed with respect to both pure components and to mixtures. In addition, several methods are presented for estimating virial coefficients.

A. General Comments Regarding Equations of State

In the most general terms an equation of state mathematically relates the pressure, volume, temperature, and composition of a substance. For a constant composition process only a relationship between pressure, volume, and temperature is necessary.

There have been many attempts to represent the volumetric behavior of substances, but no equation has been entirely successful in accurately representing actual gas behavior over the complete range of conditions of practical interest.

The simplest equation of state is the so-called "perfect gas" equation, i.e., PV = RT. Here P = absolute pressure, V = molar volume, R = the ideal gas constant, and T = temperature, degrees absolute. No gases exactly obey this equation; however, real gases approach this relationship at low pressures.

Volumetric properties of gases and vapors are frequently expressed in terms of the compressibility factor, Z, defined as the ratio of the actual specific gas volume, V, to the perfect gas volume RT/P. Only two of the quantities P, V, and T are independent; thus the compressibility factor may be considered to be a function only of T and P for a constant composition system.

Equations of state generally are of the closed-form type, containing several constants which are determined empirically. Such equations may be made fairly accurate by proper determination of the constants. In their present state of development, however, these equations may lead to serious error if used in the treatment and interpretation of compressibility data from a fundamental (virial coefficient) standpoint. A more theoretical relationship is necessary. The desired relationship is furnished by the virial equation of state. This equation is of fundamental significance, and may be derived from first principles, using the formulations of statistical mechanics. As the virial equation forms the theoretical basis for a substantial portion of the work reported herein it will be discussed in the following section; a detailed discussion of closed-form equations of state will be delayed until Section D, below.

B. The Virial Equation of State

The virial equation of state is an open-ended expression of the form

$$Z = 1 + B(T)/V + C(T)/V^2 + D(T)/V^3 + \cdots \qquad \text{(III-1)}$$

where for a pure component the coefficients B(T), C(T), D(T), . . ., are the second, third, fourth, . . . etc., virial coefficients, which are functions of temperature only.

The complete derivation of Equation III-1 is given in Chapter III of reference (23). This procedure considers interactions between all possible configurations of particles, both pairwise and higher-ordered interactions. The derivation is quite lengthy, and will not be presented here.

The virial equation may be given either as the open-ended series in reciprocal volume (as above) or as an open-ended series in pressure. The reciprocal volume series is said to be the Leiden form of the virial equation. The coefficients are said to be the Leiden virial coefficients.

The power series in pressure is given below, and is termed the Berlin form of the virial equation.

$$Z = 1 + B'(T)P + C'(T)P^2 + D'(T)P^3 + \cdots \qquad \text{(III-2)}$$

Here the coefficients are termed the Berlin virial coefficients, and are also functions of temperature only. The Berlin form was used extensively by the early German workers for representing volumetric properties of a gas, while the Leiden form was used in The Netherlands.

The Leiden form has the advantage of having theoretical significance. Also, fewer terms are usually required in the Leiden form than in the Berlin form to obtain the same degree of fit to a given set of data. Only the Leiden form will be considered in the following discussions.

The virial equation of state for a mixture may also be determined from theoretical considerations, and the result, given below, is analogous to Equation III-1 for a pure component.

$$Z_m = 1 + B_m(T)/V_m + C_m(T)/V_m^2 + D_m(T)/V_m^3 + \ldots \qquad \text{(III-3)}$$

Here the subscript m refers to a mixture. The virial coefficients are functions of both temperature and of the composition of the mixture.

Methods of determining virial coefficients are given in the following section; also relationships between mixture virial coefficients and the coefficients for pure components are discussed.

C. Virial Coefficients

In this thesis second virial coefficients are determined graphically by the following rearrangement of Equation III-1.

$$(Z - 1)V = B(T) + C(T)/V + D(T)/V^2 + \ldots \qquad \text{(III-4)}$$

Here $(Z - 1)V$ is plotted versus $(1/V)$ along an isotherm. The intercept at infinite volume $(1/V \to 0)$ equals the second virial coefficient.

After B(T) is known, C(T) may also be determined graphically from the expression

$$\lim_{(1/V \to 0)} [(Z - 1)V - B(T)]V = C(T) \qquad \text{(III-5)}$$

For the fourth virial coefficient, using previously determined B(T) and C(T) values,

$$\lim_{(1/V\to 0)} [(Z - 1)V^2 - B(T)V - C(T)]V = D(T) \qquad \text{(III-6)}$$

This procedure is referred to as the slope-intercept method, and has been employed extensively by previous investigators. This procedure is very sensitive to inaccuracies in the experimental data, especially in the low density region. The advantage of the procedure is that coefficients so determined (for pure components) are functions of temperature only.

Virial Coefficients of Mixtures

For mixtures, virial coefficients may similarly be determined by the slope-intercept method. The second, third, and fourth virial coefficients are determined from Equation III-3 according to the expressions

$$\lim_{(1/V_m\to 0)} (Z_m - 1)V_m = B_m(T) \qquad \text{(III-7)}$$

$$\lim_{(1/V_m\to 0)} [(Z_m - 1)V_m - B_m(T)]V_m = C_m(T) \qquad \text{(III-8)}$$

$$\lim_{(1/V_m\to 0)} [(Z_m - 1)V_m^2 - B_m(T)V_m - C_m(T)]V_m = D_m(T) \qquad \text{(III-9)}$$

As stated previously the virial coefficients in this case are functions of both temperature and of the composition of the mixture.

It has been shown by Mayer (35) that the virial coefficients for a mixture of N components may be expressed as

$$B_m(T) = \sum_{i}^{N} \sum_{j}^{N} B_{ij}(T) x_i x_j \qquad \text{(III-10)}$$

$$C_m(T) = \sum_{i}^{N} \sum_{j}^{N} \sum_{k}^{N} C_{ijk}(T) x_i x_j x_k \qquad \text{(III-11)}$$

In this case x_i, x_j, and x_k are the mole fractions, respectively, of species i, j, and k in the mixture. The coefficient $B_{ii}(T)$ represents the second virial coefficient for i in its pure state. The term $B_{ij}(T)$ represents the interaction between molecules of species i and j, and is said to be the second interaction or cross coefficient between i and j. Similar comments apply to the terms in Equation III-11. Here $C_{ijk}(T)$ represents ternary interactions between molecules i, j, and k. If i = j = k, the resulting C_{iii} represents the third virial coefficient for component i in its pure state.

It is important to note that, although the virial coefficients on the left side of Equations III-10 and III-11 are functions of both temperature and composition, the coefficients on the right side (including the cross coefficients) are functions of temperature only.

For a binary mixture Equations III-10 and III-11 take the form

$$B_m(T) = x_1^2 B_{11}(T) + 2x_1 x_2 B_{12}(T) + x_2^2 B_{22}(T) \qquad \text{(III-12)}$$

$$C_m(T) = x_1^3 C_{111}(T) + x_2^3 C_{222}(T) + 3x_1^2 x_2 C_{112}(T) + 3x_1 x_2^2 C_{122}(T) \quad \text{(III-13)}$$

Here it is assumed that $B_{12} = B_{21}$, and that C_{ijk} is the same for all permutations of the indices.

Empirical Relationships for Predicting Virial Coefficients

Methods of predicting virial coefficients are also of interest and will be considered in the following. The prediction of interaction second virial coefficients (for binary systems) will receive particular attention.

One method for estimating second virial coefficients is based on Pitzer's modified theorem of corresponding states (55). Here a characterizing parameter, ω, is defined by the reduced vapor pressure P_R^o at $T_R = 0.7$. The expression is as follows

$$\omega = -(\log P_R^o + 1.00)_{T_R = 0.7} \quad \text{(III-14)}$$

In this expression T_R and P_R are the reduced temperature (T/T_c) and reduced pressure (P/P_c), respectively, and ω is termed the accentric factor. A simple fluid is defined as one having $\omega = 0.0$; thus ω is a measure of the deviation from a simple fluid. The compressibility factor is then given by the relationship

$$Z = Z^o + \omega Z' \quad \text{(III-15)}$$

where Z^o = the compressibility factor for a simple fluid

Z' = the compressibility factor correction for deviation from a simple fluid.

Based upon this generalized data, an analytical expression for the reduced second virial coefficient $\left(\frac{BP_c}{RT_c}\right)$ was also presented by Pitzer. The expression is as follows

$$b = \frac{BP_c}{RT_c} = 0.1445 + 0.073\,\omega - \left(\frac{0.33 - 0.46\omega}{T_R}\right) - \left(\frac{0.1385 + 0.50\omega}{T_R^2}\right) - \left(\frac{0.0121 + 0.097\omega}{T_R^3}\right) - \left(\frac{0.0073\omega}{T_R^8}\right) \qquad \text{(III-16)}$$

Another means of estimating virial coefficients was presented by Prausnitz (56, 57). This work consists of a suitable extension to mixtures of Pitzer's (55) generalized results, and is described as follows.

For a pure component i the second virial coefficient is given as

$$\frac{B_{ii}}{V_{c_{ii}}} = \theta_B \left(\frac{T}{T_{c_{ii}}}, \omega_{ii}\right) \qquad \text{(III-17)}$$

where $V_{c_{ii}}$ and $T_{c_{ii}}$ represent the component's critical volume and temperature, respectively, and ω_{ii} is the accentric factor. The function θ_B is given in tabular form.

The interaction second virial coefficient B_{ij} is given by

$$\frac{B_{ij}}{V_{c_{ij}}} = \theta_B \left(\frac{T}{T_{c_{ij}}}, \omega_{ij}\right) \qquad \text{(III-18)}$$

The parameters $V_{c_{ij}}$, $T_{c_{ij}}$, and ω_{ij} characterize the interactions between dissimilar species; combining rules are given by Prausnitz for estimating these parameters.

The third virial coefficients were also given by Prausnitz; these coefficients are given in the form of a graph and are somewhat less

accurate than the results for second virial coefficients.

The direct estimation of the interaction second virial coefficient B_{12} from the virial coefficients B_{11} and B_{22} is also considered here. In principle B_{12} may be calculated from a selected mathematical combination of B_{11} and B_{22}, and the result substituted into Equation III-12 to yield $B_m(T)$. As a test of the combining rule, the calculated value of $B_m(T)$ is then compared with the experimental value.

In addition to being of theoretical interest a reliable combining rule of this type would be of utility in engineering calculations. If mixture second virial coefficients could be accurately determined, compressibility factors of the mixture could also be calculated to moderate pressures by use of the truncated form of the virial equation (using only the second virial coefficient). Of even greater importance, however, increased knowledge of combining rules could be used to provide additional insight into the development of an improved equation of state for mixtures. Several such combining rules for B_{12} are presented below.

The <u>linear</u> combination of B_{11} and B_{22} has the form

$$B_{12} = \frac{1}{2}(B_{11} + B_{22}) \qquad \text{(III-19)}$$

Substituting B_{12} from Equation III-19 into Equation III-12, B_m takes the simplified form

$$B_m = x_1 B_{11} + x_2 B_{22} \qquad \text{(III-20)}$$

The <u>square root</u> combination is given as

$$B_{12} = \sqrt{B_{11} B_{22}} \qquad \text{(III-21)}$$

Substituting this equation into Equation III-12, there results

$$B_m = (x_1\sqrt{B_{11}} + x_2\sqrt{B_{22}})^2 \qquad \text{(III-22)}$$

The above two combining rules are the simplest expressions that could be expected to provide a reasonable estimation of B_{12}. In addition, two slightly more complex expressions are considered below.

The Lorentz combination for B_{12} is

$$B_{12} = [(B_{11})^{1/3} + (B_{22})^{1/3}]^3 /8 \qquad \text{(III-23)}$$

With this combining rule no simplification is obtained if Equation III-23 is substituted into Equation III-12. Thus the value of B_{12} is calculated from Equation III-23, and the numerical result is substituted directly into Equation III-12 to obtain B_m.

The linear square root rule was considered only because it is similar in mathematical form to the Lorentz combination. As far as is known to the author this particular mathematical form has not been previously used for equation of state combinations of this type. The rule is

$$B_{12} = [(B_{11})^{1/2} + (B_{22})^{1/2}]^2 /4 \qquad \text{(III-24)}$$

As was the case with the Lorentz combining rule, no simplification is obtained by substituting this equation into Equation III-12.

In Chapter VI results are given for testing the four above combining rules versus the experimental methane-ethylene virial coefficients.

One additional method will be considered for making empirical estimates of virial coefficients. This method involves calculating virial coefficients directly from the virial form of empirical equations of state. The procedure will be described in Section D.

D. Empirical Equations of State

Empirical equations of state were mentioned briefly, above. Such equations are very numerous; in this work it is not proposed to present a large number of equations as examples. Moreover, three of the most important equations of state were selected for evaluation versus the experimental data. These equations are 1) the Benedict-Webb-Rubin (BWR) equation (6), 2) the Edmister generalized form of the BWR equation (20), and 3) the Redlich-Kwong (RK) equation (58). The equations will be discussed in this order.

The BWR Equation

The BWR equation is an eight constant relationship expressing pressure or compressibility factor as a function of density (reciprocal volume). The form of the equation is a power series ending with an exponential density term, the coefficients of density being functions of temperature. The equation is written as

$$P = RTd + (B_oRT - A_o - \frac{C_o}{T^2})d^2 + (bRT - a)d^3 + a\alpha d^6 + cd^3(\frac{1 + \gamma d^2}{T^2}) \exp(-\gamma d^2) \qquad \text{(III-25)}$$

where d = density.

In terms of compressibility factor the equation has the form

$$Z = 1 + (B_o - \frac{A_o}{RT} - \frac{C_o}{RT^3})d + (b - \frac{a}{RT})d^2 + \frac{a\alpha}{RT}d^5 + \frac{cd^2}{RT^3}(1 + \gamma d^2) \exp(-\gamma d^2) \qquad \text{(III-26)}$$

The empirical constants A_o, B_o, C_o, a, b, c, γ, and α are determined for a specific compound from PVT, critical, and vapor pressure data. This equation was developed primarily for hydrocarbons and their mixtures, and provides a satisfactory representation of experimental data for densities up to about twice the critical density.

For application to mixtures, the constants are determined from the corresponding constants for the pure components by the relationships

$$B_{o_m} = \sum_i^N x_i B_{o_i} \qquad \text{(Linear)}$$

$$B_{o_m} = \sum_{ij}^N x_i x_j \left[(B_{o_i})^{1/3} + (B_{o_j})^{1/3}\right]^3 /8 \qquad \text{(Lorentz)}$$

$$A_{o_m} = \left[\sum_i^N x_i (A_{o_i})^{1/2}\right]^2$$

$$C_{o_m} = \left[\sum_i^N x_i (C_{o_i})^{1/2}\right]^2$$

$$b_m = \left[\sum_i^N x_i (b_i)^{1/3}\right]^3 \qquad \text{(III-27)}$$

$$c_m = \left[\sum_i^N x_i (c_i)^{1/3}\right]^3$$

$$a_m = \left[\sum_i^N x_i (a_i)^{1/3}\right]^3$$

$$\gamma_m = \left[\sum_i^N x_i (\gamma_i)^{1/2}\right]^2$$

$$\alpha_m = \left[\sum_i^N x_i (\alpha_i)^{1/3}\right]^3$$

Here the subscript m refers to properties of the mixture, and i refers to properties of component i of the mixture, present at composition x_i. Although these rules are based on statistical mechanical considerations, they must be regarded as somewhat empirical. Both the linear and Lorentz forms for B_{o_m} are frequently used. In some cases these mixing rules have been shown to fit the experimental data for mixtures almost as well as the original equation of state fits the pure component data.

The BWR equation may be rearranged into open-ended virial form as follows. The exponential term in Equation III-26 may be expanded into a infinite power series, giving

$$\exp(-\gamma d^2) = 1 - \gamma d^2 + \frac{\gamma^2 d^4}{2} - \frac{\gamma^3 d^6}{6} + \ldots \qquad \text{(III-28)}$$

Substituting Equation III-28 into Equation III-26 and rearranging according to increasing powers of d (reciprocal volume), there results

$$Z = 1 + (B_o - \frac{A_o}{RT} - \frac{C_o}{RT^3})d + (b - \frac{a}{RT} + \frac{c}{RT^3})d^2 + \frac{\alpha a}{RT} d^5 - \frac{c\gamma^2 d^6}{2RT^3} + \ldots \qquad \text{(III-29)}$$

Comparing corresponding terms of Equations III-29 and III-1, the second and third virial coefficients are given by the BWR equation as

$$B(T) = B_o - \frac{A_o}{RT} - \frac{C_o}{RT^3} \qquad \text{(III-30)}$$

$$C(T) = b - \frac{a}{RT} + \frac{c}{RT^3} \qquad \text{(III-31)}$$

It is to be noted that, due to the mathematical form of the BWR equation, the third and fourth virial coefficients (and also other higher ordered coefficients) are missing from Equation III-29.

This equation was selected for theoretical analysis as it gives an indication of the accuracy and application obtainable from relatively complex equations of state.

The Edmister Generalized Form of the BWR Equation

The Edmister generalized form (20) of the BWR equation presents the eight constants in the equation in terms of Pitzer's (55) modified theorem of corresponding states. Here Equation III-26 is given in reduced form as

$$Z = 1 + (B'_o - \frac{A'_o}{\theta} - \frac{C'_o}{\theta^3})\rho + (b' - \frac{a'}{\theta})\rho^2 + \frac{\alpha' a'}{\theta}\rho^5 + \frac{c'}{\theta^3}\rho^2(1 + \gamma'\rho^2)\exp(-\gamma'\rho^2) \qquad \text{(III-32)}$$

where $$\rho = \frac{RT_c/P_c}{V} = \frac{d}{P_c/RT_c} = \frac{P_R}{ZT_R}$$

= reduced density. θ is defined as T/T_c = reduced temperature, and B'_o, A'_o, C'_o, b', a', c', α', and γ' are reduced constants.

The reduced constants were determined from the original BWR constants for 12 hydrocarbons by plotting them versus ω, obtaining straight lines. The equations of these lines are given as

$$B'_o = 0.1306$$

$$A'_o = 0.35 - 0.30\omega$$

$$
\begin{aligned}
C_o' &= 0.10 + 0.40\omega \\
b' &= 0.031 + 0.08\omega \\
a' &= 0.036 + 0.16\omega \\
c' &= 0.042 + 0.105\omega \\
\alpha' a' &= 0.0000875 \\
\gamma' &= 0.049 - 0.05\omega
\end{aligned}
\qquad \text{(III-33)}
$$

The specific constants are determined from these reduced constants by the expressions

$$
\begin{aligned}
B_{o_i} &= B_o' \frac{RT_{c_i}}{P_{c_i}} \\
A_{o_i} &= A_o' \frac{R^2 T^2_{c_i}}{P_{c_i}} \\
C_{o_i} &= C_o' \frac{R^2 T^4_{c_i}}{P_{c_i}} \\
b_i &= b' \frac{R^2 T^2_{c_i}}{P^2_{c_i}} \\
a_i &= a' \frac{R^3 T^3_{c_i}}{P^2_{c_i}}
\end{aligned}
\qquad \text{(III-34)}
$$

$$\alpha_i = \alpha' \frac{R^3 T_{c_i}^3}{P_{c_i}^3}$$

$$c_i = c' \frac{R^3 T_{c_i}^5}{P_{c_i}^2}$$

$$\gamma_i = \gamma' \frac{R^2 T_{c_i}^2}{P_{c_i}^2}$$

Additional relationships similar to Equations III-33 above, but giving the reduced constants as functions of critical compressibility factor Z_c, were also developed by Edmister (20). These relationships are not utilized in this work, however.

Due to the manner in which the reduced constants (Equations III-33) were determined, it was unnecessary to develop new combining rules for mixtures. From Equations III-33 and III-34 specific constants may be determined; these constants are combined for mixtures using the original BWR combining rules (Equations III-27).

In a similar manner the second and third virial coefficients for the generalized equation are given by the same expressions as before (Equations III-30 and III-31).

By evaluation of this equation the applicability of a generalized relationship is demonstrated. At the same time an opportunity is afforded to compare a generalized equation directly with a similar equation for a specific compound, the equations differing only in the

value of the constants. The comparison of the two equations, both against each other and against the experimental data, gives indications of future methods for improving the equations.

The RK Equation

The RK equation is a two constant relationship of the form

$$P = \frac{RT}{V - b} - \frac{a}{T^{1/2}V(V + b)} \qquad \text{(III-35)}$$

with the two constants a and b given as

$$a = \frac{0.4278\ R^2 T_c^{2.5}}{P_c}$$

$$b = \frac{0.0867\ R\ T_c}{P_c} \qquad \text{(III-36)}$$

For application, the equation is frequently used in the equivalent form

$$Z = \frac{1}{1 - h} - \frac{A^2}{B}\frac{h}{1 + h} \qquad \text{(III-37)}$$

where

$$A^2 = \frac{0.4278}{P_c T_R^{2.5}}$$

$$B = \frac{0.0867}{P_c T_R} \qquad \text{(III-38)}$$

$$h = \frac{BP}{Z} = \frac{0.0867\ P_R}{ZT_R}$$

This equation was developed primarily for use at temperatures above the critical.

For mixtures, the constants a and b are combined according to the relations

$$\sqrt{a_m} = \sum_i^N x_i \sqrt{a_i}$$

$$b_m = \sum_i^N x_i b_i \qquad \text{(III-39)}$$

whereas the constants A and B are determined from

$$A_m = \sum_i^N x_i A_i$$

$$B_m = \sum_i^N x_i B_i \qquad \text{(III-40)}$$

The virial form of the equation is obtained as follows. Equation III-35 is written as

$$P = RT \frac{1}{V}\left(\frac{1}{1 - \frac{b}{V}}\right) - \frac{a}{T^{1/2}} \left(\frac{1}{V}\right)^2 \left(\frac{1}{1 + \frac{b}{V}}\right) \qquad \text{(III-41)}$$

Expanding the terms $\left(\frac{1}{1 - \frac{b}{V}}\right)$ and $\left(\frac{1}{1 + \frac{b}{V}}\right)$ into an infinite series, and rearranging terms, the RK equation may be written as

$$Z = 1 + \left(b - \frac{a}{RT^{3/2}}\right) \frac{1}{V} + \left(b^2 + \frac{ab}{RT^{3/2}}\right) \left(\frac{1}{V}\right)^2$$

$$+ \left(b^3 - \frac{ab^2}{RT^{3/2}}\right) \left(\frac{1}{V}\right)^3 + \ldots \qquad \text{(III-42)}$$

Comparing corresponding terms between Equation III-42 and Equation III-1, the second and third virial coefficients are given for the RK equation as

$$B(T) = b - \frac{a}{RT^{3/2}}$$

$$C(T) = b^2 + \frac{ab}{RT^{3/2}} \qquad \text{(III-43)}$$

As contrasted to the BWR equation, all higher-ordered virial coefficients are present in this expansion. This equation differs further from the BWR equation in that the constants a and b are functions only of the critical properties of the components; the BWR constants are somewhat dependent upon the range of data covered.

In the past the RK equation has found application where highest accuracy was not required, and where relative ease of computation was desired.

No further attempt to discuss equations of state will be made at this point. A wide variety of publications and thermodynamics texts is readily available; in particular, applications of equations of state are discussed by Dodge (14) and by Edmister (19).

CHAPTER IV

EXPERIMENTAL APPARATUS

The physical description and operating characteristics of the experimental equipment are presented in this chapter. Mathematical equations that characterize the apparatus are presented, and the advantages and disadvantages of the apparatus are discussed.

A. Description of Equipment

General operating features of the entire system will be discussed first, before the detailed descriptions of each section of the apparatus.

General Description of Apparatus

The apparatus to be described is of the constant volume-constant mass (isochoric) type, which type of apparatus for PVT measurements has been discussed in Chapter II. This particular apparatus is similar in design to that of Michels (47), the principal difference being in the constant temperature bath. The Michels cryostat used a stirred liquid to insure thermal equilibrium; the present design uses an air thermostat.

The apparatus is shown schematically in Figure 1; connections to the interrelated Burnett apparatus are also shown in this figure. The apparatus consists of a double-walled air thermostat containing a jacketed constant volume cell. The controlled temperature region

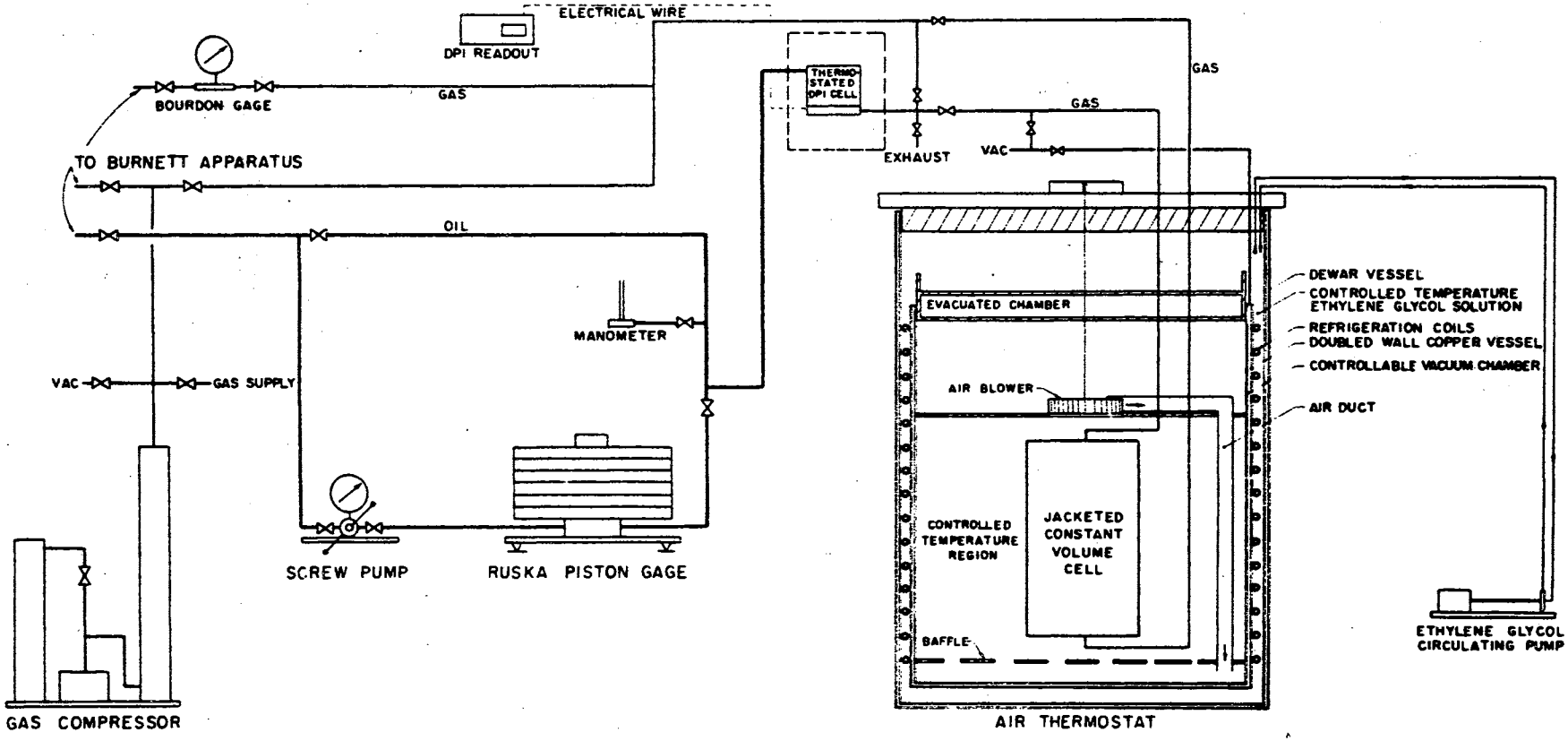

Figure 1

Schematic Diagram of Apparatus for Isochoric Heating and Cooling

of the thermostat, containing the constant volume cell, consists of a recirculating air stream whose temperature is controlled by the addition of a small amount of heat through an electronic temperature regulating device. The double-walled vessel is placed in a dewar vessel, containing a constant temperature refrigerated liquid such as ethylene glycol, the liquid serving as a heat sink for the thermostat.

The pressure of the sample is determined by means of the Ruska Instrument Corporation piston gage. The oil of the pressure balance system is separated from the gas sample by the thermostated differential pressure indicator (DPI) cell.[1/] This cell consists of two chambers, separated by a flexible metal diaphragm, the zero position of which is detected electronically and indicated by the DPI readout. The DPI cell is placed outside the air thermostat because the high pressure oil would solidify if subjected to the prevailing low temperatures. The DPI cell was continuously maintained at a temperature slightly above ambient; a temperature of approximately 95°F was found to be practical. An interconnecting valve was placed outside the air thermostat between the DPI cell and bomb. The necessary balancing pressure of the oil is generated by the screw pump.

A hand-operated gas compressor is used for charging the cell and its surrounding pressure jacket to the desired pressures, the nominal

---

[1/] The jacketed constant volume cell will be referred to as the "bomb", whereas the differential pressure indicator cell will be termed the "DPI cell." The controlled temperature region of the air thermostat will be referred to as the "cryostat."

value of pressure being indicated on the bourdon gage. The pressure jacket around the bomb is used to offset any change of bomb volume due to the stresses set up by the internal sample pressure. The gas sample is injected into the main chamber of the bomb through the gas line shown leading into the top of the bomb. Gas is injected into the surrounding pressure jacket of the bomb via the gas line leading into the bottom of the bomb.

Provision is made for subjecting the necessary portion of the apparatus to the vacuum system. The temperatures of the cryostat and DPI cell are determined by calibrated thermocouples.

A run consists of charging the bomb and DPI cell to a high density and observing the pressures corresponding to a pre-selected series of temperature levels. Since the mass and volume are constant, the run thus follows an isochor, or constant density path. At any point on the isochor the simultaneous knowledge of the three quantities pressure, temperature, and density is sufficient to determine the volumetric properties at that temperature and pressure. The density is determined as follows.

A reference temperature of 77°F is established; along this isotherm the compressibility of the sample has been independently determined from the Burnett apparatus. Each isochoric run includes the reference isotherm as the upper temperature; at this temperature the pressure, temperature, and density are simultaneously known, and the value of

density for the entire isochor may thus be determined.[2/]

Additional isochors are run, at successively decreasing densities. The density for each isochor is established at the beginning of each run by exhausting a small amount of the sample to the atmosphere. The same series of temperature levels is selected along each isochor so that the final results may be given as either isothermal or isochoric data. Temperatures of 77, 60, 40, and 20°F were used in this work.

A small correction is required for the amount of sample in the DPI cell. A mass balance, given in Appendix N, shows that this correction requires the value of the ratio of the volume of the DPI cell to the volume of the bomb. It is convenient if this ratio is determined when the DPI cell and bomb are at the same temperature.

To determine the volume ratio the system is rinsed with a gas of known volumetric properties, evacuated, and the cryostat temperature is adjusted to that of the DPI cell (95°F). The valve between the bomb and DPI cell is closed, and the DPI cell only is charged with a sample of the same gas. After equilibrium has been attained the DPI cell pressure is measured, and the temperatures of both bomb and DPI cell are measured.

[2/] As will be shown later, the value so calculated at the reference isotherm is not a true density, but a run constant. The difference is due to the volume of gas in the DPI cell and capillary lines. Only the run constant is required in the calculations along the isochor; the true density exists as a constant known fraction of the run constant, and could be simply calculated if desired.

The valve is then opened, and the sample allowed to expand into the bomb. The system is allowed to equilibrate, and the final pressure and the temperatures of both volumes are measured. The known volumetric properties of the sample at each of the above pressures allow the volume ratio to be calculated.

A small correction for the amount of gas in the capillary line is also required. This correction is discussed in Appendix N.

For all values of pressure, the jacket pressure must be continuously maintained at the proper value to eliminate the effect of internal pressure on the bomb volume. This correction is discussed in Appendix K. The effect of temperature on the bomb volume must be considered. This correction is calculated from the dimensions of the bomb and the linear temperature expansion coefficient for the material; the equation is derived in Appendix H.

Additional details of specific sections of the apparatus are given in the following.

Cryostat

For maintenance of low temperatures a double-walled copper can, 26 inches in height and 11 1/8 inches in outside diameter, was used. This vessel is shown in Plate I and was illustrated schematically in Figure 1. The can was formed from a 1/16 inch sheet of hard copper by Spincraft, Inc., of Milwaukee, Wisconsin. The double walls were firmly braced internally by supporting strips of heat resistant Johns-Mansville transite, before joining the walls together at the top by silver soldering. A single steel support was located in the space between the double walls at the bottom of the cans.

Plate I

Double-walled Vessel with Upper Chamber

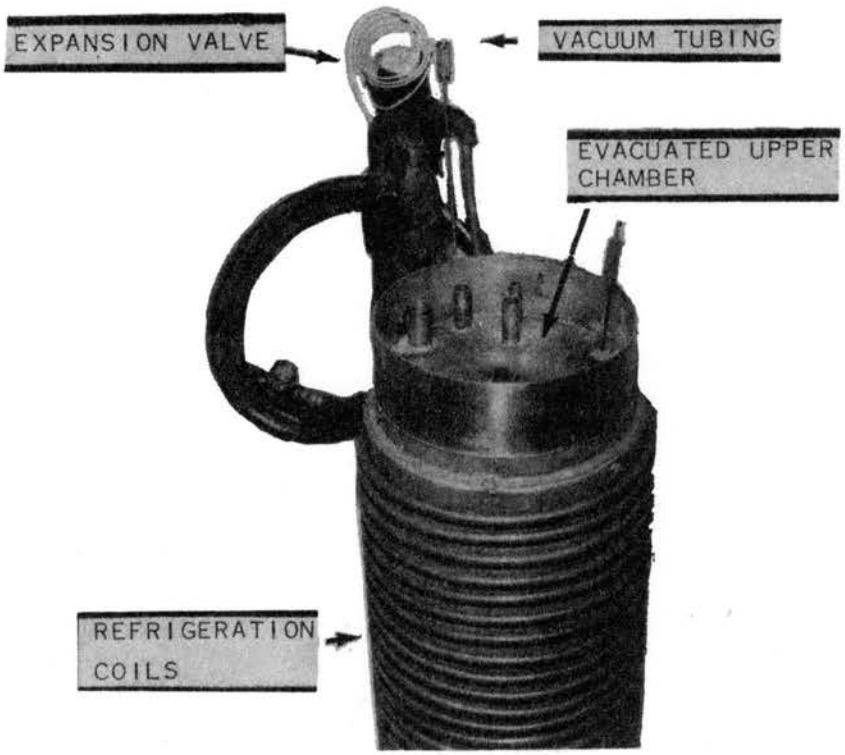

A 1/8 inch OD stainless steel vacuum line was silver soldered between the double walls of the can and connected to the vacuum system. An absolute pressure of approximately 25 microns was maintained in the space between the outer surface of the inside wall and the inner surface of the outside wall. All walls of the vessel were plated with nickel and then polished. The plating and polishing of the walls and the maintenance of a vacuum between the walls thus insured the desired small amount of heat transfer by conduction and radiation through the annular space.

An evacuated upper chamber was fitted into the mouth of the double-walled cans. This chamber was formed from stainless steel and was then nickel plated and polished to minimize radiation heat transfer. The chamber was evacuated and sealed at an absolute pressure of about one micron. The upper portion of the evacuated chamber serves as a container for a refrigerating medium such as liquid nitrogen or a mixture of dry ice and iso-octane.

The heat sink for the cryostat was maintained by an ordinary Freon-12 closed loop refrigeration system. Twenty turns of 1/2 inch OD refrigeration type copper tubing were concentrically wrapped and soldered around the outer surface of the outside wall of the double-walled cans. These coils served as the evaporator for the refrigeration system. The double-walled vessel with refrigeration coils was then placed inside a stainless steel dewar (Sulfrian Model No. SJ-2, 76 liter, 13 inches inside diameter). The outer wall of the steel dewar was insulated from the surrounding with a layer of fibre-glass insulating material. A four-inch thick section of styrofoam insulating material was fitted into the top of the dewar, to further minimize

heat transfer between the surroundings and the cryostat. A disassembled view of the insulated dewar, double-walled copper can, and bomb is shown in Plate II.

The space between the outside wall of the double-walled vessel and the inside wall of the dewar was filled with approximately three gallons of ethylene glycol solution which could be circulated by an external centrifugal pump (Figure 1). The solution consisted of 60% by volume commercial "Prestone" antifreeze and 40% by volume water, thus providing a liquid with a freezing point of approximately -50°F. The refrigeration system used a PAR 1/3 HP refrigeration compressor unit. The 1/2 ton Freon-12 expansion valve (Plate I) was adjusted so as to provide a suction side pressure of about zero psig to the compressor and a discharge side pressure of about 120 psig.

The compressor was allowed to run continuously, reaching equilibrium with the surroundings and with the particular temperature of the cryostat. The temperature of the ethylene glycol solution was affected by ambient temperature and by the level of the cryostat temperature. Any changes in ambient temperature were gradual and thus did not markedly upset the temperature control. The effect of the cryostat temperature on the ethylene glycol solution temperature (Table III) gives an indication of the rate of heat transfer between these two regions. The change in ethylene glycol solution temperature is considerable, and is indicative of conduction heat transfer to the ethylene glycol solution through the upper portion of the cryostat. This has a small effect on the temperature control inside the cryostat.

Plate II

Major Components of Cryostat--Disassembled View

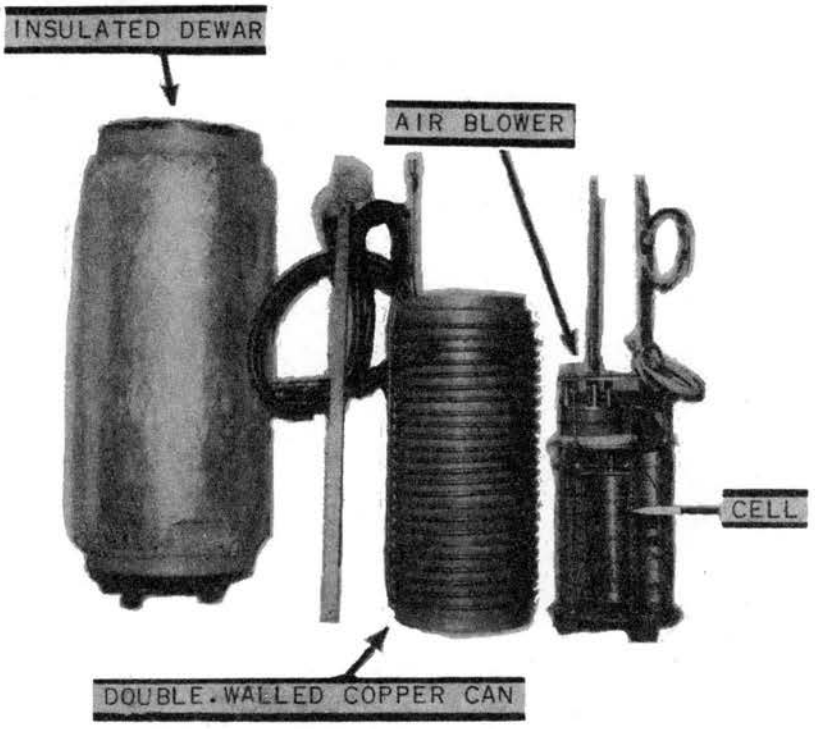

TABLE III

EFFECT OF CRYOSTAT TEMPERATURE ON THE ETHYLENE GLYCOL SOLUTION TEMPERATURE

Cryostat Temperature, °F	20	40	60	77
Ethylene Glycol Solution Temperature, °F	-18	-13	-9	-6

The air in the cryostat was continuously circulated at atmospheric pressure by means of a squirrel-cage type air blower supported on a mounting plate about three inches above the top of the bomb. A view of the bomb and the internal arrangement of the cryostat is given in Plate III. The air is recirculated via a two-inch ID aluminum air duct. The return air is distributed over a baffle located in the bottom part of the controlled temperature region; this distributing baffle helps insure uniformity of temperature by thorough mixing of the return air. The blower was rated at 100 CFM of air at no-load conditions, with a blower speed of 1750 RPM.

It was necessary to place the driving motor for the blower completely outside the cryostat (Figure 1) or the dissipated heat would upset the temperature control. The motor was separated from the blower by means of a steel shaft, supported by bearings at the top, bottom, and center, and interrupted in the center by a flexible coupling.

Initially a 1/45 HP series-type motor was used. This arrangement was found to be unsatisfactory, as any changes in line voltage or changes in loading characteristics produced a change of speed in the motor. This was observed to affect the temperature control.

Plate III

Internal Arrangement of Cryostat

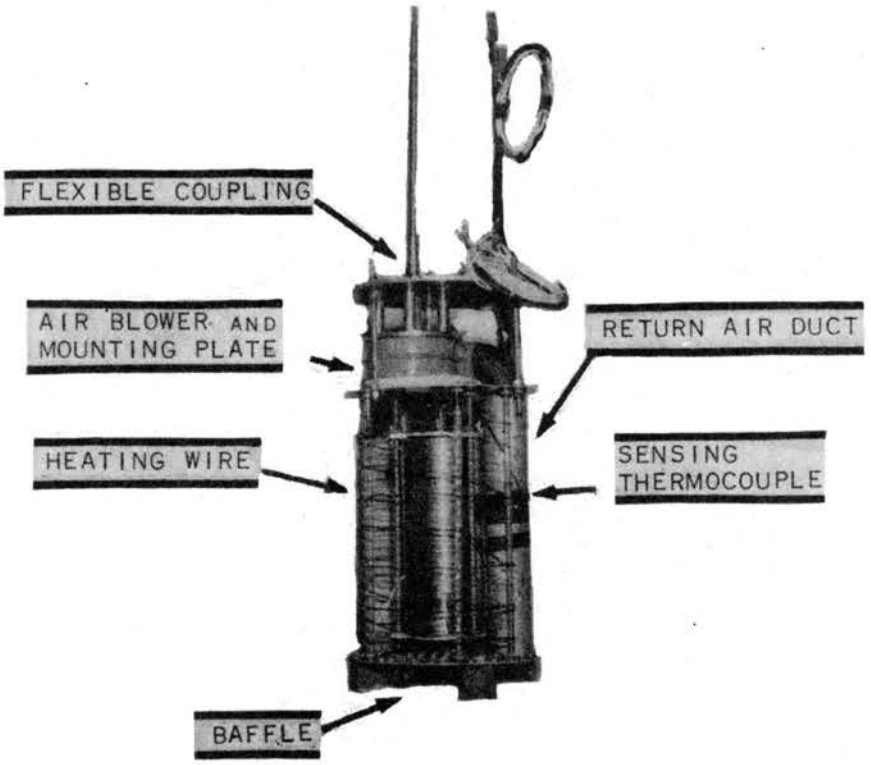

This motor was thus replaced by a 1/15 HP constant speed hysteresis synchronous motor. This unit had a rated speed of 1800 RPM, and was observed periodically with a stroboscope to operate precisely at rated speed, both at full load and at no load.

No convenient method to measure the rate of air circulation was available, but it was thought to be somewhat less (perhaps by a factor of 50%) than the rated circulation rate at no load (100 CFM) due to the pressure drop through the return air duct and across the air distribution baffles.

The bomb is shown in Plate III resting on aluminum supports approximately two inches above the distribution air baffle.

The optimum control of temperature is achieved by removing only a small amount of heat from the system via the heat sink and by adding a corresponding small amount of heat through a temperature controller. The control heater consisted of approximately 45 feet of nichrome wire (Driver Company "Tophet A" size 40) having a resistance of 20 ohms. This control wire was supported in the main circulating air stream by vertical glass rods (Plate III) which were located concentrically around the bomb. The entire amount of heat to the cryostat was added through these control heaters, no auxiliary heaters being used. The automatic temperature controller for the process will be described presently.

The location of the sensing thermocouple was quite important in the control of temperature. The thermocouple was located in the return air duct, located vertically about midway in the duct. It was found helpful to lag the bare thermocouple lightly with a thin piece of absorbent cotton. With this arrangement the temperature of the cryostat

could be maintained constant to within $\pm$ 0.02°K for a period of four to six hours, sufficiently long to make a corresponding equilibrium reading of pressure and temperature.

All high pressure valves in that portion of the apparatus between the bomb and the DPI cell were 15,000 psi 1/8 inch Ermeto-type valves (High Pressure Equipment Co.). The valves have a freely rotating stem and turn easily under maximum pressure. All tubing, unions, and tees were Autoclave Engineering Company "Tubeline" series.

The Jacketed Bomb

The bomb was fabricated from type 303 stainless steel in the OSU Research Apparatus Development Laboratory. An assembly drawing of the bomb is shown in Figure 2. The bomb assembly is circular in cross section and is formed from three parts--a lower part, an upper part, and the jacket. The upper and lower parts were welded together at A and B, and the welds were machined flush to the cylinder walls. This portion of the bomb was then tested with oil to 15,000 psi. After pressure testing, this inner portion of the bomb was inserted into the pressure jacket and was welded at C and D. These welds were then machined flush to the wall, and the jacket portion of the bomb was pressure tested with oil to 15,000 psi. Seats for Ruska connectors were provided for the tubing connections for both inner bomb volume and jacket volume. The internal dimensions of the completed bomb assembly are such that the outer jacket pressure P_o should be 0.8024 times the inner pressure P_i for the elimination of volume changes due to wall stresses. This relationship is developed in Appendix K.

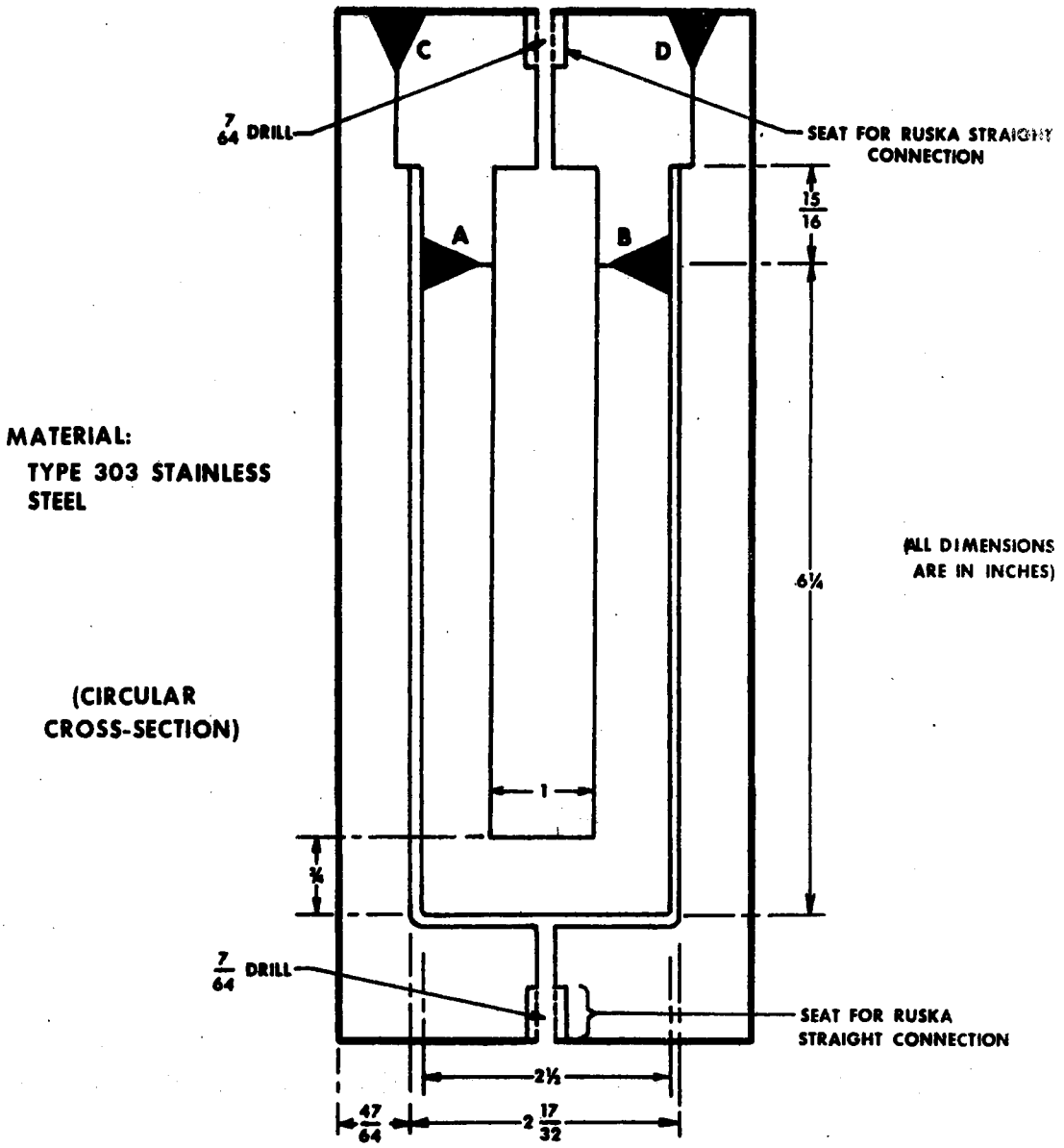

Figure 2

Jacketed Bomb Assembly

The DPI Cell and Thermostat

The DPI cell is of Ruska design (Cat. No. 2413). The cell consists of two pressure chambers separated by a thin stainless steel diaphragm. The diaphragm deflects vertically as a result of any differential pressure, and the deflection positions a core within a differential transformer coil located within the upper pressure chamber. The coil-core relationship causes an electrical output which is a function of the diaphragm displacement. The electrical output is detected and indicated by an electronic null indicator, or readout box (Ruska Cat. No. 2416).

The DPI cell will withstand a maximum overpressure of 15,000 psi. The cell and readout box arrangement can detect a differential pressure of 0.0002 psi.

For purposes of establishing the zero reference point of the DPI cell and readout box, an oil filled open-end manometer was connected into the oil system between the DPI cell and the Ruska piston gage (Figure 1). The manometer was constructed from approximately 30 inches of 7 mm OD soft glass tubing. A short end was sealed with epoxy resin into a standard high-pressure valve. By means of a cathetometer, the exact point on the vertical section of the manometer was located to correspond with the height of the diaphragm inside the DPI cell. This point was marked for future reference.

The zero shift of the DPI cell with operating pressure was determined by Ruska, and a calibration curve was furnished by them. This correction is on the order of two to three parts per million parts.

In order to measure the temperature of the thermostated DPI cell, a calibrated copper-constantan adjustable pipe clamp thermocouple (Conax Cat. No. CL-64-CC) was clampled around the DPI cell near the bottom of the cell in the section where the sample was confined. Several turns of refrigeration-type 1/4 inch OD copper tubing were then clamped around the cell and pipe clamp thermocouple, and provision was made to circulate controlled temperature water through the copper coils.

The entire DPI cell, thermocouple, and copper tubing were placed inside an insulated thermostated box (illustrated schematically in Figure 1). The outer walls of the thermostated box were made of transite; the transite walls were then lined on the inside with sections of one-inch thick styrofoam.

The controlled temperature water to the copper coils was circulated via a constant temperature circulating system (Precision Scientific Company). This unit uses a mercury-in-glass regulating mechanism and is designed to circulate a liquid at a rate of three GPM at a six foot head. Using tap water as a heat sink, this bath would maintain a constancy of circulated water temperature of 0.05°F for several hours, depending on the temperature changes of the surrounding room.

The DPI cell and surrounding thermostat were maintained at a constant temperature for all values of temperature of the bomb; thus, no change in the cell zero point with temperature must be considered. It is convenient to maintain a temperature slightly above ambient conditions; in this case 95°F was used.

With this arrangement the DPI cell temperature was constant to about 0.1°F for a period of four to six hours.

Control of Temperature

The automatic temperature control system consists of six major components: 1) primary element, 2) set point unit, 3) null detector, 4) current adjusting type (C.A.T.) control unit, 5) silicon controlled rectifier (SCR), and 6) control heaters. These are discussed in more detail as follows, with reference to Figure 3.

The primary element (or sensing device) provides an emf output proportional to the value of the controlled variable (in this case, temperature). A copper-constantan thermocouple was used for the primary element here.

The set point unit is basically a potentiometer with an emf output that can be set to a given signal level. The emf output from the set point unit is connected in series opposition with the emf output from the primary element. The emf difference, if any, between the primary element and the set point unit is a measure of the deviation of the controlled temperature from its set point. This emf difference, or error voltage, is then fed into a null detector.

The range of application of the control arrangement is determined by the range of emf output to which the set point unit potentiometer can be set. The subject potentiometer is setable directly to any value within the range -10 to + 45 millivolts. The direct setability of the set point unit is 0.0005 millivolts (mv), which corresponds to about 0.1°K. By interpolation, the unit may be set to within approximately 0.00005 mv, or 0.01°K.

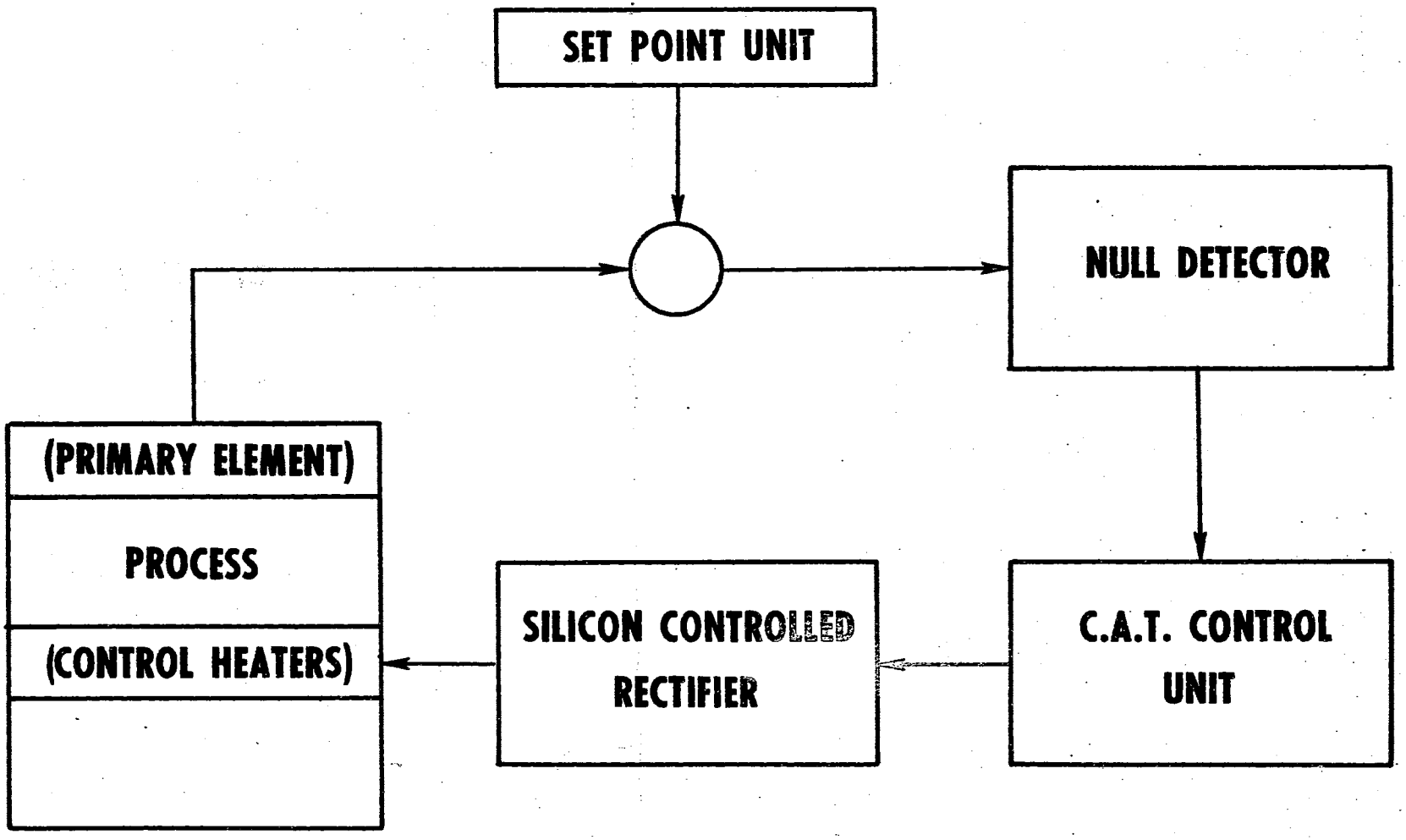

Figure 3

Diagram of Automatic Temperature Control System

The null detector is a high gain, high sensitivity, microvolt amplifier. It detects any error voltage from the set point unit and amplifies it to a level suitable for use as an input to the control unit. The null detector for this system is a Leeds and Northrup electronic DC null detector (Cat. No. 9834-2). This unit contains a variable sensitivity and a readout scale for the error voltage.

The control unit is a Leeds and Northrup series 60 C.A.T. model. This unit has three modes of control action (proportional, reset, and rate controls), and its function is to provide continuous corrective control action based on the size, rate of change, and duration of the error voltage. It does this by providing an output current (0 to 5 milliamps DC) which is proportional to the input heat requirement for the controlled temperature process. This output current goes to the final control device, which is a silicon controlled rectifier unit.

It was necessary to ground electrically this portion of the temperature control system. For this purpose a 1/2 inch diameter solid copper rod was driven 10 feet into the earth, and was connected to an insulated 12-gauge copper lead-in wire. This wire served to ground only the electrical gear in the Thermodynamics Laboratory.

The SCR is a Fincor power package (Model No. 1200-2.2-11A) manufactured exclusively for the Leeds and Northrup Co. This unit produces an AC output voltage that is proportional to the DC current from the C.A.T. control unit. This output voltage supplies current to the process control heaters, and may range from zero to 110 volts. For a particular application, the minimum and maximum values of the SCR output are adjusted by means of potentiometers in the circuit.

For this application, the output voltage varies linearly from zero to a maximum of 40 volts.

Measurement of Temperature

For the determination of temperature of the sample in the bomb, a calibrated copper-constantan thermocouple was fastened to its outside surface. The thermocouple was calibrated over the temperature range -40 to +95°F versus an NBS platinum resistance thermometer.

The temperature of the sample in the DPI cell (nominally 95°F) was determined by the copper-constantan thermocouple fastened to the outside surface of the DPI cell. The thermocouple was calibrated over the temperature range 80 to 115°F versus the NBS thermometer. Illustrations of the potentiometer and thermocouple circuitry are given in Figures 4 and 5.

The potentiometer is a Leeds and Northrup type K-3 universal potentiometer, with a scale range of zero to 1.6110 volts. The scale may be read directly to 0.0005 mv, and may be read by interpolation to within 0.0001 mv. For this application 0.0001 mv is roughly equivalent to 0.002°K. The galvanometer is a standard Leeds and Northrup DC galvanometer with self-contained lamp and scale reading device.

The accuracy of the potentiometer is 0.0005 mv or, 0.01°K. The accuracy of the thermocouple calibrations for the bomb and for the DPI cell is estimated at 0.01 to 0.02°K, or roughly equivalent to the accuracy of the potentiometer. Details on the NBS thermometer and the thermocouple calibrations are given in Appendix A.

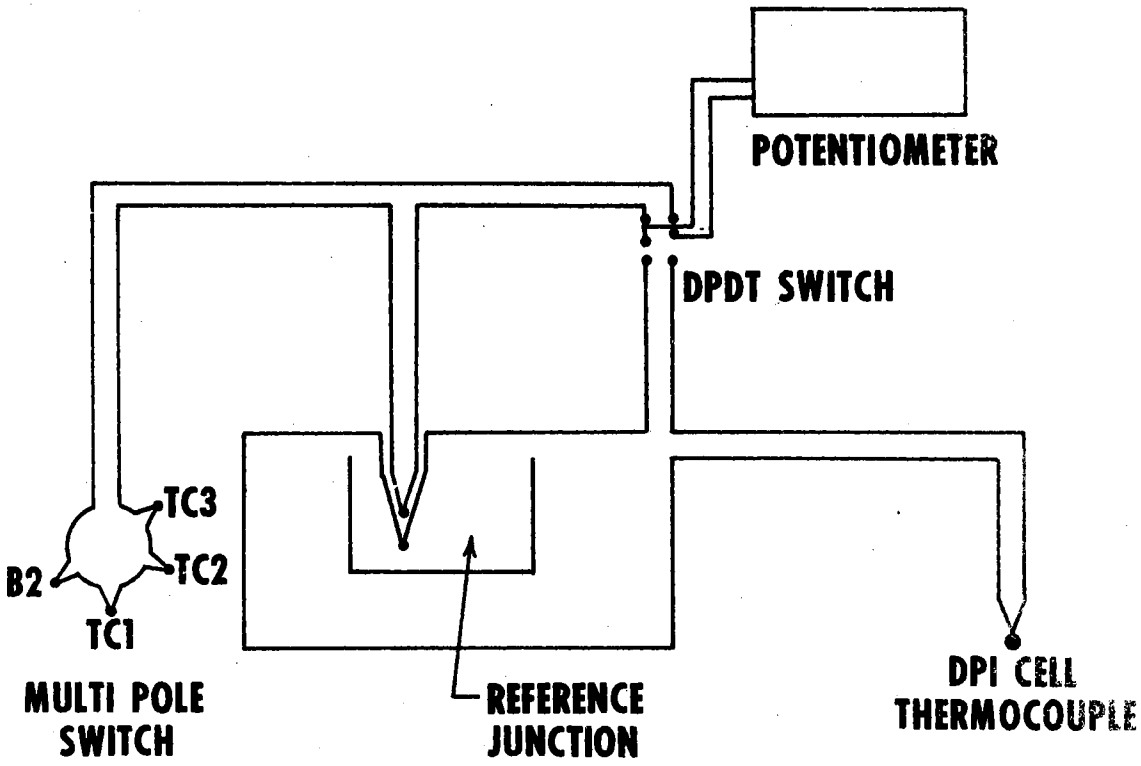

Figure 4

Thermocouple Circuit Diagram

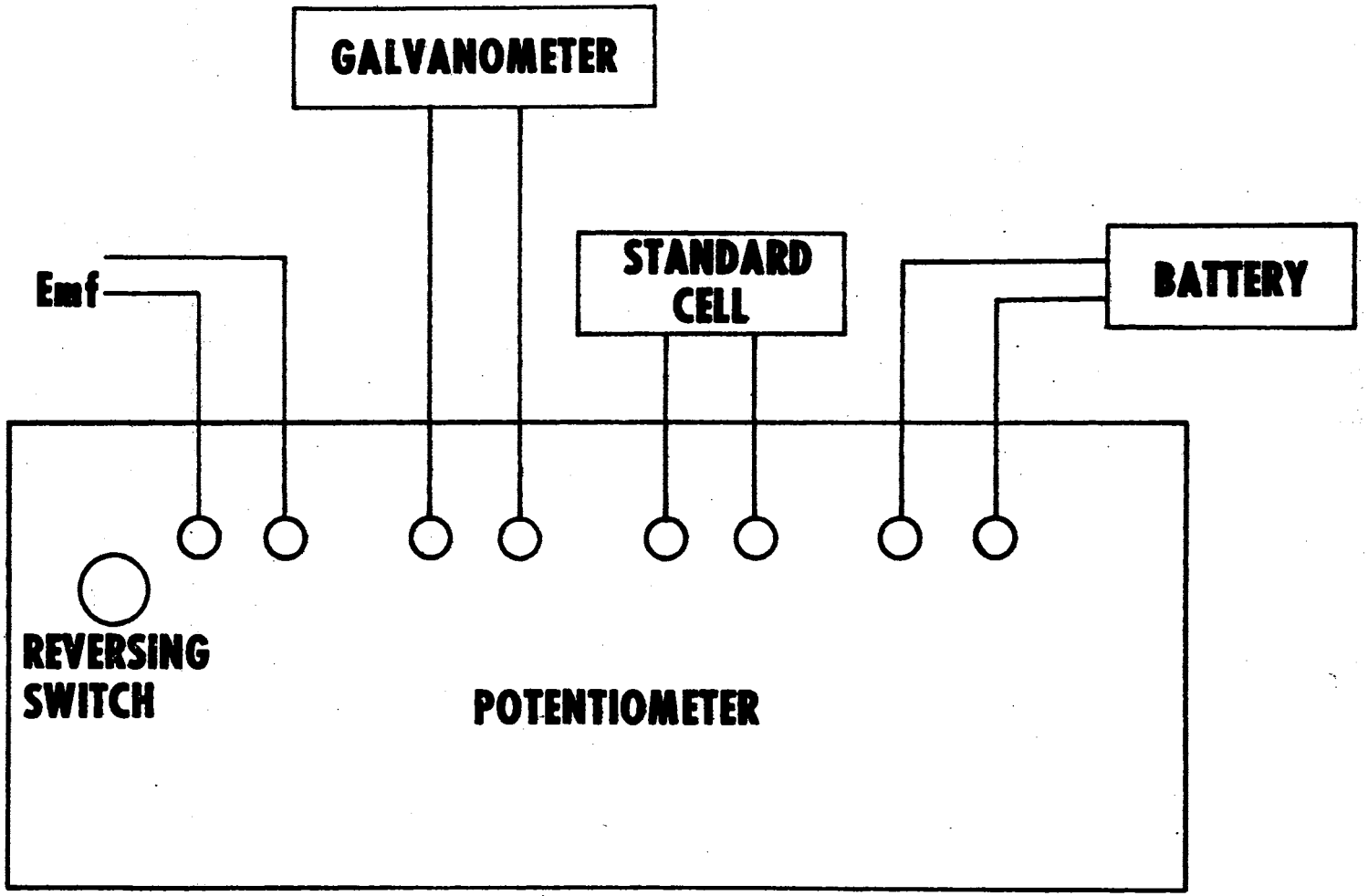

Figure 5

Diagram of K-3 Potentiometer and Galvanometer

It is necessary to make a mass correction for the small amount of the sample contained in the capillary tube, as discussed previously. For this purpose the average temperatures of different sections of the capillary are required. To estimate the average temperatures, three copper-constantan thermocouples (TC1, TC2, and TC3--Figure 4) were fastened at equidistant intervals along the length of the tube. Standard thermocouple charts were used to determine the temperatures from these thermocouples. The ambient temperature of the laboratory was determined from standard mercury-in-glass thermometers, which were certified to be accurate to 0.05°F.

Measurement of Pressure

As stated previously, the gas sample is separated from the high pressure oil system by the DPI cell. The oil pressure is generated with the screw pump and is measured with the Ruska piston gage. The instrument has a stated accuracy of one part in 10,000 parts over the range six - 12,140 psi, with the calibration being directly traceable to NBS. The calibration data and specifications for the gage are presented in Appendix J. A sample calculation of a pressure point is given in Appendix B.

Although the assembled apparatus was satisfactorily tested at pressures up to 12,000 psia, data was taken only to pressures of 2400 psia. In the derivation of virial coefficients by the slope-intercept procedure it is important to have a considerable amount of data in the low pressure region. Points at higher pressures have little effect on the determination of virial coefficients by this procedure.

The oil used in the system is a specially developed oil with a density of 0.85 grams/cc and a viscosity of 160 SSU at 25°C. A head correction of 0.031 psi per vertical inch of oil head is given by Ruska for use in making head corrections.

Standard Ruska 1/8 inch needle valves (Cat No. 2005) were used throughout the Ruska equipment.

A 16,000 psi Acco Helicoid bourdon gage with 200 psi subdivisions was mounted on the screwpump. Two alternate bourdon gages were connected into the gas side of the high pressure system. These bourdon gages were used principally during the charging of the bomb, and were valved off from the system after the charging was completed. These two gages are 1) a 20,000 psi XFO Maxisafe gage with 200 psi subdivisions, and 2) a Crosby AIH 5,000 psi gage with 50 psi subdivisions. For clarity the Crosby AIH 5,000 psi gage is omitted from Figure 1. All three of the above bourdon gages were calibrated versus the Ruska piston gage. The calibrations are given in Appendix D.

Barometric pressure was determined by means of a Texas Instruments servo-nulling pressure gage. The instrument has an accuracy of 0.015%; operating characteristics and calibration of the gage are presented in Appendix C.

Auxiliary Apparatus

The vacuum system consisted of a mechanical pump (Welch Scientific) and a CVC type VMF-10 diffusion pump. The VMF-10 pump has an ultimate rated pressure of 10^{-6} millimeters mercury.

The McLeod gage is a Virtis 5.0 millimeter range unit. The gage was located so as to be able to measure the absolute pressure at any

portion of the apparatus connected to the vacuum system.

A Gaertner cathetometer was used for all vertical measurements. By means of a vernier scale attachment, this instrument could be read directly to 0.005 centimeters. The instrument was used for making all vertical measurements associated with the calibration of the apparatus.

The gas compressor is a 15,000 psi hand operated pump (Autoclave Engineers). This unit was used both for charging the sample into the cell, and also for injecting gas into the jacket itself. The pump is a positive displacement, reciprocating piston type with displacement per stroke of 0.115 cubic inches.

B. Advantages and Disadvantages of the Isochoric Apparatus

The chief advantage of the apparatus is that, given the volumetric properties of the sample along the reference isotherm (77°F), the volumetric properties at lower temperatures may be determined solely from the experimental measurement of pressure and temperature. The temperature may be determined to within 0.02°K, and the pressure may be determined to one part in 10,000 parts.

Due to the insulating effect of the gas-filled pressure jacket surrounding the bomb, the temperature fluctuations in the air bath ($\pm$0.02°K) are largely damped out before affecting the inner sample temperature. By observing the pressure fluctuations inside the cell, it was estimated that the actual temperature fluctuations of the sample were approximately $\pm$ 0.01°K, or roughly one-half the fluctuations in the air bath.

It is of practical interest to measure the volumetric properties of mixtures within the two-phase and the subcooled liquid regions. For many types of PVT apparatus (such as the Burnett apparatus) this is difficult, due to possible non-equilibrium conditions prevailing in the mixture. For the isochoric apparatus, an isochor may be cooled directly into the liquid or two-phase regions, without additional complications.

The use of the air bath, rather than the liquid bath (as used by Michels), introduces the disadvantage of a long period of time required to obtain equilibrium following a change of temperature. This is due to the relatively low overall heat transfer coefficient between the circulating air and the bomb. Also, the insulating effect of the surrounding pressure jacket further complicates this effect. As the data are taken isochorically, rather than isothermally, only one data point is taken between temperature changes.

Each successive isochor is run as nearly as possible at the same levels of temperature as the previous run. With the most careful work, it is yet necessary to make a small temperature correction in combining the volumetric observations to obtain final densities for each isotherm.

Any inaccuracies in the compressibility factors of the reference isotherm will introduce corresponding inaccuracies into the isochoric data. For this reason the accuracy of the isochoric data cannot be greater than the accuracy of the reference isotherm compressibility factors.

C. Characterizing Equations for the Apparatus

All equations that characterize the apparatus are developed in Appendix N. The equations will be briefly summarized in the following.

To determine the isochoric run constant D the cryostat is charged and allowed to reach equilibrium at 77°F, and the temperatures and pressures of all portions of the system are measured. The run constant is then determined from

$$D = [F(T_B - 95) + 0.003868]D_{BT} + 0.01263\ D_D + 0.01537\ D_5 + 0.01511\ D_4 + 0.003794\ (D_3 + D_2) + 0.003273\ D_1 \qquad \text{(N-20)}$$

D_{BT} is the density of the sample in the bomb at 77°F (determined from the compressibility factor from the reference isotherm). The quantities D_D, D_5, D_4, D_3, D_2, and D_1 are densities representing the correction for the amount of sample in the DPI cell and exposed capillary line. The function $F(T_B - 95)$ is the correction for the effect of temperature on the bomb volume.

The quantity D is constant along the isochor. From a knowledge of D, the compressibility factors at other temperatures along the isochor are determined from

$$Z_{BT} = \left(\frac{P}{RT}\right)_{BT} \left[\frac{F(T_B - 95) + 0.003868}{DEN}\right] \qquad \text{(N-21)}$$

where

$$DEN = D - 0.01263\ D_D - 0.01537\ D_5 - 0.01511\ D_4 - 0.003794\ (D_3 + D_2) - 0.003273\ D_1 \quad \text{(N-22)}$$

The densities D_D, D_5, D_4, D_3, D_2, and D_1 involve the unknown compressibility factors Z_D, Z_5, Z_4, Z_3, Z_2, and Z_1 at the temperatures T_D, T_5, T_4, T_3, T_2, and T_1, respectively. These temperatures lie approximately in the range from ambient temperature to 0°F. Since the terms involving these densities are relatively small compared to the other terms, Equations N-20 and N-21 are first solved using the approximation $Z_D = Z_5 = Z_4 = Z_3 = Z_2 = Z_1 =$ unity. From the assumptions a value of D may be calculated at the reference isotherm from Equation N-20; then values of Z_{BT} may be calculated over the experimental temperature range of 77 to 20°F, using Equation N-21. From these calculated values more accurate values of Z_D, Z_5, Z_4, Z_3, Z_2, and Z_1 may be interpolated and used to recalculate values of D and Z_{BT} from Equations N-20 and N-21.

This iterative procedure is continued until no significant change in the calculated value of D and Z_{BT} occurs. Since the terms involving D_D, D_5, D_4, D_3, D_2, and D_1 are small, normally about two iterations are sufficient for this convergence. A sample calculation is given in Appendix F.

D. Some Experimental Difficulties

The Heat Sink Temperature

Initially it was desired to maintain temperatures from ambient down to about the sublimation temperature (-78°C) of dry ice. A mixture of dry ice and liquid iso-octane was used as a heat sink in the space between the outer wall of the copper can and the inner wall of the dewar. This arrangement was found to be unsatisfactory for periods of time in excess of about two hours; as the dry ice began to sublime, considerable temperature gradients formed in the cold liquid, upsetting the temperature control.

The installation of the mechanical refrigeration system with copper evaporator coils helped considerably in elimating these temperature gradients. A thermistor-operated on-off unit was initially placed in the compressor circuit, controlling the temperature of the refrigerant ethylene glycol solution; however, the on-off cycle of the refrigeration unit was observed to upset the temperature control system. The on-off control unit was thus abandoned, and the refrigeration unit was allowed to operate continuously. This arrangement was found to provide the most satisfactory heat sink.

Vibrations in the Blower Shaft

The excessive length (about 20 inches) of shaft between the air blower and motor was found to cause pronounced vibrations in the shaft. To overcome this problem it was necessary to support the shaft at the top with a close-fitting "oil-lite" type bronze bearing, and at the bottom and center by steel roller bearings. Between the center and

upper bearings the shaft was interrupted by a steel flexible universal-joint type coupling.

Temperature Control

Considerable difficulty was encountered in the temperature control of the cryostat due to small voltage fluctuations within the automatic temperature control system. These fluctuations were principally due to two separate factors: 1) the relatively high inherent electrical "noise" in the primary temperature circuit, and 2) the instability of the automatic reference junction compensator. These disturbances are discussed as follows.

The electrical noise in the circuit results in improper corrections being made to the output voltage to the final control device. With reference to Figure 3, the emf output from the set point unit is connected in series opposition with the generated thermocouple emf. The emf difference is continuously monitored, and is used to determine the output control voltage. For the range of temperature encountered in this work the generated thermocouple emf was between -0.2 and +1.2 mv. When compared to this relatively low value of emf, the electrical noise level in the primary circuit was sufficiently high to affect the proper operation of the entire temperature control system. The problem of the inherently high electrical noise level in the system was never eliminated. Temperature control of within $\pm 0.02°K$ could be achieved with this arrangement.

The automatic reference junction compensator between the sensing thermocouple and the set point unit was observed to be sensitive to rapid fluctuations in ambient temperature. A fluctuation in ambient

temperature caused by opening a door into the main laboratory was observable almost immediately on the null detecting device. This problem was largely overcome by insulating the automatic reference junction compensator with fibre glass insulation. Also, the installation of additional air conditioning equipment helped damp out rapid changes in the ambient temperature.

Elimination of High Pressure Leaks

Considerable effort was required to eliminate all leaks in the gas side portion of the system. Separate portions of the system were successively isolated and charged to a high pressure. The pressure was then measured and the system allowed to stand for 24 to 48 hours, whereupon the pressure was remeasured. These tests were quite time consuming, and were further complicated by any day-to-day change in ambient temperature, especially in the portions of the apparatus containing the exposed capillaries. All leaks were eliminated.

CHAPTER V

EXPERIMENTAL PROCEDURE

The preliminary adjustments to the automatic temperature control system are discussed at the first of this chapter, as this phase of the experimental work was quite important.

This is followed by a discussion of the experimental details of the measurement of pressure and temperature. Considerable attention is given to the operation of the Ruska piston gage.

Next, the preparation of the apparatus for taking a data point is discussed, followed by the details of the actual taking of the data point and the lining out of the apparatus for the next data point.

Lastly, the experimental determination of isochoric volumetric properties in the two-phase region is discussed.

A. General Experimental Details

Adjusting Automatic Temperature Control System to the Process

The automatic temperature control system is illustrated schematically in Figure 3. The control unit uses three modes of control action--proportional, reset, and rate modes of control. The combined settings for these modes of control establish the characteristics of the heat input to the cryostat; the proper setting of each particular mode of control action is determined separately.

The proper setting for the proportional mode of control was first determined. For the determination of this setting, the reset and rate modes of control were set to zero. The "proportional band" setting is a measure of the amount that the controlled variable (temperature) must change (from its set point position) in order to produce a full scale change in the output voltage to the control heaters.

In adjusting the proportional band it is desirable to start with a fairly wide setting and then decrease the setting in a stepwise fashion until the optimum value is reached. It is generally desirable to use a relatively narrow proportional band, thus making the temperature control system sensitive to small temperature variations.

At each successively lower setting of the proportional band, small "upsets" were thrown into the process by slightly moving the level of the set point temperature. If the effect of such an upset caused the controlled temperature to "cycle" excessively, the proportional band setting was too narrow. The optimum setting is the lowest value that may be continuously used without introducing a cycling tendency into the process.

For this application a proportional band of about 40% was found to be adequate. There was no observable change in the required proportional band with the level of temperature; thus the 40% setting was used exclusively.

After selecting the proper proportional band, the setting for the rate mode of control action was determined. Here the proportional band was maintained at its 40% position and the reset control action remained at zero. Rate control setting involves the proper determination

of the "rate time," expressed in minutes. The effect of rate control action is to produce a magnitude of change in the output voltage that is proportional to the rate of deviation of the controlled temperature from the set point.

The proper procedure for determining the rate time setting is to increase the rate time setting (in a stepwise fashion) from its zero position. At each setting an upset is manually introduced into the process to detect any tendency to cycle. The rate time should be set as high as possible without inducing cycling. In this case the rate action was observed to introduce some cycling tendency at low rate times of 0.05 to 0.10 minutes. This was indicative that, due to the physical nature of the process, rate action was undesirable. Accordingly the rate time setting was permanently turned back to its zero position.

After selecting the proper settings for proportional band and rate time, the setting for the reset mode of control was determined. In reset control, the rate of change of the control voltage is continuously proportional to the magnitude of the deviation of the controlled temperature from its set point. The "reset rate" is expressed in repeats per minute, i.e., the number of times per minute that the effect of the proportional control is repeated by the control action. Reset action is commonly used for temperature control application, and imparts a stability to the process.

The reset rate should be as high as practical without causing the controlled variable to cycle continuously. A reset rate of from 0.1 to 0.3 repeats per minute was found to be adequate for this

application, after the process had become completely "lined out." During the period of time when the system was rapidly approaching thermal equilibrium (after a set point change), reset rates as high as 1.0 repeat/minute were used with the 40% proportional band setting. In this case the higher reset rate helped significantly in stabilizing the process and in bringing the process to equilibrium more quickly. The reset rate was then gradually decreased to 0.1 to 0.3 repeats per minute, when the system had attained equilibrium.

The variable sensitivity of the null detector (Figure 3) has a maximum setting of ten units. The proper setting is that in which the output control voltage is as steady as possible, considering all upsets encountered by the entire control system. A setting of 7.5 to 8.5 units was found to be optimum. Initially the maximum setting of ten units was used; occasionally, however, this setting was observed to produce an increased fluctuation in the control voltage, resulting in instability of the system.

Adjustment of DPI Cell Temperature

In general, very little attention was required for this portion of the system. Since the insulated lead-in lines from the circulating water bath would absorb a small amount of heat from the surroundings (depending upon the ambient temperature) it was periodically necessary to adjust the set point temperature of the water bath. Regulation of the temperature level was accomplished by simply adjusting a leveling screw in the mercury-in-glass mechanism.

Operation of the Ruska Piston Gage and DPI Cell

Periodically, it was necessary to check the zero position of the DPI cell and readout. The oil-filled reference manometer for this purpose was described in Chapter IV. The procedure is given as follows.

After bleeding the oil system and making certain that no air was present, the gas side of the DPI cell was opened to the atmosphere via the exhaust valve (Figure 1). With the DPI readout set at a low sensitivity value, the oil of the pressure balance system was maintained at about one atmosphere pressure via the screw pump, and the valve to the reference manometer was opened.

The oil was brought to the reference mark of the manometer, and the DPI readout was zeroed at low sensitivity by means of the "zero adjust" knob. The sensitivity was then increased to its normal operating range (about 3/4 maximum sensitivity) and the readout was more finely zeroed. After the zeroing procedure was completed, the isolating valve between the manometer and the high pressure system was closed.

The shift of the DPI cell zero point with operating temperature did not have to be considered, as the DPI cell remained at the same temperature level for all values of the cryostat temperature. As a high overpressure of the DPI cell might tend to shift the zero point, the DPI cell was always overpressured from the same side (the oil side), and the overpressure was held to within 100 psi in most cases.

The zero point was redetermined each time the entire system was opened to the atmosphere; generally this occurred each time a new sample was charged to the system. Any change in the zero point was observed to be negligible.

Initially, in the determination of a pressure, the valves between the screw pump and Ruska piston gage were closed (Figure 1); then the DPI cell was balanced at low sensitivity versus the screw pump. The necessary balancing pressure of the oil was then read as accurately as possible from the calibrated bourdon gage atop the screw pump; and the DPI cell, containing the high pressure oil, was also valved off.

The screw pump was then brought back to atmospheric pressure, and the valve to the piston gage opened. Proper masses were added to the piston gage, and the gage balanced versus the screw pump, until the same oil balancing pressure as above was indicated by the calibrated bourdon gage.

The pressure of the oil of the piston gage was then approximately equal to the oil pressure of the isolated DPI cell; thus the valve separating the piston gage and the DPI cell was opened carefully. The approximate balance was then indicated by the readout box. At this point the masses of the piston gage were set in rotation, with the readout box remaining set at low sensitivity.

By increasing the readout box sensitivity, with the masses in rotation, it could be determined whether mass needed to be added or subtracted from the piston gage. In general the masses of 0.01 pound and below were directly placed on (or taken from) the gage, without stopping the rotation.

For masses larger than 0.01 pound it was necessary to use the following procedure in adjusting the amount of mass. The DPI cell (at approximate balance) was valved off, the rotation of the masses was stopped, and the masses on the gage were lowered with the screw

pump. After the necessary adjustments to the amount of mass were made, the masses were again raised, the valve to the DPI cell was reopened, and approximate balance was again confirmed on the readout box. The masses were then placed in rotation again.

As the DPI cell was balanced at each value of sensitivity setting, the sensitivity was increased and the above balancing procedure repeated.

The DPI cell was assumed to be completely balanced, and the pressure point was taken, whenever the DPI readout was maintained at balance for fifteen minutes at normal operating sensitivity (3/4 maximum) with the masses being in rotation. The pressure was always determined at 3/4 maximum sensitivity, since the DPI zero point was determined at this setting.

The point was taken with the line on the rotating sleeve weight corresponding as nearly as possible with the engraved reference mark on the index post of the piston gage.

The piston gage temperature was then read and recorded to the nearest 0.1°C, and a reading was made of the Texas Instruments barometer and its temperature.

The calculational procedure for the pressure determination, including corrections for the head of oil, gives the absolute pressure, psia, at the level of the diaphragm of the DPI cell. The sample calculation of an experimental pressure point is presented in Appendix B.

Measurement of Temperature

The following temperatures were measured with thermocouples, using the K-3 potentiometer.

1) T_D, the temperature of the DPI cell

2) T_{BT}, the temperature of the bomb

3) T_3, T_2, and T_1, the temperatures along the capillary tube.

A diagram of the thermocouple circuit and potentiometer is given in Figures 4 and 5; the thermocouple calibrations are discussed in Appendix A. The temperatures T_D and T_{BT} were determined both before and after a pressure measurement, and an average value was taken.

The potentiometer standard cell was zeroed before each individual measurement, and normal balancing procedures were followed with the potentiometer.

The temperatures T_4 and T_5 were determined from ordinary mercury-in-glass thermometers.

Volume Ratio Calibration

The significance of the ratio of the volume of the DPI cell to the volume of the bomb has been discussed previously. The experimental details of this determination will be given below.

This determination requires that a gas of known volumetric properties be available. Airco prepurified nitrogen was used in this case; specifications and purities for this gas are presented in Appendix E. Also it was convenient if the ratio was determined with the bomb and DPI cell at the same temperature; the cryostat was thus adjusted to a temperature of 95°F.

The entire gaseous portion of the system, including the gas compressor, was successively evacuated (to 100 microns or less) and rinsed with the nitrogen; finally the interconnecting valve between the bomb and the DPI cell was closed and the gas compressor was filled with the nitrogen.

The DPI cell was then charged to about 2500 psi. After equilibrium was attained the pressure of the gas in the DPI cell was measured with the piston gage, and the small residual gas pressure in the bomb (about 100 microns) was measured with the McLeod gage.[1/] Temperatures of all portions of the system were read and recorded, and the barometric pressure was noted. The interconnecting valve was then opened, allowing the nitrogen to expand into the bomb.

After the system had again reached equilibrium the pressure was determined on the piston gage; from this reading the proper bomb jacket pressure was determined, and gas to this pressure was admitted to the pressure jacket. The calibrated 5,000 psi Crosby bourdon gage was used to determine the jacket pressure.

After the bomb had again attained equilibrium, the system pressure was again determined, and all temperatures were measured. The barometer was again read and recorded.

From the above readings and the known volumetric properties of the nitrogen, the volume ratio V_D/V_B was then determined from Equation N-10. After several such calibrations the average value (V_D/V_B = 0.01263) was determined. A sample calculation is given in Appendix E.

[1/] Caution must be exercised in the use of the glass McLeod gage, especially when one portion of the system is open to the McLeod gage and the other portion of the system is under a pressure. For safety an auxiliary needle valve was placed between the McLeod gage and the system. The valve remains closed unless the gage is being used.

B. Preparing Apparatus for Taking a Data Point

Estimation of Charging Pressures

In the treatment of the experimental data, the isochoric compressibility factors are presented as isotherms. In the theoretical treatment of the data the points along the isotherm should, for convenience, be spaced at approximately equal intervals of density. As the cell is charged for each isochor to a known pressure (as indicated by the bourdon gage), rather than to a known density, the required charging pressure may only be estimated.

In this series of measurements the Redlich-Kwong equation of state was used to estimate the charging pressures required to produce compressibility factors at equally spaced values of density. The compressibility factor Z was first calculated as a function of pressure P along an isotherm. Secondly, the compressibility factor was calculated as a function of the density along the same isotherm. Two plots were then made--one of Z versus P, the second of Z versus density. The calculated compressibilities corresponding to evenly spaced values of density were read from the first plot; then the pressures corresponding to each of these values of compressibility factor were read from the second plot. The pressures so determined were used as the experimental charging pressures for the isochoric determinations.

The same procedure was used for each system studied. For the four intermediate mixtures the conventional mixing rules (Equation III-39) were used. It should be emphasized that any inaccuracies in the RK equation do not affect the accuracy of the experimental measurements. This procedure only represents a simple approximation

for spacing the compressibility factors equally with respect to density.

Charging Procedure

Prior to charging the system for an isochoric measurement, the gas compressor was rinsed, evacuated, and filled with the sample from the gas supply bottles. The entire gaseous portion of the system was then rinsed and evacuated, and the cryostat temperature was adjusted to the reference temperature (77°F). With the interconnecting valve remaining open the DPI cell and bomb were charged to the pre-selected initial pressure. The required pressure for the jacket of the bomb was determined (as described in Appendix K) and was admitted to the jacket. This pressure was measured with the 5000 psi calibrated bourdon gage.

C. Taking a Data Point

After the bomb had been allowed to line out for about ten hours, a data point was taken. The actual taking of the data point requires

1) determination of the temperature of all portions of the system,
2) measurement of the system gage pressure, and
3) measurement of the barometric pressure.

The operation of the pressure and temperature measuring apparatus was discussed above. Details of the operation of the Texas Instruments barometer are given in Appendix C.

The total time required for determination of the pressure with the piston gage was from 30 minutes to one hour. Due to this expiration of time the temperatures were determined both before and after the pressure measurement, and the average value taken.

The data point at the reference temperature was used to compute the run constant, D, for that isochor, using Equation N-20. The measurements at the other temperature levels on that isochor were used in Equation N-21 to compute the compressibility factor at that temperature.

D. Preparing Apparatus for Next Data Point

After completing the taking of a data point, the temperature of the cryostat was changed to the next value as follows.

The sensitivity of the null detector portion of the control system was set to a low value (about three units), and the set point unit was set at the proper value corresponding to the desired temperature. The reset rate of the control unit was increased from its normal operating value of about 0.2 repeats per minute to a higher value of 1.0 repeat per minute. The proportional band setting was unchanged from its normal operating value of 40%. With these settings, the control system exhibited an increased stability during the period that the circulating air temperature was changing rapidly.

As the air temperature began to closely approach the set point temperature (as indicated by the null detector) the null detector sensitivity was increased in a stepwise fashion, allowing time for the system to stabilize after each sensitivity increase. With each

sensitivity increase the reset rate was decreased, also in a stepwise manner, until the normal reset rate setting was again reached.

A considerable time was required for changing temperatures within the bomb itself. After the set point temperature was changed by 20°F the circulating air would restabilize within an hour; the temperature of the sample within the bomb, however, required a much longer period. The most sensitive test of constancy of temperature within the inner portion of the bomb was the pressure change as indicated by the DPI readout. Experimental observations of the DPI readout after a 20°F temperature change indicated that about six to eight hours were required for complete equilibrium to be attained. It was desirable to take the data according to a regular schedule; hence it was decided to take one single data point each 12 hours. This schedule allowed roughly two hours for taking the data point and changing the temperature of the circulating air to the next level; the remaining ten hours were utilized for obtaining equilibrium inside the bomb.

Expansion to the Next Isochor

The above procedure was continued until all temperature levels on the isochor had been covered. The experimental procedure for the first isochor had then been completed. The density for the next isochor was obtained by exhausting slowly a small portion of the sample to the atmosphere, via the exhaust valve.

In this case there are two convenient temperatures at which this expansion may be made.

1) The bomb may be returned to the starting temperature of the reference isotherm (77°F) and the expansion of the sample to the second isochor made at this temperature.

2) Alternately the expansion may be made at the existing lower temperature (20°F); the second isochor is then run in the reverse direction of the first, starting at 20°F and increasing the temperature stepwise to 77°F, thus including the reference isotherm as the last point on the isochor.

Several attempts were made to raise the temperature to 77°F from 20°F before making the expansion. These attempts showed that the apparatus was more difficult to restabilize after this large change in temperature. This was thought to be due to the insulating effect of the gas in the surrounding pressure jacket. Thus, the second, fourth (and all even-numbered) isochors were determined starting from 20°F and increasing the temperature to 77°F. The first, third, fifth (and all odd-numbered) isochors were determined in the normal manner, starting at 77°F and decreasing the temperature to 20°F. The temperature at which the expansion is made has no effect on the data;[2/] the only requirement is that the reference isotherm be included on the isochor.

E. Combining of Data to Isotherms and Isochors

Isotherms

The temperature levels along each isochor were maintained as closely as possible to the even temperature levels 77, 60, 40, and

---

[2/] An exception is made for the case of the two-phase region. See Section F, below.

20°F. After all isochors had been determined for a given sample it was desirable to combine the experimental data points into isotherms. This made necessary the correction of the compressibility factors to the exact even temperature levels. Normally this correction was on the order of 0.1 to 0.2°F.

If an experimental compressibility factor Z_{P,T_x} is determined at pressure P and temperature T_x, the compressibility factor Z_{P,T_o} at pressure P and the exact temperature level T_o is given by

$$Z_{P,T_o} = Z_{P,T_x} + \int_{T_x}^{T_o} \left(\frac{\partial Z}{\partial T}\right)_{P,T_x} dT \qquad (V\text{-}1)$$

As the temperature T_x was very close to the temperature T_o, Equation V-1 is written as

$$Z_{P,T_o} = Z_{P,T_x} + \left(\frac{\partial Z}{\partial T}\right)_{P,T_x} (T_o - T_x) \qquad (V\text{-}2)$$

The term $\left(\frac{\partial Z}{\partial T}\right)_{P,T_x}$ was evaluated graphically from the data. At each pressure large plots of Z versus T were made, and the slope of the line read off at each of the temperatures 77, 60, 40, and 20°F. These slopes $\left(\frac{\partial Z}{\partial T}\right)_{P,T_x}$ were then plotted versus pressure at each of the above four temperatures, and smooth curves drawn through the points. This procedure was quite satisfactory, as the last term of Equation V-2 is small compared to the other two terms in the equation.

Isochors

Due to the effect of the sample in the exposed capillary line, the experimental data does not follow an exact isochor. For use in future equation of state development the isothermal data (from above) was also smoothed to isochors. By using a procedure similar to that above, the compressibility factor Z_{T_o,ρ_x} (at temperature T_o and density ρ_x) was corrected to the compressibility factor $Z_{T_o,\rho}$ (at temperature T_o and the exact value of density ρ for the sample at the reference isotherm) from the equation

$$Z_{T_o,\rho} = Z_{T_o,\rho_x} + \left(\frac{\partial Z}{\partial \rho}\right)_{T_o,\rho_x} (\rho - \rho_x) \qquad \text{(V-3)}$$

As with the corrections to isotherms the last term in the above equation was relatively small; thus the term $\left(\frac{\partial Z}{\partial \rho}\right)_{T_o,\rho_x}$ was satisfactorily evaluated graphically from the data.

F. Special Procedure for the Two-phase Region

As has been discussed in Chapter IV, no theoretical reason exists why the isochoric apparatus may not be used for determining volumetric properties of pure components or of mixtures in the two-phase region.

In general the experimental procedure is the same as for a sample above its critical temperature, except for the temperature of expansion to the next isochor. For a pure compound, after an isochor has been run into the two-phase region, the sample must be heated back to the single-phase region before changing to the next isochor by removal of a portion of sample. This is because there is no change in

the sample pressure with the expansion in the two-phase region; thus there is no way to ascertain from the pressure measurements when the desired density has been reached. For a mixture this expansion must also be made in the single-phase region, to avoid composition changes of the sample.

CHAPTER VI

PRESENTATION AND CALCULATIONAL TREATMENT OF EXPERIMENTAL DATA

In this chapter the experimental compressibility factor data from the isochoric measurements is presented. The data for methane, ethylene, and four intermediate mixtures covers the range 260 to 2400 psia at temperatures of 20, 40, 60, and 77°F. For the pure ethylene, the measurements extend into the two-phase region. The 77°F data represents the reference isotherm from the Burnett apparatus.

The compressibility factors were compared versus the BWR equation (6) and the Edmister generalized form of the BWR equation (20). The second and third Leiden virial coefficients were derived by the slope-intercept method, and were used to calculate interaction second virial coefficients. The experimental second and third virial coefficients were compared versus the BWR equation (both original and generalized forms) and the RK equation (58). Four empirical rules were evaluated for estimating B_{12} from the pure component virial coefficients B_{11} and B_{22}.

A. Presentation of Data

Volumetric Data

The experimental compressibility factor data is shown in Tables IV and V. The reference isotherm (77°F) data from the Burnett apparatus

TABLE IV

METHANE-ETHYLENE COMPRESSIBILITY FACTOR DATA

99.0 per cent methane

	P psia	Z	(Z - 1)V ft^3/lb mole	1/V lb mole/ft^3
77.00°F[1/]	2346.859	0.8230	-0.3575	0.49513
	2106.929	0.8241	-0.3962	0.44392
	1787.913	0.8352	-0.4434	0.37170
	1521.457	0.8523	-0.4765	0.30996
	1233.124	0.8742	-0.5136	0.24492
	920.962	0.9023	-0.5513	0.17722
	643.814	0.9295	-0.5862	0.12027
	294.144	0.9672	-0.6212	0.05281
60.00°F	2198.660	0.8002	-0.4056	0.49270
	1973.511	0.8044	-0.4447	0.43995
	1685.260	0.8183	-0.4921	0.36931
	1440.195	0.8379	-0.5258	0.30819
	1172.875	0.8631	-0.5619	0.24370
	879.878	0.8955	-0.5933	0.17619
	617.179	0.9241	-0.6337	0.11976
	283.240	0.9653	-0.6591	0.05261
40.00°F	2040.432	0.7695	-0.4662	0.49453
	1841.992	0.7763	-0.5056	0.44251
	1575.790	0.7945	-0.5555	0.36986
	1355.413	0.8176	-0.5901	0.30918
	1109.302	0.8465	-0.6282	0.24440
	837.025	0.8832	-0.6609	0.17674
	589.651	0.9156	-0.7027	0.12010
	272.087	0.9616	-0.7282	0.05277
20.00°F	1876.944	0.7337	-0.5358	0.49695
	1698.841	0.7440	-0.5771	0.44359
	1464.603	0.7663	-0.6295	0.37132
	1266.041	0.7934	-0.6665	0.30999
	1043.526	0.8267	-0.7068	0.24522
	792.452	0.8681	-0.7440	0.17735
	560.900	0.9049	-0.7895	0.12041
	260.247	0.9560	-0.8329	0.05289

[1/] Reference isotherm data (31).

TABLE IV (CONTINUED)

78.8 per cent methane

	P psia	Z	(Z - 1)V ft^3/lb mole	1/V lb mole/ft^3
77.00°F[1/]	2316.386	0.7492	-0.4672	0.53684
	2008.996	0.7538	-0.5320	0.46276
	1758.562	0.7678	-0.5839	0.39769
	1498.063	0.7907	-0.6362	0.32897
	1238.213	0.8196	-0.6877	0.26232
	969.847	0.8552	-0.7350	0.19684
	694.161	0.8949	-0.7803	0.13469
	319.019	0.9513	-0.8360	0.05820
60.00°F	2140.096	0.7194	-0.5260	0.53342
	1868.855	0.7282	-0.5906	0.46017
	1643.159	0.7458	-0.6435	0.39508
	1408.976	0.7725	-0.6956	0.32706
	1170.654	0.8047	-0.7487	0.26087
	922.510	0.8440	-0.7958	0.19598
	663.507	0.8873	-0.8405	0.13409
	306.943	0.9486	-0.8855	0.05802
40.00°F	1956.938	0.6804	-0.5958	0.53637
	1717.497	0.6937	-0.6633	0.46170
	1521.246	0.7154	-0.7177	0.39657
	1313.980	0.7464	-0.7724	0.32829
	1099.708	0.7833	-0.8276	0.26181
	872.425	0.8273	-0.8780	0.19665
	631.520	0.8753	-0.9266	0.13455
	294.121	0.9431	-0.9777	0.05816
20.00°F	1761.730	0.6358	-0.6766	0.53826
	1562.079	0.6545	-0.7452	0.46365
	1393.956	0.6805	-0.8028	0.39792
	1214.260	0.7160	-0.8620	0.32945
	1026.410	0.7577	-0.9208	0.26317
	821.081	0.8072	-0.9758	0.19762
	598.192	0.8609	-1.0307	0.13499
	280.963	0.9358	-1.1010	0.05833

[1/] Reference isotherm data (31).

TABLE IV (CONTINUED)

57.2 per cent methane

	P psia	Z	(Z - 1)V ft^3/lb mole	1/V lb mole/ft^3
77.00°F[1/]	2227.785	0.6564	-0.5831	0.58930
	1952.979	0.6602	-0.6616	0.51363
	1712.099	0.6746	-0.7384	0.44067
	1526.559	0.6968	-0.7971	0.38040
	1229.021	0.7471	-0.8854	0.28564
	988.482	0.7949	-0.9499	0.21592
	675.034	0.8609	-1.0217	0.13615
	349.326	0.9292	-1.0855	0.06518
60.00°F	2041.475	0.6186	-0.6445	0.59175
	1804.906	0.6268	-0.7228	0.51635
	1592.594	0.6449	-0.8019	0.44283
	1432.770	0.6698	-0.8609	0.38359
	1160.848	0.7268	-0.9539	0.28639
	941.507	0.7788	-1.0206	0.21679
	647.201	0.8504	-1.0964	0.13647
	337.506	0.9243	-1.1563	0.06548
40.00°F	1817.319	0.5690	-0.7236	0.59563
	1618.876	0.5817	-0.8060	0.51901
	1445.548	0.6057	-0.8859	0.44509
	1309.766	0.6333	-0.9507	0.38568
	1079.373	0.6977	-1.0477	0.28849
	882.112	0.7554	-1.1232	0.21777
	613.304	0.8348	-1.2057	0.13701
	322.507	0.9161	-1.2782	0.06565
20.00°F	1584.507	0.5124	-0.8117	0.60078
	1428.087	0.5305	-0.8978	0.52300
	1293.648	0.5587	-0.9811	0.44978
	1186.067	0.5913	-1.0489	0.38969
	988.770	0.6642	-1.1612	0.28920
	819.825	0.7282	-1.2427	0.21870
	577.547	0.8164	-1.3361	0.13744
	307.065	0.9057	-1.4316	0.06586

[1/] Reference isotherm data (31).

TABLE IV (CONTINUED)

38.4 per cent methane

	P psia	Z	(Z - 1)V ft^3/lb mole	1/V lb mole/ft^3
77.00°F[1/]	2142.716	0.5677	-0.6596	0.65536
	1967.034	0.5608	-0.7211	0.60903
	1515.253	0.5871	-0.9214	0.44813
	1471.531	0.5947	-0.9433	0.42964
	1211.778	0.6557	-1.0730	0.32089
	1013.872	0.7121	-1.1628	0.24739
	738.983	0.7961	-1.2651	0.16118
	412.744	0.8907	-1.3584	0.08046
60.00°F	1911.035	0.5204	-0.7283	0.65843
	1768.497	0.5165	-0.7875	0.61398
	1386.246	0.5523	-0.9947	0.45008
	1353.163	0.5605	-1.0153	0.43291
	1129.740	0.6279	-1.1534	0.32265
	956.435	0.6899	-1.2475	0.24860
	704.301	0.7806	-1.3563	0.16180
	397.772	0.8828	-1.4509	0.08080
40.00°F	1636.795	0.4583	-0.8133	0.66607
	1519.081	0.4584	-0.8764	0.61797
	1230.777	0.5048	-1.0891	0.45471
	1203.197	0.5145	-1.1132	0.43612
	1028.869	0.5902	-1.2605	0.32509
	882.701	0.6589	-1.3654	0.24984
	661.690	0.7589	-1.4829	0.16261
	378.107	0.8706	-1.5974	0.08099
20.00°F	1343.923	0.3895	-0.9108	0.67035
	1266.777	0.3927	-0.9691	0.62664
	1065.097	0.4516	-1.1969	0.45814
	1046.383	0.4624	-1.2229	0.43957
	919.727	0.5472	-1.3868	0.32653
	805.823	0.6226	-1.5011	0.25146
	615.589	0.7330	-1.6366	0.16315
	358.209	0.8558	-1.7738	0.08132

[1/] Reference isotherm data (31).

TABLE IV (CONTINUED)

18.4 per cent methane

	P psia	Z	(Z - 1)V ft^3/lb mole	1/V lb mole/ft^3
77.00°F	2285.548	0.4648	-0.6269	0.85379
	1894.508	0.4363	-0.7477	0.75394
	1537.437	0.4401	-0.9231	0.60656
	1287.002	0.4757	-1.1161	0.46976
	1154.221	0.5210	-1.2453	0.38466
	1072.243	0.5588	-1.3243	0.33317
	765.436	0.7120	-1.5450	0.18630
	454.276	0.8422	-1.6849	0.09366
60.00°F	1931.400	0.4038	-0.6951	0.85773
	1620.145	0.3810	-0.8118	0.76244
	1332.245	0.3916	-0.9973	0.61004
	1139.865	0.4296	-1.1989	0.47573
	1041.131	0.4802	-1.3370	0.38874
	980.449	0.5181	-1.4202	0.33936
	721.265	0.6910	-1.6511	0.18718
	435.270	0.8298	-1.8093	0.09406
40.00°F	1526.336	0.3277	-0.7740	0.86868
	1279.820	0.3098	-0.8960	0.77030
	1082.616	0.3259	-1.0881	0.61955
	953.565	0.3699	-1.3093	0.48195
	900.272	0.4246	-1.4551	0.39546
	855.580	0.4694	-1.5610	0.33992
	665.797	0.6586	-1.8108	0.18852
	410.818	0.8117	-1.9954	0.09439
20.00°F	1108.631	0.2448	-0.8583	0.87992
	936.589	0.2317	-0.9784	0.78530
	827.228	0.2577	-1.1904	0.62358
	771.330	0.3088	-1.4243	0.48532
	742.455	0.3637	-1.6046	0.39654
	715.113	0.4030	-1.7319	0.34469
	604.362	0.6212	-2.0043	0.18902
	385.233	0.7896	-2.2200	0.09478

1/ Reference isotherm data (31)

TABLE IV (CONTINUED)

ethylene

	P psia	Z	(Z - 1)V ft^3/lb mole	1/V lb mole/ft^3
77.00°F[1]	1669.761	0.3714	-0.8052	0.78063
	1259.190	0.3252	-1.0037	0.67232
	1037.278	0.3437	-1.2524	0.52402
	925.779	0.4523	-1.5411	0.35540
	753.259	0.6071	-1.8237	0.21544
	469.314	0.7931	-2.0137	0.10275
60.00°F	1311.832	0.2992	-0.8914	0.78624
	1001.621	0.2630	-1.0792	0.68294
	870.902	0.2932	-1.3270	0.53264
	826.468	0.4103	-1.6326	0.36120
	698.690	0.5746	-1.9510	0.21803
	447.465	0.7776	-2.1554	0.10318
40.00°F	911.012[2]	0.2118	-0.9824	0.80233
	688.266[3]	0.1846	-1.1725	0.69545
	682.022[3]	0.2306	-1.3949	0.55159
	680.794[3]	0.3450	-1.7798	0.36803
	629.469	0.5326	-2.1206	0.22040
	419.560	0.7553	-2.3621	0.10359
20.00°F	524.628[3]	0.1257	-1.0780	0.81109
	524.308[3]	0.1452	-1.2185	0.70155
	527.619[3]	0.1842	-1.4663	0.55632
	528.809[3]	0.2742	-1.9374	0.37462
	519.920[3]	0.4563	-2.4563	0.22135
	389.754	0.7281	-2.6146	0.10399

[1] Reference isotherm data (31).

[2] Single-phase liquid point. The critical temperature and critical pressure of ethylene are 49.82°F and 742.1 psia, respectively (69).

[3] Two-phase point.

TABLE V

METHANE-ETHYLENE DATA, SMOOTHED TO ISOCHORS

		60.00°F		40.00°F		20.00°F	
	$1/V$[1] lb moles/ft^3	P psia	Z	P psia	Z	P psia	Z
99.0 per cent methane							
	0.49513	2208.985	0.8000	2042.749	0.7694	1870.758	0.7340
	0.44392	1989.944	0.8038	1847.183	0.7760	1699.895	0.7439
	0.37170	1694.801	0.8176	1582.344	0.7939	1466.009	0.7662
	0.30996	1447.351	0.8373	1358.408	0.8173	1265.902	0.7934
	0.24492	1178.207	0.8626	1111.457	0.8463	1042.384	0.8268
	0.17722	884.553	0.8950	839.014	0.8829	792.016	0.8682
	0.12027	619.614	0.9238	590.417	0.9155	560.283	0.9050
	0.05281	284.264	0.9652	272.304	0.9616	259.883	0.9560
78.8 per cent methane							
	0.53684	2152.893	0.7191	1958.346	0.6803	1757.811	0.6361
	0.46276	1878.003	0.7277	1720.858	0.6935	1559.793	0.6548
	0.39769	1652.208	0.7449	1524.738	0.7150	1393.693	0.6806
	0.32897	1415.769	0.7717	1316.124	0.7461	1212.981	0.7163
	0.26232	1176.041	0.8039	1101.383	0.7830	1023.942	0.7583
	0.19684	925.724	0.8433	873.004	0.8271	818.300	0.8076
	0.13469	666.190	0.8869	632.101	0.8752	597.093	0.8612
	0.05820	307.824	0.9484	294.323	0.9431	280.385	0.9359

[1] Density values correspond to those of the reference isotherm, Table IV.

TABLE V (CONTINUED)

$1/V$[1] lb moles/ft^3	60.00°F P psia	60.00°F Z	40.00°F P psia	40.00°F Z	20.00°F P psia	20.00°F Z
57.2 per cent methane						
0.58930	2033.643	0.6188	1800.855	0.5699	1561.022	0.5146
0.51363	1802.013	0.6291	1605.142	0.5828	1408.961	0.5329
0.44067	1586.591	0.6456	1435.500	0.6075	1276.873	0.5629
0.38040	1424.539	0.6715	1297.914	0.6363	1169.204	0.5971
0.28564	1158.565	0.7273	1071.550	0.6996	980.579	0.6669
0.21592	938.635	0.7795	876.460	0.7570	812.258	0.7308
0.13615	645.925	0.8507	610.845	0.8367	573.219	0.8179
0.06518	336.090	0.9246	320.395	0.9167	304.215	0.9067
38.4 per cent methane						
0.65536	1901.246	0.5202	1609.844	0.4581	1313.845	0.3895
0.60903	1756.495	0.5169	1502.983	0.4600	1246.474	0.3974
0.44813	1381.779	0.5529	1218.306	0.5070	1050.048	0.4552
0.42964	1345.372	0.5615	1190.613	0.5168	1031.493	0.4664
0.32089	1125.807	0.6291	1020.879	0.5933	911.467	0.5518
0.24739	953.341	0.6910	877.384	0.6614	798.713	0.6272
0.16118	702.291	0.7813	657.458	0.7607	610.400	0.7357
0.08046	396.348	0.8833	375.916	0.8713	355.071	0.8573

[1] Density values correspond to those of the reference isotherm, Table IV.

TABLE V (CONTINUED)

18.4 per cent methane						
		60.00°F		40.00°F		20.00°F
$1/V$[1] lb moles/ft^3	P psia	Z	P psia	Z	P psia	Z
0.85379	1918.387	0.4029	1495.697	0.3267	1054.348	0.2399
0.75394	1601.953	0.3810	1252.454	0.3098	899.219	0.2317
0.60656	1325.336	0.3918	1065.844	0.3277	816.173	0.2614
0.46976	1131.219	0.4318	944.103	0.3748	763.160	0.3156
0.38466	1035.696	0.4828	890.230	0.4316	735.991	0.3717
0.33317	974.354	0.5244	850.923	0.4763	710.361	0.4142
0.18630	719.067	0.6921	660.925	0.6616	599.659	0.6253
0.09366	433.792	0.8305	408.409	0.8132	381.889	0.7921
ethylene						
0.78063	1291.232	0.2966	863.970	0.2064	524.002	0.1309
0.67232	986.097	0.2630	680.505	0.1846	519.815	0.1502
0.52402	867.068	0.2967	681.964	0.2427	526.539	0.1952
0.35540	823.326	0.4154	675.580	0.3545	527.808	0.2896
0.21544	694.692	0.5782	625.328	0.5413	516.348	0.4656
0.10275	446.096	0.7785	417.247	0.7573	386.900	0.7315

[1] Density values correspond to those of the reference isotherm, Table IV.

is shown in Table IV. Table IV represents the data before smoothing to exact isochors; in Table V the data (at 60, 40, and 20°F) has been smoothed to the densities of the reference isotherm. The data was smoothed to isochors, as isochoric data is frequently used in equation of state development. All calculations reported herein, however, were based on the data of Table IV.

An error analysis of the data is given in Section C below, and a sample calculation of a compressibility factor is presented in Appendix F.

Second Virial Coefficients

Leiden second virial coefficients were determined from the data using the slope-intercept technique, described previously.

Initially, values of B(T) were determined at each temperature as intercepts on a plot of $(Z - 1)V$ versus $1/V$ (Equation III-4). These initial values of B(T) were improved somewhat in the determination of third virial coefficients. This is explained as follows. According to Equation III-5 plots of $[(Z - 1)V - B(T)]V$ versus $1/V$ were constructed, the intercept being the third virial coefficient. At each temperature several values of B(T) were assumed, using the initial value of B(T) as a starting value. The adjustments to B(T) were made in stepwise fashion, with increments of 0.001 ft^3/lb mole (approximately 0.06 cm^3/gm mole). It was found that a small adjustment in B(T) resulted in a considerable change in the function $[(Z - 1)V - B(T)]V$. This procedure was continued until the value of B(T) was determined that would produce the most linearity of the function $[(Z - 1)V - B(T)]V$ at low densities. The maximum revision in B(T) from the initial value

was ± 0.5 cm^3/gm mole. This revision corresponds to approximately ± 0.3 to $\pm 1.2\%$, depending on temperature and composition.

The second virial coefficients were determined in units of ft^3/lb mole, and were then converted to units of cm^3/gm mole for analysis.

The virial coefficients representing the 99.0% methane are compared below (Table VI) with the published values of Douslin (16) for methane. Douslin's data is given in 25°C intervals, the lowest temperature being 0°C. The only direct comparison is at 77°F. Values for comparison at the other temperatures were determined by carefully plotting Douslin's data on large (22 inch × 34 inch) sheets, and interpolating the values. Errors introduced by this procedure are estimated to be less that 0.1 cm^3/gm mole. The estimated accuracy of Douslin's data is 0.1 to 0.7 cm^3/gm mole.

TABLE VI

COMPARISON OF METHANE VIRIAL COEFFICIENTS

$-B(T)$, cm^3/gm mole

T, °F	Douslin (16)	This Investigation
77	42.82	41.14
60	46.50	44.64
40	51.24	49.32
32	53.35	--
20	56.65	54.94
per cent methane	99.994	99.0

From the composition analysis (Appendix G) the chief impurity in the methane sample is seen to be nitrogen (0.6%) with lesser amounts of the impurities carbon dioxide, ethane, and propane.

In principle the effect of impurities is described by Equation III-10, given as

$$B_m(T) = \sum_i^N \sum_j^N B_{ij}(T) x_i x_j \qquad \text{(III-10)}$$

For the 99.0% methane sample only the coefficients involving interactions with methane (methane-nitrogen, methane-carbon dioxide, methane-ethane, and methane-propane) need be considered, the sum of all other terms being less than the total correction by at least two orders of magnitude.

All of the above coefficients were available from the literature with the exception of the methane-nitrogen coefficients. These coefficients were evaluated by the method of Prausnitz (56, 57) discussed previously. A sample calculation is given in Appendix M.

Using Equation III-10 and the above interaction coefficients the composition corrections to the 99.0% methane coefficients (Table VI) were evaluated. The calculation produced a negligible correction to the coefficient at each temperature level. As an example, the total correction at 77°F was +0.13 cm^3/gm mole. In this case the correction is of the incorrect sign; to explain the difference between the experimental value and Douslin's value (at 77°F), a total correction of -1.68 cm^3gm mole would be required. It was generally concluded that the difference between experimental (99.0%) coefficients and Douslin's coefficients cannot be explained by Equation III-10.

From the above comparisons the experimental coefficients are consistently higher (algebraically) than Douslin's values by an average of approximately 1.8 cm^3/gm mole. Considering the accuracy of Douslin's values, the experimental coefficients are estimated to be accurate to approximately 1.5 cm^3/gm mole.

For the calculational analysis of the virial coefficient data (Section B) the pure component virial coefficients B_{11} (methane) and B_{22} (ethylene) are combined empirically to obtain estimates of the methane-ethylene interaction coefficient B_{12}. In order to make reliable tests of these empirical rules it was desired to avoid introducing any uncertainty due to differences in the pure component coefficients. Accordingly, the virial coefficient data of Douslin was used to represent the pure methane, both for second and third virial coefficients.

The ethylene virial coefficients were also determined by the slope-intercept method. The critical temperature of ethylene is 49.82°F (69); thus it was seen (Table IV) that a considerable portion of the low temperature ethylene data (at 20 and 40°F) consists of points in the two-phase region. At these sub-critical temperatures the slope-intercept procedure proved unsatisfactory, and the virial coefficients could not be determined. A plot of the function (Z - 1)V versus 1/V exhibits pronounced curvature through the two-phase region, making extrapolation to the origin impossible.

As the 77 and 60°F isotherms lie close to the critical isotherm, these points also exhibit a certain degree of curvature. This is to be expected. It was possible, however, to determine the virial

coefficients at these temperatures by the slope-intercept method.

The values at 77 and 60°F are shown in Table VII, compared with the results of Michels (39). As with Douslin's methane data the only exact comparison between these two sets of data is at 77°F. Michels' value at 60°F was determined graphically, by interpolation of the data. The error introduced by this procedure is less than 0.1 cm^3/gm mole. As was the case with the methane data the values from this investigation are higher (algebraically) than the literature values. From these comparisons the ethylene coefficients are estimated to be accurate to approximately 1.4 cm^3/gm mole.

TABLE VII

COMPARISON OF ETHYLENE VIRIAL COEFFICIENTS

-B(T), cm^3/gm mole

T, °F	Michels (39)	This Investigation
77	140.33	139.0
60	149.95	148.4

As stated above, the virial coefficients at 40 and 20°F could not be satisfactorily determined from the isochoric data. For this reason the results of Michels were used at these temperatures. For the calculational analysis of the data (Section B) it was decided to also use the values of Michels at 77 and 60°F, in order to preserve all possible internal consistency of the data.

The second virial coefficients for the four intermediate mixtures were determined by the slope-intercept procedure. The impurities in the intermediate mixtures are all hydrocarbons that are similar in characteristics to the methane and ethylene. The largest impurity is the 0.4% propane that is present in the 78.8% methane/20.7% ethylene mixture. The correction for the impurities was made using Equation III-10. For this correction the required interaction coefficients are available in the literature, with the exception of the ethylene-ethane and ethylene-propane coefficients. These coefficients were estimated from the method of Prausnitz; the total correction ranges from +0.69 to +1.70 cm^3/gm mole. The resultant coefficients are shown in Tables VIII and IX, both before and after making the composition corrections.

The second virial coefficients from Table IX (corrected for impurities) are illustrated graphically in Figures 6 and 7. In Figure 6 the virial coefficients are plotted versus temperature at constant composition; in Figure 7 the coefficients are plotted versus composition at constant temperature.

Third Virial Coefficients

Leiden type third virial coefficients were determined, using the slope-intercept technique (Equation III-5). The derivation of third virial coefficients is similar to that of second virial coefficients in that the initial estimate of the third coefficient is further improved via deriving fourth virial coefficients, and adjusting thirds to obtain reasonable fourths. In each case slightly different values of C(T) (in steps of ± 0.005 ft^6/lb $mole^2$, or approximately

TABLE VIII

METHANE-ETHYLENE SECOND VIRIAL COEFFICIENTS, UNCORRECTED FOR COMPOSITION

per cent methane	100.0[1]	78.8[2]	57.2[2]	38.4[2]	18.4[2]	0.0[3]
	$-B_m$, cm^3/gm mole					
T, °F						
77	42.82	54.81	71.36	90.71	114.06	140.33
60	46.50	58.87	76.47	97.20	121.61	149.95
40	51.24	64.61	84.03	106.38	133.22	162.58
20	56.65	71.54	93.08	117.43	145.52	175.95

[1] Douslin (16).

[2] This investigation.

[3] Michels (39), ethylene.

TABLE IX

METHANE-ETHYLENE SECOND VIRIAL COEFFICIENTS, CORRECTED FOR COMPOSITION

per cent methane	100.0[1]	79.2[2]	57.4[2]	38.5[2]	18.4[2]	0.0[3]
	$-B_m$, cm^3/gm mole					
T, °F						
77	42.82	53.44	70.17	90.02	114.06	140.33
60	46.50	57.41	75.19	96.45	121.61	149.95
40	51.24	63.03	82.65	105.57	133.22	162.58
20	56.65	69.84	91.58	116.56	145.52	175.95

[1] Douslin (16).

[2] This investigation.

[3] Michels (39), ethylene.

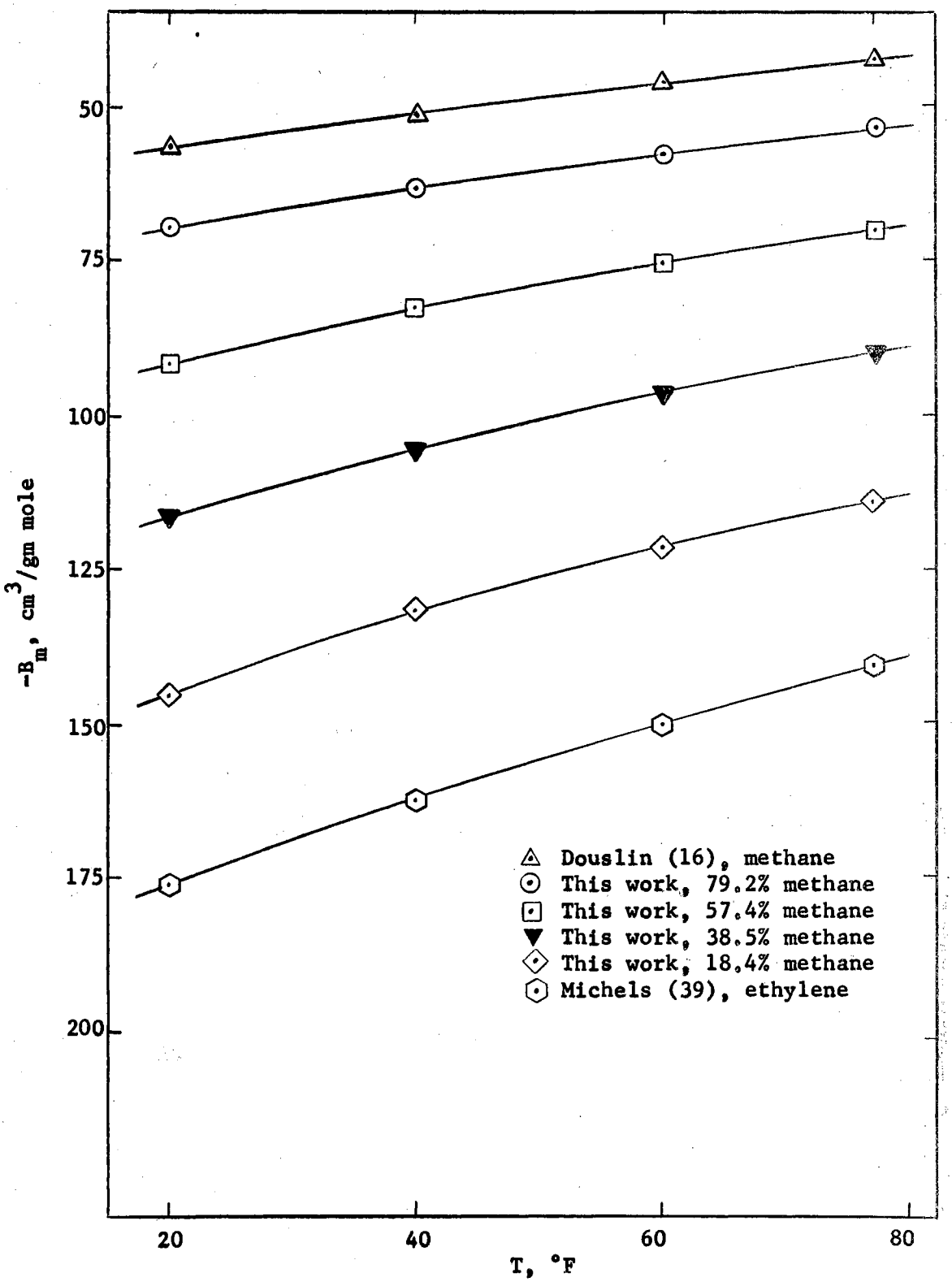

Figure 6

Experimental Second Virial Coefficients Versus Temperature

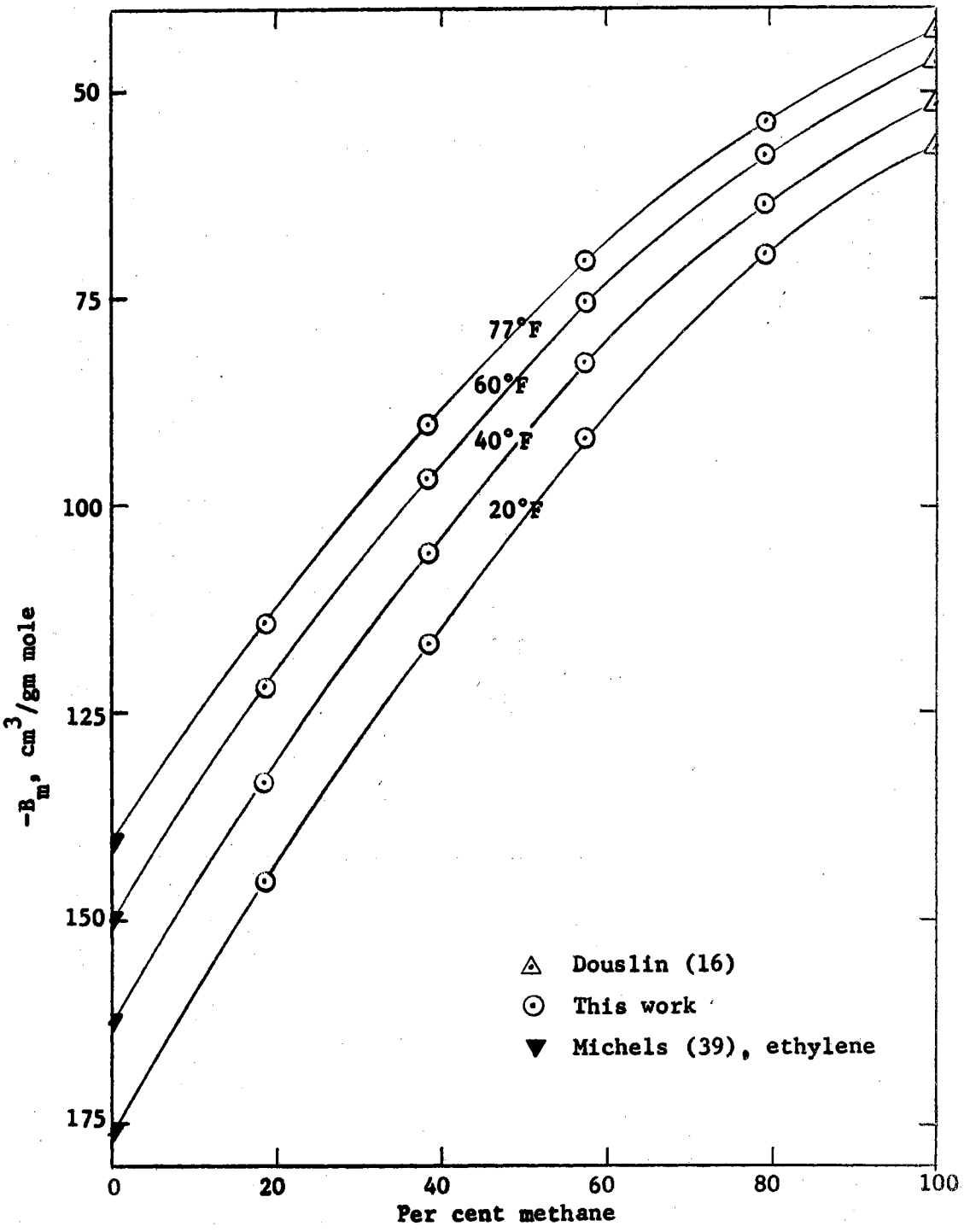

Figure 7

Experimental Second Virial Coefficients Versus Composition

0.2×10^2 $cm^6/gm\ mole^2$) were assumed at each temperature, using the original value as an initial estimate.

Due to considerable scatter of the values of the term $[(Z - 1)V^2 - B(T)V - C(T)]V$ in the plot versus 1/V it was difficult to determine reliable values of the fourth virial coefficients. By proper choice of the third virial coefficient, the values of the function $[(Z - 1)V^2 - B(T)V - C(T)]V$ were determined which exhibited the most systematic variation with both temperature and composition. Although this method was valuable in improving the third virial coefficients, the resulting fourth virial coefficients exhibited considerable scatter. Thus the fourth virial coefficients are not reported.

The maximum adjustment to the third virial coefficients by this procedure was 2.0×10^2 $cm^6/gm\ mole^2$. This value corresponds to roughly 2.0 to 8.0%, depending on temperature and composition. The absolute accuracies of the third virial coefficients are difficult to evaluate, as these coefficients are quite sensitive to errors in both compressibility factor data and second virial coefficients.

In principle, correction for impurities in the third virial coefficients can be made by use of Equation III-11. This correction was not made in this case, as a sufficiently reliable means is not available for estimating the interaction third virial coefficients.

Values of the third virial coefficient are presented in Table X. The values were determined in units of $ft^6/lb\ mole^2$, and were then converted to $cm^6/gm\ mole^2$ for analysis.

TABLE X

METHANE-ETHYLENE THIRD VIRIAL COEFFICIENTS

per cent methane	100.0[1]	78.8[2]	57.2[2]	38.4[2]	18.4[2]	0.0[3]
	C_m, $cm^6/gm\ mole^2 \times 10^{-2}$					
T, °F						
77	23.70	28.2	34.7	45.5	60.0	76.43
60	24.60	29.2	36.6	48.5	62.8	80.5
40	25.60	30.9	40.0	53.3	68.3	85.9
20	26.85	33.6	44.5	59.0	74.6	91.7

[1] Douslin (16).

[2] This investigation.

[3] Michels (39), ethylene.

B. Theoretical and Calculational Analysis of Data

In this section the data is treated from four separate viewpoints. These are:

1) the theoretical determination of B_{12} from Equation III-12,

2) empirical methods of estimating B_{12},

3) comparisons of compressibility factors versus equations of state, and 4) comparisons of virial coefficients with equations of state. The viewpoints are discussed in this order.

Theoretical Determination of B_{12}

As discussed in Chapter III the virial coefficients for a mixture are expressed in terms of the pure component coefficients and interaction coefficients by Equation III-12. As mixture coefficients and pure component coefficients are known, the interaction coefficients may be calculated directly.

For these calculations the virial coefficient data of Table IX was used. Equation III-12 was rearranged to the form

$$B_{12} = \frac{B_m - x_1^2 B_{11} - x_2^2 B_{22}}{2x_1 x_2} \qquad \text{(VI-1)}$$

and values of B_{12} were calculated at each temperature for each composition. The results are given in Table XI.

Theoretically B_{12} is a function of temperature only. In Table XI the B_{12} are seen to vary slightly with composition. This variation is

TABLE XI

METHANE-ETHYLENE INTERACTION SECOND VIRIAL COEFFICIENTS

units cm^3/gm mole

	x_1, mole fraction methane	x_2, mole fraction ethylene	B_m (experimental)	B_{12} [1]	B_{12} [2] (lms)	B_m [3] (calculated)	B_m difference (calc - exp)
77°F	1.000	0.000	-42.82	--	--	--	--
	0.792	0.208	-53.44	-62.25	-63.38	-53.81	-0.37
	0.574	0.426	-70.17	-62.25		-70.57	-0.40
	0.385	0.615	-90.02	-64.61		-89.43	0.59
	0.184	0.816	-114.06	-63.84		-113.92	0.14
	0.000	1.000	-140.33	--	--	--	--
60°F	1.000	0.000	-46.50	--	--	--	--
	0.792	0.208	-57.41	-66.03	-67.59	-57.92	-0.51
	0.574	0.426	-75.19	-66.78		-75.59	-0.40
	0.385	0.615	-96.45	-69.35		-95.62	0.83
	0.184	0.816	-121.61	-67.24		-121.72	-0.11
	0.000	1.000	-149.95	--	--	--	--

[1] Calculations based on Equation VI-1 and data of Table IX.

[2] Least mean squares value.

[3] From Equation III-12, using B_{12}(lms).

TABLE XI (CONTINUED)

units cm^3/gm mole

	x_1, mole fraction methane	x_2, mole fraction ethylene	B_m (experimental)	B_{12}	B_{12} (lms)	B_m (calculated)	B_m difference (calc - exp)
40°F	1.000	0.000	-51.24	--	--	--	--
	0.792	0.208	-63.03	-72.40	-75.28	-63.98	-0.95
	0.574	0.426	-82.65	-74.15		-83.20	-0.55
	0.385	0.615	-105.57	-77.04		-104.73	0.84
	0.184	0.816	-133.22	-77.36		-132.60	0.62
	0.000	1.000	-162.58	--	--	--	--
20°F	1.000	0.000	-56.65	--	--	--	--
	0.792	0.208	-69.84	-81.02	-85.31	-71.25	-1.41
	0.574	0.426	-91.58	-83.81		-92.32	-0.74
	0.385	0.615	-116.56	-87.88		-115.35	1.21
	0.184	0.816	-145.52	-88.06		-144.69	0.83
	0.000	1.000	-175.95	--	--	--	--

standard deviation =

0.74 cm^3/gm mole

not unexpected, however, and is relatively small for interaction coefficients determined in this manner.

Values of B_{12} were also calculated from Equation III-12, using the method of least squares. The resulting values are also shown in Table XI. Using these least squares values of B_{12}, values of B_m were recalculated from Equation III-12. The values so calculated are seen to agree reasonably well with the experimental values of B_m, for all temperatures and compositions. The agreement between the experimental data and Equation III-12 is indicative of a fairly high degree of internal consistency in the data.

Empirical Estimations of B_{12}

Several methods were evaluated for estimating B_{12} from the pure component B_{11} and B_{22}. The different empirical methods were discussed in Chapter III; they will be briefly summarized below.

linear: $$B_{12} = \frac{1}{2}(B_{11} + B_{22}) \qquad \text{(III-19)}$$

square root: $$B_{12} = \sqrt{B_{11}B_{22}} \qquad \text{(III-21)}$$

Lorentz: $$B_{12} = \left[(B_{11})^{1/3} + (B_{22})^{1/3}\right]^3/8 \qquad \text{(III-23)}$$

linear square root: $$B_{12} = \left[(B_{11})^{1/2} + (B_{22})^{1/2}\right]^2/4 \qquad \text{(III-24)}$$

The results of the empirical estimations are shown in Tables XII through XV. The B_{12} values so estimated were used in Equation III-12 to recalculate values of B_m. These B_m values were then compared versus the experimental values of B_m. Using this procedure the best fit to the experimental values was provided by the square root combining rule; this rule gave a standard deviation of 6.2 cm^3/gm mole. In order of

TABLE XII

LINEAR COMBINING RULE ESTIMATION OF B_{12}

units cm^3/gm mole

	x_1, mole fraction methane	x_2, mole fraction ethylene	B_m [1/] (experimental)	B_{12} [2/] (linear)	B_m [3/] (calculated)	B_m difference (calc - exp)
77°F	1.000	0.000	-42.82	--	--	--
	0.792	0.208	-53.44	-91.57	-63.10	-9.66
	0.574	0.426	-70.17		-84.36	-14.19
	0.385	0.615	-90.02		-102.79	-12.77
	0.184	0.816	-114.06		-122.39	-8.33
	0.000	1.000	-140.33	--	--	--
60°F	1.000	0.000	-46.50	--	--	--
	0.792	0.208	-57.41	-98.23	-68.02	-10.61
	0.574	0.406	-75.19		-90.57	-15.38
	0.385	0.615	-96.45		-110.12	-13.67
	0.184	0.816	-121.61		-130.92	-9.31
	0.000	1.000	-149.95	--	--	--

1/ Table IX.

2/ Equation III-19.

3/ Equation III-12.

TABLE XII (CONTINUED)

40°F	1.000	0.000	-51.24	--	--	--
	0.792	0.208	-63.03	-106.91	-74.40	-11.37
	0.574	0.426	-82.65		-98.67	-16.02
	0.385	0.615	-105.57		-119.71	-14.14
	0.184	0.816	-133.22		-142.09	-8.87
	0.000	1.000	-162.58	--	--	--
20°F	1.000	0.000	-56.65	--	--	--
	0.792	0.208	-69.84	-116.30	-81.46	-11.37
	0.574	0.426	-91.58		-107.47	-15.89
	0.385	0.615	-116.56		-130.02	-13.46
	0.184	0.816	-145.52		-154.00	-8.48
	0.000	1.000	-175.95	--	--	--

standard deviation =

12.4 cm^3/gm mole

TABLE XIII

SQUARE ROOT COMBINING RULE ESTIMATION OF B_{12}

units cm^3/gm mole

	x_1, mole fraction methane	x_2, mole fraction ethylene	B_m [1] (experimental)	B_{12} [2] (square root)	B_m [3] (calculated)	B_m difference (calc - exp)
77°F	1.000	0.000	-42.82	--	--	--
	0.792	0.208	-53.44	-77.52	-58.47	-5.03
	0.574	0.426	-70.17		-77.48	-7.31
	0.385	0.615	-90.02		-96.13	-6.11
	0.184	0.816	-114.06		-118.17	-4.11
	0.000	1.000	-140.33	--	--	--
60°F	1.000	0.000	-46.50	--	--	--
	0.792	0.208	-57.41	-83.50	-63.17	-5.76
	0.574	0.426	-75.19		-83.37	-8.18
	0.385	0.615	-96.45		-103.15	-6.70
	0.184	0.816	-121.61		-126.49	-4.88
	0.000	1.000	-149.95	--	--	--

[1] Table IX.

[2] Equation III-21.

[3] Equation III-12.

TABLE XIII (CONTINUED)

40°F	1.000	0.000	-51.24	--	--	--
	0.792	0.208	-63.03	-91.27	-69.25	-6.22
	0.574	0.426	-82.65		-91.02	-8.37
	0.385	0.615	-116.56		-112.31	-6.74
	0.184	0.816	-133.22		-137.40	-4.18
	0.000	1.000	-162.58	--	--	--
20°F	1.000	0.000	-56.56	--	--	--
	0.792	0.208	-69.84	-99.84	-76.04	-6.20
	0.574	0.426	-91.58		-99.42	-7.84
	0.385	0.615	-116.56		-122.22	-5.66
	0.184	0.816	-145.52		-149.06	-3.54
	0.000	1.000	-175.95	--	--	--

standard deviation =

6.2 cm^3/gm mole

TABLE XIV

LORENTZ COMBINING RULE ESTIMATION OF B_{12}

units cm^3/gm mole

	x_1, mole fraction methane	x_2, mole fraction ethylene	B_m [1] (experimental)	B_{12} [2] (Lorentz)	B_m [3] (calculated)	B_m difference (calc - exp)
77°F	1.000	0.000	-42.82	--	--	--
	0.792	0.208	-53.44	-82.17	-60.00	-6.56
	0.574	0.426	-70.17		-79.76	-9.59
	0.385	0.615	-90.02		-98.34	-8.32
	0.184	0.816	-114.06		-119.56	-5.50
	0.000	1.000	-140.33	--	--	--
60°F	1.000	0.000	-46.50	--	--	--
	0.792	0.208	-57.41	-88.38	-64.77	-7.36
	0.574	0.426	-75.19		-85.75	-10.56
	0.385	0.615	-96.45		-105.46	-9.01
	0.184	0.816	-121.61		-127.96	-6.35
	0.000	1.000	-149.95	--	--	--

[1] Table IX.

[2] Equation III-23.

[3] Equation III-12.

TABLE XIV (CONTINUED)

40°F	1.000	0.000	-51.24	--	--	--
	0.792	0.208	-63.03	-96.45	-70.95	-7.92
	0.574	0.426	-82.65		-93.56	-11.00
	0.385	0.615	-105.57		-114.76	-9.19
	0.184	0.816	-133.22		-138.95	-5.73
	0.000	1.000	-162.58	--	--	--
20°F	1.000	0.000	-56.65	--	--	--
	0.792	0.208	-69.84	-105.29	-77.84	-8.00
	0.574	0.426	-91.58		-102.09	-10.51
	0.385	0.615	-116.56		-124.81	-8.25
	0.184	0.816	-145.52		-150.69	-5.17
	0.000	1.000	-175.95	--	--	--

standard deviation =

8.3 cm^3/gm mole

TABLE XV

LINEAR SQUARE ROOT ESTIMATION OF B_{12}

units cm^3/gm mole

	x_1, mole fraction methane	x_2, mole fraction ethylene	B_m [1/] (experimental)	B_{12} [2/] (Linear square root)	B_m [3/] (calculated)	B_m difference (calc - exp)
77°F	1.000	0.000	-42.82	--	--	--
	0.792	0.208	-53.44	-84.55	-60.79	-7.35
	0.574	0.426	-70.17		-80.92	-10.75
	0.385	0.615	-90.02		-99.46	-9.44
	0.184	0.816	-114.06		-120.28	-6.22
	0.000	1.000	-140.33	--	--	--
60°F	1.000	0.000	-46.50	--	--	--
	0.792	0.208	-57.41	-90.86	-65.59	-8.18
	0.574	0.426	-75.19		-86.97	-11.78
	0.385	0.615	-96.45		-106.64	-10.19
	0.184	0.816	-121.61		-128.70	-6.22
	0.000	1.000	-149.95	--	--	--

1/ Table IX.

2/ Equation III-24.

3/ Equation III-12.

TABLE XV (CONTINUED)

40°F	1.000	0.000	-51.24	--	--	--
	0.792	0.208	-63.03	-99.09	-71.82	-8.79
	0.574	0.426	-82.65		-94.85	-12.20
	0.385	0.615	-105.57		-116.01	-10.44
	0.184	0.816	-133.22		-139.75	-6.53
	0.000	1.000	-162.58	--	--	--
20°F	1.000	0.000	-56.65	--	--	--
	0.792	0.208	-69.84	-108.07	-78.75	-8.91
	0.574	0.426	-91.58		-103.45	-11.87
	0.385	0.615	-116.56		-126.12	-9.56
	0.184	0.816	-145.52		-151.53	-6.01
	0.000	1.000	-175.95	--	--	--

standard deviation =

9.3 cm^3/gm mole

increasing standard deviations the remaining three methods are arranged as Lorentz (8.3 cm^3/gm mole), linear square root (9.3 cm^3/gm mole), and linear (12.4 cm^3/gm mole). The poor fit given by the linear method is not surprising, as this method represents an oversimplification.

Comparisons of Compressibility Factors Versus Equations of State

The experimental compressibility factors (Table IV) were compared versus the BWR equation and the Edmister generalized BWR equation. The results are shown in Table XVI.

For the BWR equation the constants, in English units, as tabulated by Benedict et al (5) were used for the hydrocarbons. For the 99.0% methane sample the constants for carbon dioxide as tabulated by Eakin and Ellington (18) were used. For the mixtures the constant B_{o_m} was determined by the linear combining rule. For use in the generalized BWR equation the accentric factor for ethylene was required. This value was determined from the definition (Equation III-14), using the vapor pressure data of York and White (69). The resulting value was $\omega = +0.087$.

From Table XVI it is seen that both of the equations generally predict compressibility factors that are lower than the experimental values. For the 99.0% methane sample and the four intermediate mixtures the generalized BWR equation provides a slightly better fit than does the original BWR equation. For the ethylene sample the original BWR equation provides the better fit. Considering all of the data points together, the standard deviations from the experimental compressibility factors are given as 0.015 for the generalized BWR equation and 0.022 for the original equation.

TABLE XVI

COMPARISONS OF COMPRESSIBILITY FACTORS VERSUS EQUATIONS OF STATE

99.0 per cent methane

	1/V lb moles/ft^3	Z(exp)[1]	Z(BWR)[2]	Z difference (calc-exp)	Z(GEN BWR)[3]	Z difference (calc-exp)
77.00°F	0.49513	0.8230	0.8143	-0.0087	0.8176	-0.0054
	0.44392	0.8241	0.8176	-0.0065	0.8222	-0.0019
	0.37170	0.8352	0.8288	-0.0064	0.8347	-0.0005
	0.30996	0.8523	0.8443	-0.0080	0.8506	-0.0017
	0.24492	0.8742	0.8663	-0.0079	0.8725	-0.0017
	0.17722	0.9023	0.8954	-0.0069	0.9007	-0.0016
	0.12027	0.9295	0.9245	-0.0050	0.9287	-0.0008
	0.05281	0.9672	0.9645	-0.0027	0.9666	-0.0006
60.00°F	0.49270	0.8002	0.7894	-0.0108	0.7928	-0.0074
	0.43995	0.8044	0.7954	-0.0089	0.8002	-0.0042
	0.36931	0.8183	0.8101	-0.0082	0.8161	-0.0022
	0.30819	0.8379	0.8285	-0.0094	0.8350	-0.0029
	0.24370	0.8631	0.8537	-0.0094	0.8600	-0.0031
	0.17619	0.8955	0.8862	-0.0093	0.8917	-0.0038
	0.11976	0.9241	0.9181	-0.0060	0.9224	-0.0017
	0.05261	0.9653	0.9617	-0.0036	0.9638	-0.0015

[1] Table IV.

[2] Equation III-26.

[3] Equation III-32.

TABLE XVI (CONTINUED)

40.00°F	0.49453	0.7695	0.7575	-0.0120	0.7610	-0.0085
	0.44251	0.7763	0.7663	-0.0100	0.7712	-0.0051
	0.36986	0.7945	0.7854	-0.0091	0.7916	-0.0029
	0.30918	0.8176	0.8073	-0.0103	0.8140	-0.0036
	0.24440	0.8465	0.8366	-0.0099	0.8431	-0.0034
	0.17674	0.8832	0.8735	-0.0097	0.8792	-0.0040
	0.12010	0.9156	0.9094	-0.0062	0.9138	-0.0018
	0.05277	0.9616	0.9577	-0.0039	0.9600	-0.0016
20.00°F	0.49695	0.7337	0.7226	-0.0111	0.7263	-0.0074
	0.44359	0.7440	0.7346	-0.0094	0.7399	-0.0041
	0.37132	0.7663	0.7580	-0.0083	0.7646	-0.0017
	0.30999	0.7934	0.7840	-0.0094	0.7911	-0.0023
	0.24522	0.8267	0.8176	-0.0091	0.8245	-0.0022
	0.17735	0.8681	0.8594	-0.0087	0.8654	-0.0027
	0.12041	0.9049	0.8996	-0.0053	0.9043	-0.0006
	0.05289	0.9560	0.9534	-0.0026	0.9557	-0.0003
		standard deviations		0.008		0.004

TABLE XVI (CONTINUED)

78.8 per cent methane

	1/V lb moles/ft^3	Z(exp)	Z(BWR)	Z difference (calc-exp)	Z(GEN BWR)	Z difference (calc-exp)
77.00°F	0.53684	0.7492	0.7317	-0.0175	0.7328	-0.0164
	0.46276	0.7538	0.7383	-0.0156	0.7427	-0.0111
	0.39769	0.7678	0.7524	-0.0154	0.7588	-0.0090
	0.32897	0.7907	0.7757	-0.0150	0.7832	-0.0075
	0.26232	0.8196	0.8062	-0.0134	0.8139	-0.0057
	0.19684	0.8552	0.8437	-0.0115	0.8508	-0.0045
	0.13469	0.8949	0.8860	-0.0089	0.8917	-0.0032
	0.05820	0.9513	0.9470	-0.0043	0.9499	-0.0014
60.00°F	0.53342	0.7194	0.6995	-0.0199	0.7013	-0.0181
	0.46017	0.7282	0.7102	-0.0180	0.7152	-0.0130
	0.39508	0.7458	0.7281	-0.0177	0.7351	-0.0107
	0.32706	0.7725	0.7551	-0.0174	0.7632	-0.0093
	0.26087	0.8047	0.7895	-0.0153	0.7976	-0.0071
	0.19598	0.8440	0.8307	-0.0133	0.8381	-0.0059
	0.13409	0.8873	0.8770	-0.0103	0.8829	-0.0044
	0.05802	0.9486	0.9430	-0.0006	0.9459	-0.0027

TABLE XVI (CONTINUED)

40.00°F	0.53637	0.6804	0.6583	-0.0221	0.6608	-0.0196
	0.46170	0.6937	0.6735	-0.0202	0.6795	-0.0143
	0.39657	0.7154	0.6955	-0.0199	0.7033	-0.0121
	0.32829	0.7464	0.7272	-0.0192	0.7360	-0.0105
	0.26181	0.7833	0.7664	-0.0169	0.7752	-0.0081
	0.19665	0.8273	0.8128	-0.0145	0.8207	-0.0066
	0.13455	0.8753	0.8643	-0.0110	0.8706	-0.0047
	0.05816	0.9431	0.9373	-0.0058	0.9405	-0.0026
20.00°F	0.53826	0.6358	0.6134	-0.0224	0.6171	-0.0187
	0.46365	0.6545	0.6333	-0.0212	0.6404	-0.0143
	0.39792	0.6805	0.6598	-0.0207	0.6687	-0.0118
	0.32945	0.7160	0.6964	-0.0197	0.7061	-0.0099
	0.26317	0.7577	0.7405	-0.0172	0.7501	-0.0076
	0.19762	0.8072	0.7926	-0.0146	0.8012	-0.0060
	0.13499	0.8609	0.8502	-0.0107	0.8570	-0.0039
	0.05833	0.9358	0.9310	-0.0048	0.9344	-0.0014
			standard deviations:	0.016		0.010

TABLE XVI (CONTINUED)

57.2 per cent methane

	1/V lb moles/ft^3	Z(exp)	Z(BWR)	Z difference (calc-exp)	Z(GEN BWR)	Z difference (calc-exp)
77.00°F	0.58930	0.6564	0.6346	-0.0218	0.6320	-0.0244
	0.51363	0.6602	0.6385	-0.0218	0.6415	-0.0187
	0.44067	0.6746	0.6546	-0.0200	0.6613	-0.0133
	0.38040	0.6968	0.6768	-0.0200	0.6853	-0.0115
	0.28564	0.7471	0.7279	-0.0192	0.7375	-0.0097
	0.21592	0.7949	0.7780	-0.0169	0.7870	-0.0079
	0.13615	0.8609	0.8484	-0.0125	0.8553	-0.0056
	0.06518	0.9292	0.9225	-0.0067	0.9263	-0.0029
60.00°F	0.59175	0.6186	0.5935	-0.0251	0.5918	-0.0268
	0.51635	0.6268	0.6012	-0.0256	0.6051	-0.0217
	0.44283	0.6449	0.6212	-0.0237	0.6288	-0.0161
	0.38359	0.6698	0.6461	-0.0237	0.6555	-0.0143
	0.28639	0.7268	0.7042	-0.0226	0.7146	-0.0122
	0.21679	0.7788	0.7590	-0.0198	0.7686	-0.0102
	0.13647	0.8504	0.8360	-0.0144	0.8433	-0.0071
	0.06548	0.9243	0.9161	-0.0082	0.9202	-0.0041

TABLE XVI (CONTINUED)

40.00°F	0.59563	0.5690	0.5412	-0.0278	0.5409	-0.0281
	0.51901	0.5817	0.5538	-0.0279	0.5593	-0.0224
	0.44509	0.6057	0.5786	-0.0271	0.5877	-0.0180
	0.38568	0.6333	0.6075	-0.0258	0.6184	-0.0149
	0.28849	0.6977	0.6727	-0.0250	0.6843	-0.0134
	0.21777	0.7554	0.7344	-0.0210	0.7450	-0.0104
	0.13701	0.8348	0.8196	-0.0152	0.8276	-0.0072
	0.06565	0.9161	0.9080	-0.0081	0.9124	-0.0037
20.00°F	0.60078	0.5124	0.4841	-0.0283	0.4857	-0.0267
	0.52300	0.5305	0.5017	-0.0288	0.5092	-0.0213
	0.44978	0.5587	0.5307	-0.0279	0.5418	-0.0169
	0.38969	0.5913	0.5638	-0.0275	0.5765	-0.0148
	0.28920	0.6642	0.6389	-0.0253	0.6520	-0.0122
	0.21870	0.7282	0.7070	-0.0212	0.7188	-0.0094
	0.13744	0.8164	0.8014	-0.0150	0.8102	-0.0062
	0.06586	0.9057	0.8988	-0.0069	0.9036	-0.0021
			standard deviations:	0.022		0.015

TABLE XVI (CONTINUED)

38.4 per cent methane

	1/V lb moles/ft^3	Z(exp)	Z(BWR)	Z difference (calc-exp)	Z(GEN BWR)	Z difference (calc-exp)
77.00°F	0.65536	0.5677	0.5461	-0.0216	0.5374	-0.0304
	0.60903	0.5608	0.5408	-0.0200	0.5379	-0.0229
	0.44813	0.5871	0.5686	-0.0185	0.5780	-0.0092
	0.42964	0.5947	0.5760	-0.0187	0.5861	-0.0086
	0.32089	0.6557	0.6373	-0.0185	0.6494	-0.0063
	0.24739	0.7121	0.6962	-0.0159	0.7079	-0.0042
	0.16118	0.7961	0.7837	-0.0124	0.7930	-0.0031
	0.08046	0.8907	0.8835	-0.0072	0.8889	-0.0018
60.00°F	0.65843	0.5204	0.4957	-0.0247	0.4882	-0.0322
	0.61398	0.5165	0.4932	-0.0233	0.4915	-0.0250
	0.45008	0.5523	0.5302	-0.0221	0.5410	-0.0113
	0.43291	0.5605	0.5380	-0.0225	0.5495	-0.0110
	0.32265	0.6279	0.6064	-0.0216	0.6198	-0.0081
	0.24860	0.6899	0.6708	-0.0190	0.6836	-0.0063
	0.16180	0.7806	0.7661	-0.0145	0.7762	-0.0044
	0.08080	0.8828	0.8740	-0.0088	0.8799	-0.0029

TABLE XVI (CONTINUED)

40.00°F	0.66607	0.4583	0.4322	-0.0261	0.4261	-0.0322
	0.61797	0.4584	0.4329	-0.0255	0.4332	-0.0251
	0.45471	0.5048	0.4802	-0.0246	0.4931	-0.0117
	0.43612	0.5145	0.4897	-0.0248	0.5034	-0.0111
	0.32509	0.5902	0.5663	-0.0239	0.5816	-0.0086
	0.24984	0.6589	0.6383	-0.0206	0.6526	-0.0063
	0.16261	0.7589	0.7431	-0.0158	0.7542	-0.0047
	0.08100	0.8706	0.8620	-0.0086	0.8685	-0.0021
20.00°F	0.67035	0.3895	0.3628	-0.0267	0.3594	-0.0301
	0.62664	0.3927	0.3668	-0.0259	0.3693	-0.0234
	0.45814	0.4516	0.4260	-0.0256	0.4416	-0.0010
	0.43957	0.4624	0.4368	-0.0256	0.4530	-0.0094
	0.32653	0.5472	0.5229	-0.0243	0.5405	-0.0067
	0.25146	0.6226	0.6016	-0.0210	0.6178	-0.0048
	0.16315	0.7330	0.7177	-0.0153	0.7301	-0.0029
	0.08132	0.8558	0.8483	-0.0075	0.8554	-0.0004
		standard deviations:		0.021		0.015

TABLE XVI (CONTINUED)

18.4 per cent methane

	1/V lb moles/ft^3	Z(exp)	Z(BWR)	Z difference (calc-exp)	Z(BEN BWR)	Z difference (calc-exp)
77.00°F	0.85379	0.4648	0.5795	0.1147	0.5229	0.0581
	0.75394	0.4363	0.4709	0.0346	0.4456	0.0093
	0.60656	0.4401	0.4317	-0.0084	0.4336	-0.0065
	0.46976	0.4757	0.4637	-0.0120	0.4772	0.0015
	0.38466	0.5210	0.5096	-0.0114	0.5258	0.0048
	0.33317	0.5588	0.5477	-0.0111	0.5641	0.0053
	0.18630	0.7120	0.7023	-0.0097	0.7150	0.0030
	0.09366	0.8422	0.8361	-0.0061	0.8436	0.0014
60.00°F	0.85773	0.4038	0.5061	0.1023	0.4496	0.0458
	0.76244	0.3810	0.4090	0.0280	0.3836	0.0026
	0.61004	0.3916	0.3787	-0.0129	0.3824	-0.0092
	0.47573	0.4296	0.4175	-0.0121	0.4328	0.0032
	0.38874	0.4802	0.4685	-0.0117	0.4865	0.0063
	0.33936	0.5181	0.5075	-0.0106	0.5257	0.0076
	0.18718	0.6910	0.6785	-0.0125	0.6925	0.0015
	0.09406	0.8298	0.8231	-0.0067	0.8312	0.0014

TABLE XVI (CONTINUED)

40.00°F	0.86868	0.3277	0.4213	0.0935	0.3628	0.0351
	0.77030	0.3098	0.3281	0.0183	0.3036	-0.0062
	0.61955	0.3259	0.3110	-0.0149	0.3167	-0.0092
	0.48195	0.3699	0.3590	-0.0109	0.3771	0.0072
	0.39546	0.4246	0.4144	-0.0102	0.4351	0.0105
	0.33992	0.4694	0.4619	-0.0075	0.4827	0.0133
	0.18852	0.6586	0.6472	-0.0114	0.6628	0.0042
	0.09439	0.8117	0.8063	-0.0054	0.8153	0.0036
20.00°F	0.87992	0.2448	0.3262	0.0814	0.2662	0.0214
	0.78530	0.2317	0.2422	0.0105	0.2170	-0.0147
	0.62358	0.2577	0.2385	-0.0192	0.2476	-0.0100
	0.48532	0.3088	0.2971	-0.0118	0.3187	0.0099
	0.39654	0.3637	0.3596	-0.0041	0.3837	0.0200
	0.34469	0.4030	0.4076	0.0046	0.4315	0.0285
	0.18902	0.6212	0.6134	-0.0078	0.6310	0.0098
	0.09478	0.7896	0.7872	-0.0024	0.7973	0.0077
		standard deviations:		0.037		0.017

TABLE XVI (CONTINUED)

ethylene

	1/V lb moles/ft^3	Z(exp)	Z(BWR)	Z difference (calc-exp)	Z(GEN BWR)	Z difference (calc-exp)
77.00°F	0.78063	0.3714	0.3773	0.0059	0.3485	-0.0229
	0.67232	0.3252	0.3226	-0.0026	0.3208	-0.0044
	0.52402	0.3437	0.3435	-0.0002	0.3606	0.0169
	0.35540	0.4523	0.4468	-0.0055	0.4687	0.0164
	0.21544	0.6071	0.6053	-0.0018	0.6227	0.0156
	0.10275	0.7931	0.7887	-0.0044	0.7984	0.0053
60.00°F	0.78624	0.2992	0.3033	0.0041	0.2750	-0.0242
	0.68294	0.2630	0.2591	-0.0039	0.2578	-0.0052
	0.53264	0.2932	0.2889	-0.0043	0.3080	0.0148
	0.36120	0.4103	0.4010	-0.0093	0.4254	0.0150
	0.21803	0.5746	0.5725	-0.0021	0.5917	0.0171
	0.10318	0.7776	0.7722	-0.0055	0.7828	0.0051

TABLE XVI (CONTINUED)

40.00°F	0.80233	0.2118	0.2159	0.0041	0.1855	-0.0263
	0.69545	0.1846	0.1775	-0.0071	0.1772	-0.0074
	0.55159	0.2306	0.2156	-0.0150	0.2369	0.0063
	0.36803	0.3450	0.3425	-0.0025	0.3701	0.0251
	0.22040	9.5326	0.5309	-0.0017	0.5525	0.0199
	0.10359	0.7553	0.7507	-0.0046	0.7625	0.0072
20.00°F	0.81109	0.1257	0.1116	-0.0141	0.0820	-0.0437
	0.70155	0.1452	0.0883	-0.0569	0.0911	-0.0541
	0.55632	0.1842	0.1430	-0.0412	0.1683	-0.0159
	0.37460	0.2742	0.2786	0.0044	0.3102	0.0360
	0.22135	0.4563	0.4868	0.0305	0.5113	0.0549
	0.10399	0.7281	0.7264	-0.0017	0.7398	0.0117
			standard deviations:	0.017		0.024

Total standard deviations (all compositions):	Z(BWR)	Z(GEN BWR)
	0.022	0.015

Comparisons of Experimental Second Virial Coefficients with Equations of State

In Table XVII the experimental second virial coefficients are compared with the coefficients from the BWR equation, the Edmister generalized form of the BWR equation, and the RK equation.

For the original and the generalized forms of the BWR equation both linear and Lorentz combining rules for B_o were used. For all equations the coefficients were calculated in units of ft^3/lb mole, and were then converted to cm^3/gm mole for analysis. The tabulated experimental coefficients correspond to those in Table IX, corrected for impurities. To make a direct comparison, therefore, the mixing rules for a two-component system were applied in all of the above equations.

The Edmister generalized form of the BWR equation is seen to provide a better fit than the other equations tested. Using the linear combining rule for B_o, the standard deviation from the 24 experimental data points was 3.14 cm^3/gm mole. Using the original BWR equation the corresponding standard deviation was 5.99 cm^3/gm mole (linear B_o), and for the RK equation a value of 7.37 cm^3/gm mole resulted.

The agreement of the generalized BWR equation is quite good, although the value of 3.14 cm^3gm/mole is larger than the estimated error of the experimental virial coefficients (1.5 cm^3/gm mole). Both for the generalized and original forms of the BWR equation the linear combination rule for B_o appears to be slightly better than the Lorentz rule. The difference in standard deviations between the two combining rules is small, however (0.08 cm^3/gm mole for the generalized form, and 0.10 cm^3/gm mole for the original form) and does not represent a significant improvement.

TABLE XVII

SECOND VIRIAL COEFFICIENTS FROM EQUATIONS OF STATE

Composition, per cent methane	T, °F	$-B_m$, cm^3/gm mole Experimental[1]	BWR[2] (Linear B_o)	BWR (Lorentz B_o)	Generalized BWR[2] (Linear B_o)	Generalized BWR (Lorentz B_o)	RK[4]
100.0	77.00	42.82	43.60 (-0.78)[3]	43.60 (-0.78)	40.70 (+2.12)	40.70 (+2.12)	45.43 (-2.61)
	60.00	46.50	47.13 (-0.63)	47.13 (-0.63)	44.14 (+2.36)	44.14 (+2.36)	49.15 (-2.65)
	40.00	51.24	51.69 (-0.45)	51.69 (-0.45)	48.59 (+2.65)	48.59 (+2.65)	53.93 (-2.69)
	20.00	56.65	56.76 (-0.11)	56.76 (-0.11)	53.52 (+3.13)	53.52 (+3.13)	59.21 (-2.56)
79.2	77.00	53.44	59.02 (-5.58)	59.12 (-5.68)	55.62 (-2.18)	55.74 (-2.30)	61.71 (-8.27)
	60.00	57.41	63.63 (-6.22)	63.72 (-6.31)	60.08 (-2.67)	60.20 (-2.79)	66.34 (-8.93)
	40.00	63.03	69.61 (-6.58)	69.71 (-6.68)	65.86 (-2.83)	65.99 (-2.96)	72.29 (-9.26)

[1] Table IX.

[2] Equation III-30.

[3] Difference (calculated - experimental).

[4] Equation III-43.

TABLE XVII (CONTINUED)

	20.00	69.84	76.31 (-6.47)	76.41 (-6.57)	72.33 (-2.49)	72.45 (-2.61)	78.87 (-9.03)
57.4	77.00	70.17	77.92 (-7.75)	78.07 (-7.90)	73.84 (-3.67)	74.03 (-3.86)	80.94 (-10.77)
	60.00	75.19	83.88 (-8.69)	84.02 (-8.83)	79.56 (-4.37)	79.75 (-4.56)	86.62 (-11.43)
	40.00	82.65	91.65 (-9.00)	91.79 (-9.14)	87.02 (-4.37)	87.20 (-4.55)	93.94 (-11.29)
	20.00	91.58	100.40 (-8.82)	100.55 (-8.97)	95.39 (-3.81)	95.58 (-4.00)	102.02 (-10.44)
38.5	77.00	90.02	96.58 (-6.56)	96.72 (-6.70)	91.78 (-1.76)	91.96 (-1.94)	99.39 (-9.37)
	60.00	96.45	103.89 (-7.44)	104.02 (-7.57)	98.76 (-2.31)	98.94 (-2.49)	106.09 (-9.64)
	40.00	105.57	113.46 (-7.89)	113.60 (-8.03)	107.88 (-2.31)	108.06 (-2.49)	114.70 (-9.13)
	20.00	116.56	124.28 (-7.72)	124.42 (-7.86)	118.16 (-1.60)	118.34 (-1.78)	124.22 (-7.66)

TABLE XVII (CONTINUED)

18.4	77.00	114.06	118.74 (-4.68)	118.83 (-4.77)	113.03 (+1.03)	113.15 (+0.91)	120.84 (+6.78)
	60.00	121.61	127.67 (-6.06)	127.75 (-6.14)	121.52 (+0.09)	121.63 (-0.02)	128.70 (-7.09)
	40.00	133.22	139.40 (-6.18)	139.49 (-6.27)	132.64 (+0.58)	132.75 (+0.47)	138.81 (-5.59)
	20.00	145.52	152.71 (-7.19)	152.80 (7.28)	145.21 (+0.31)	145.33 (+0.19)	149.98 (-4.46)
0.0	77.00	140.33	141.11 (-0.78)	141.11 (-0.78)	134.46 (+5.87)	134.46 (+5.87)	142.13 (-1.80)
	60.00	149.95	151.69 (-1.74)	151.69 (-1.74)	144.47 (+5.48)	144.47 (+5.48)	151.14 (-1.19)
	40.00	162.58	165.64 (-3.06)	165.64 (-3.06)	157.62 (+4.96)	157.62 (+4.96)	162.72 (-0.14)
	20.00	175.95	181.49 (-5.54)	181.49 (-5.54)	172.53 (+3.42)	172.53 (+3.42)	175.52 (+0.43)
standard deviation, cm^3/gm mole:			5.99	6.09	3.14	3.22	7.37

The experimental virial coefficients are compared graphically versus the three equations of state in Figures 8, 9, and 10. Due to the small difference between linear and Lorentz forms of B_o, only the linear form is shown.

Comparisons of Experimental Third Virial Coefficients with Equations of State

In Table XVIII the experimental third virial coefficients are compared with the above three equations of state.

The expressions for the third virial coefficient from these equations are given by Equations III-31 and III-43. For both forms of the BWR equation the third virial coefficient is independent of the linear and Lorentz combining rules, as the constant B_o does not appear in the expression.

The experimental third virial coefficients were not corrected for impurities. In order to make a direct comparison with equations of state, therefore, the mixing rules were written so as to include the impurities. This procedure involves expanding the mixing rules to N terms (N being the number of components in the system), each term containing a composition term and a pure component constant. From Appendix G the maximum value of N = 4 for both the 57.2% methane and the 78.8% methane system.

As with the second virial coefficients the overall fit of the Edmister generalized form of the BWR equation is better than that of the other equations. For the 24 experimental points the standard deviations were 2.1×10^2 $cm^6/gm\ mole^2$ (generalized BWR), 3.7×10^2 $cm^6/gm\ mole^2$ (original BWR), and 12.8×10^2 $cm^6/gm\ mole^2$ (RK). In Figures 11, 12, and 13 the experimental coefficients are compared graphically versus coefficients from the equations of state.

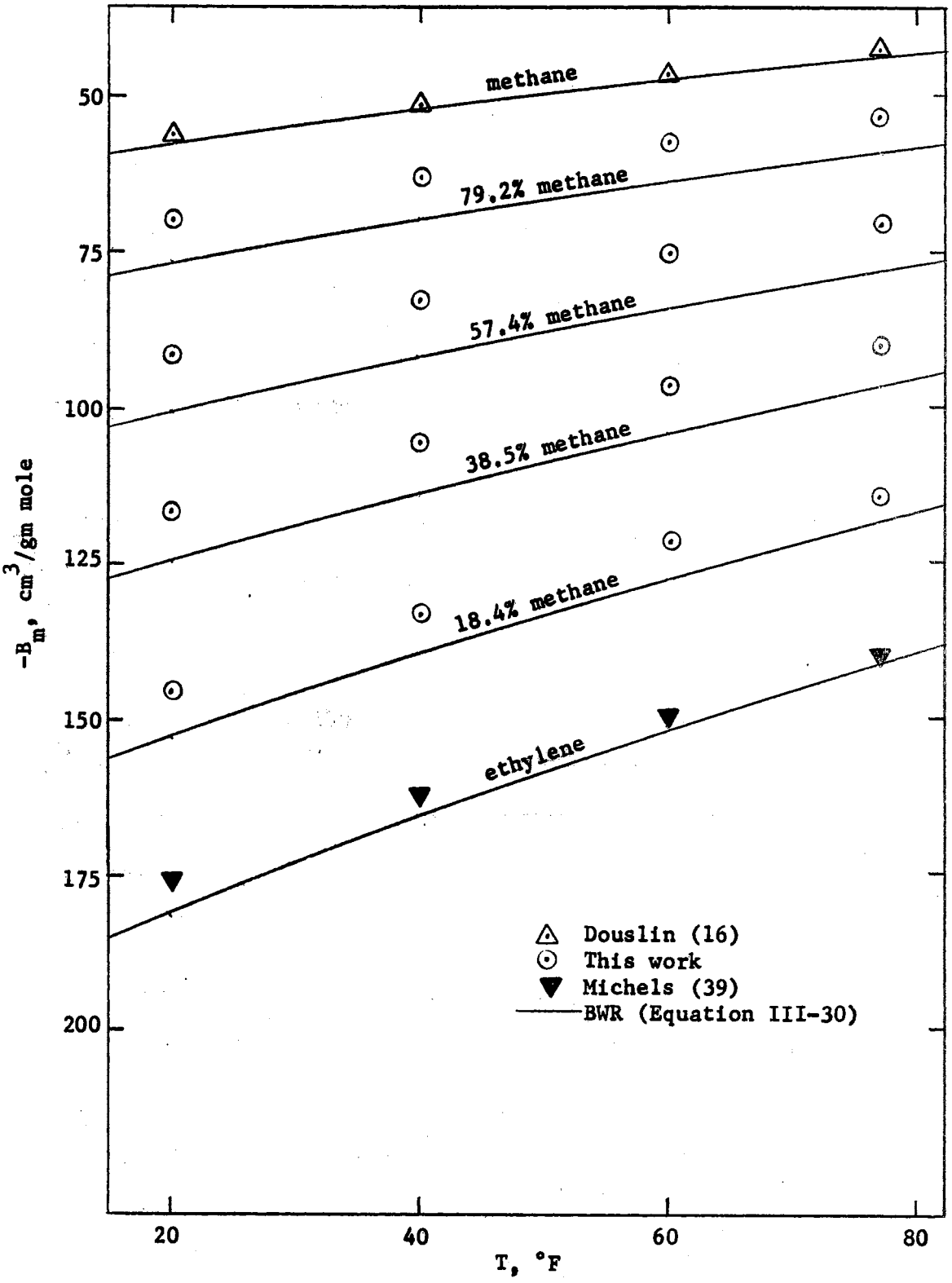

Figure 8

Second Virial Coefficients from BWR Equation

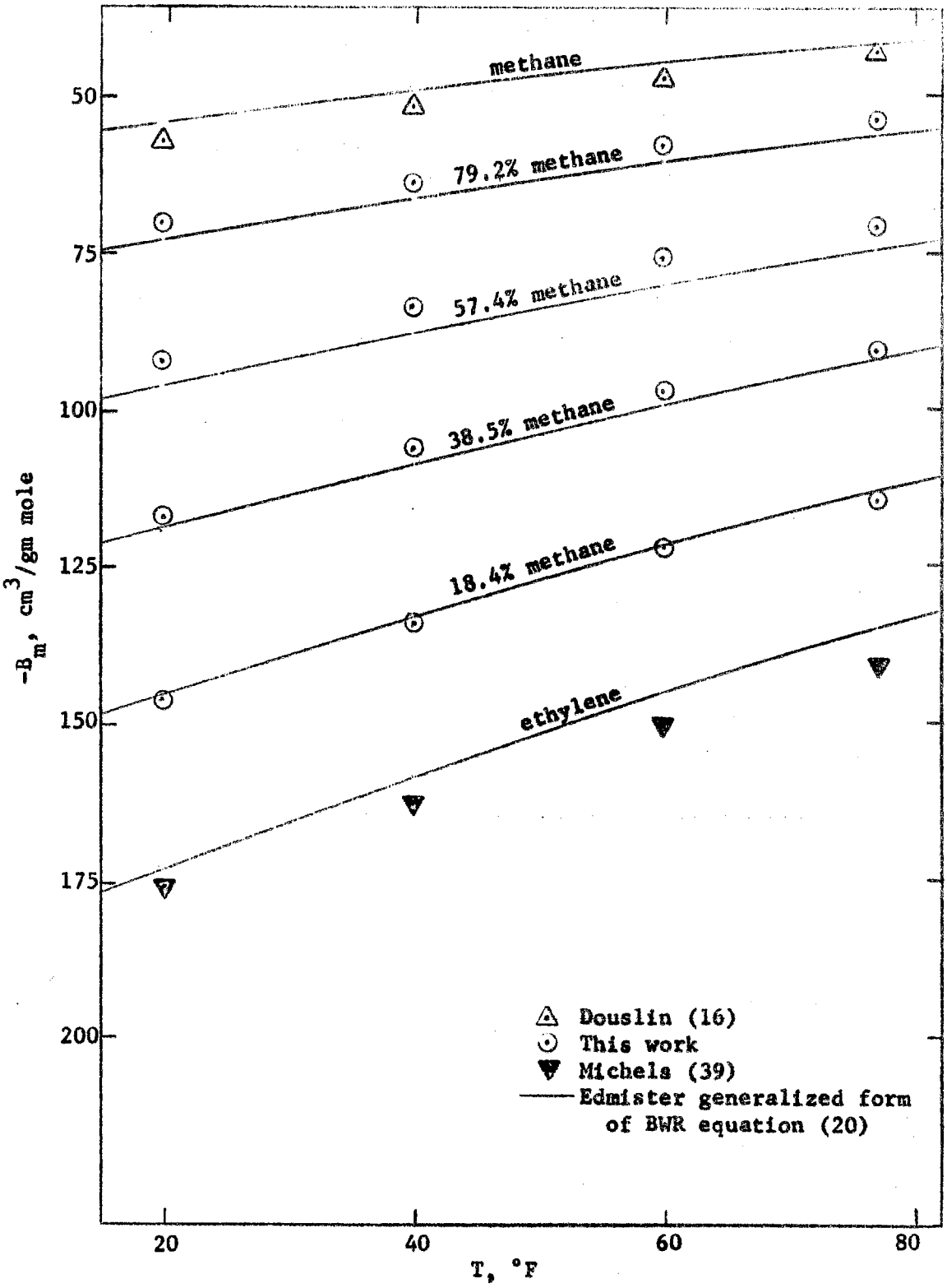

Figure 9

Second Virial Coefficients from Edmister Generalized BWR Equation

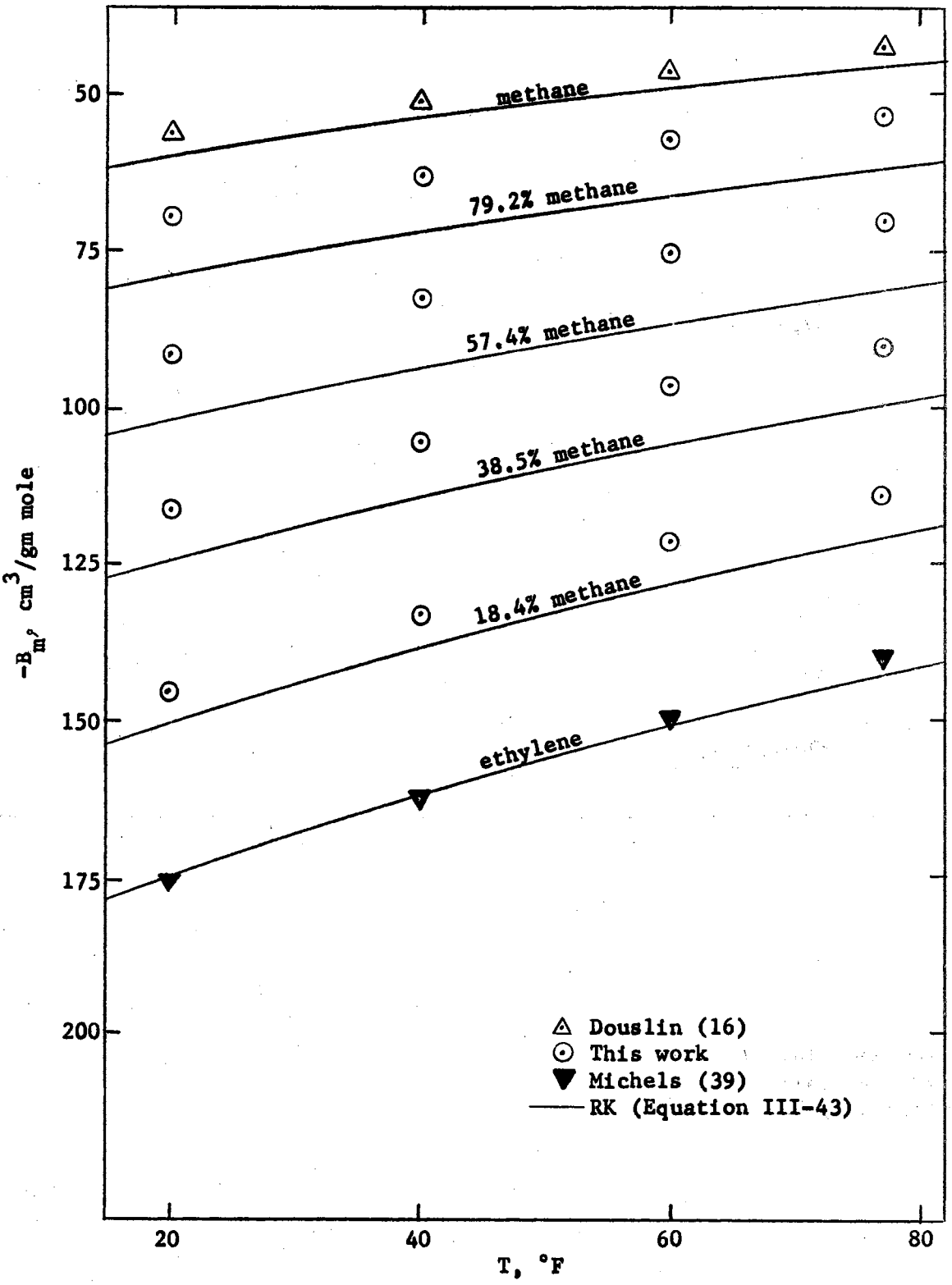

Figure 10

Second Virial Coefficients from RK Equation

TABLE XVIII

THIRD VIRIAL COEFFICIENTS FROM EQUATIONS OF STATE

C_m, $cm^6/gm\ mole^2 \times 10^{-2}$

Composition, per cent methane	T, °F	Experimental[1]	BWR[2]	Generalized BWR[2]	RK[4]
100.0	77.00	23.70	25.3 (+1.60)[3]	22.3 (-1.40)	31.1 (+7.40)
	60.00	24.60	25.8 (+1.20)	22.7 (-1.90)	32.2 (+7.60)
	40.00	25.60	26.6 (+1.00)	23.4 (-2.20)	33.6 (+8.00)
	20.00	26.85	27.6 (+0.75)	24.3 (-2.55)	35.2 (+8.35)
78.8	77.00	28.2	32.5 (+4.3)	28.7 (+0.5)	40.4 (+12.2)
	60.00	29.2	33.6 (+4.4)	29.7 (+0.5)	41.9 (+12.7)

[1] Table X.

[2] Equation III-31.

[3] Difference (calculated - experimental).

[4] Equation III-43.

TABLE XVIII (CONTINUED)

	40.00	30.9	35.3 (+4.4)	31.3 (+0.4)	43.8 (+12.9)
	20.00	33.6	37.3 (+3.7)	33.2 (-0.4)	45.9 (+12.3)
57.2	77.00	34.7	41.4 (+6.7)	37.1 (+2.4)	51.1 (+16.4)
	60.00	36.6	43.5 (+6.9)	39.0 (+2.4)	53.0 (+16.4)
	40.00	40.0	46.4 (+6.4)	41.8 (+1.8)	55.6 (+15.6)
	20.00	44.5	50.0 (+5.5)	45.3 (+0.8)	58.3 (+13.8)
38.4	77.00	45.5	51.1 (+5.6)	46.4 (+0.9)	61.9 (+16.4)
	60.00	48.5	54.2 (+5.7)	49.4 (+0.9)	64.3 (+15.8)
	40.00	53.3	58.7 (+5.4)	53.7 (+0.4)	67.4 (+14.1)
	20.00	59.0	64.1 (+5.1)	58.9 (-0.1)	70.8 (+11.8)

TABLE XVIII (CONTINUED)

18.4	77.00	60.0	63.4 (+3.4)	58.6 (-1.4)	74.8 (+14.8)
	60.00	62.8	68.0 (+5.2)	63.1 (+0.3)	77.8 (+15.0)
	40.00	68.3	74.6 (+6.3)	69.4 (+1.1)	81.6 (+13.3)
	20.00	74.6	82.6 (+8.0)	77.0 (+2.4)	85.9 (+11.3)
0.0	77.00	76.43	77.27 (+0.84)	72.65 (-3.78)	88.48 (+12.05)
	60.00	80.5	83.7 (+3.2)	78.8 (-1.7)	92.1 (+11.6)
	40.00	85.9	92.6 (+6.7)	87.4 (+1.5)	96.7 (+10.8)
	20.00	91.7	103.6 (+11.9)	97.8 (+6.1)	101.8 (+10.1)
standard deviation, $cm^6/gm\ mole^2 \times 10^{-2}$:			3.7	2.1	12.8

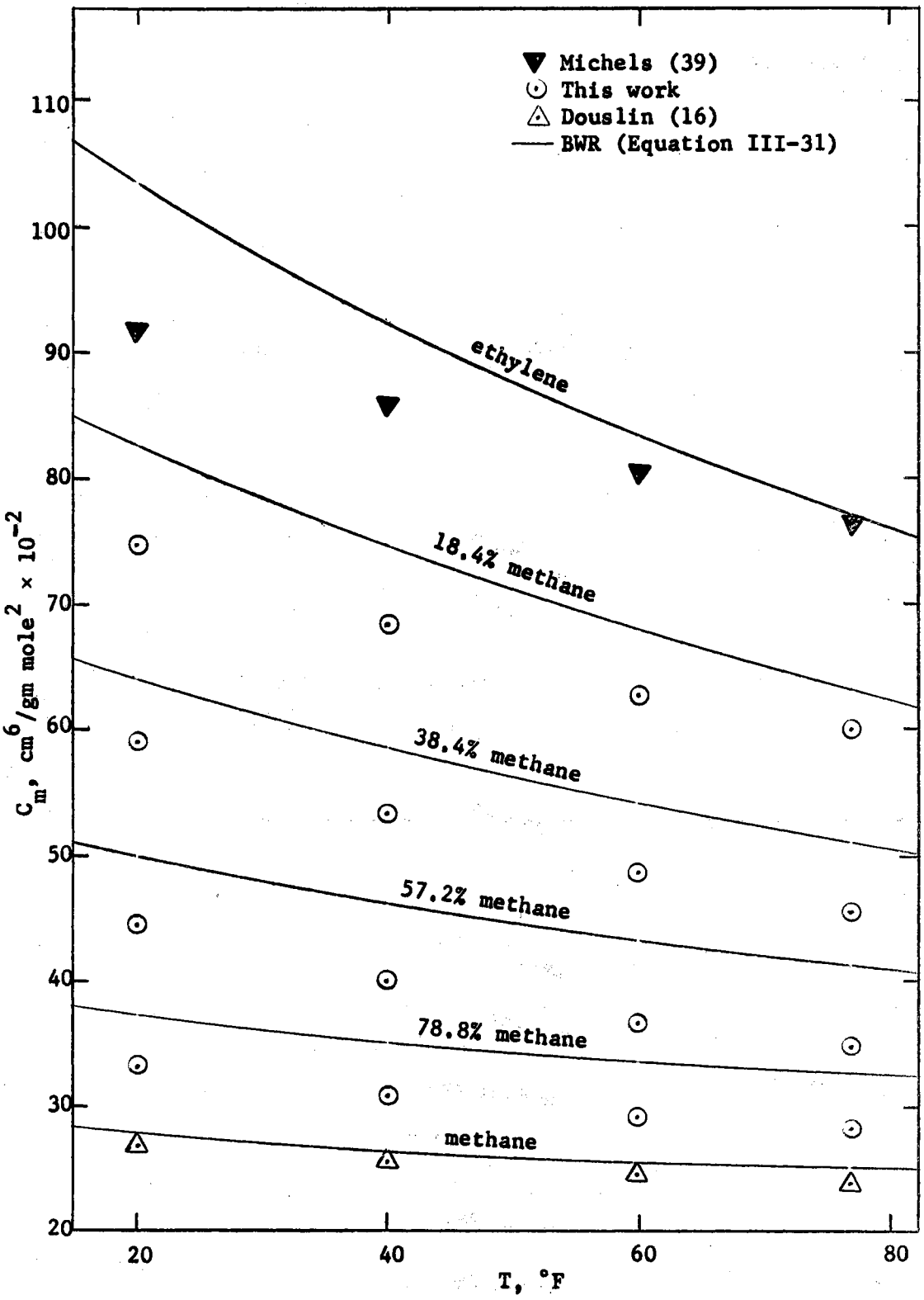

Figure 11

Third Virial Coefficients From BWR Equation

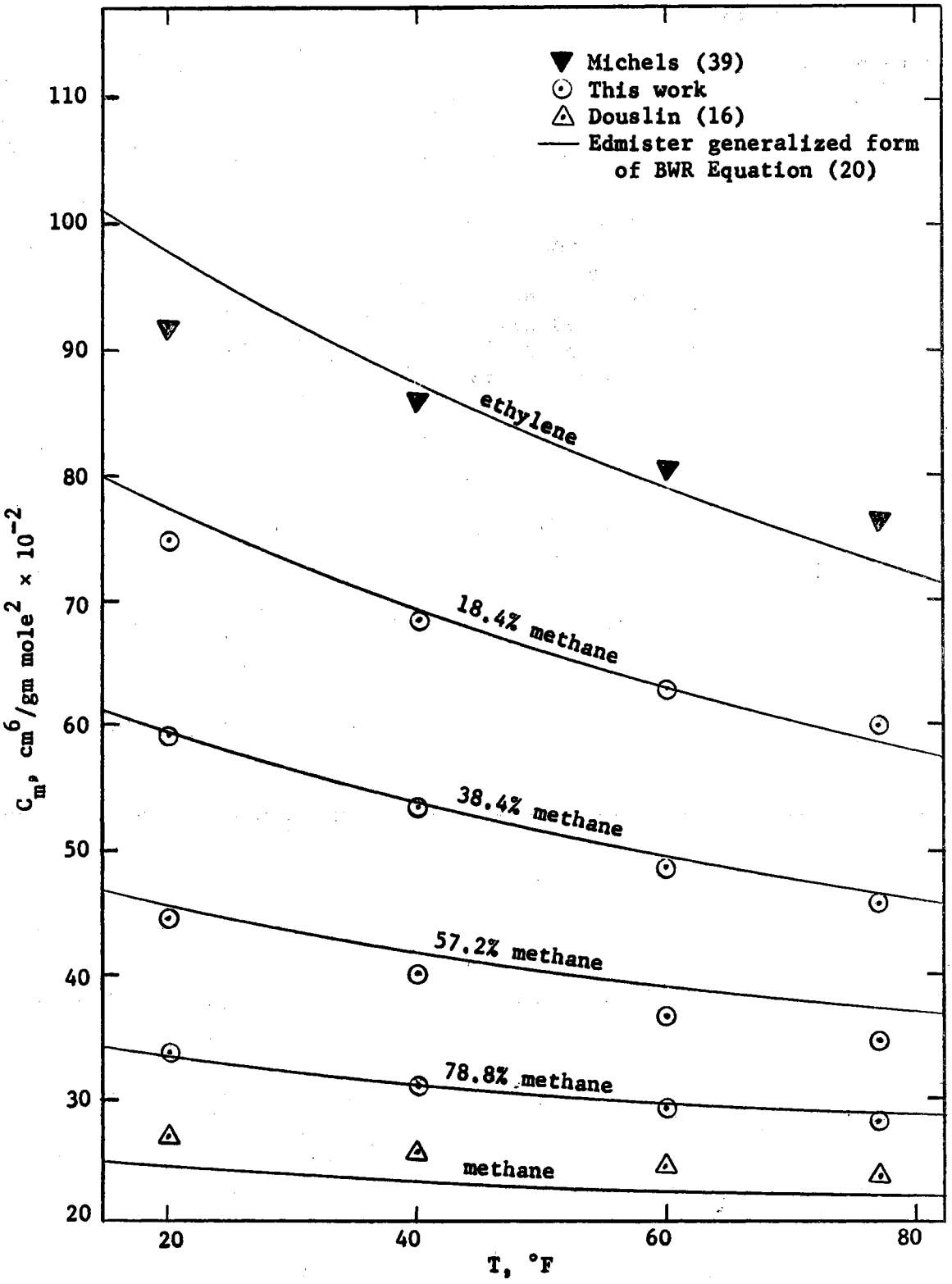

Figure 12

Third Virial Coefficients from Edmister Generalized BWR Equation

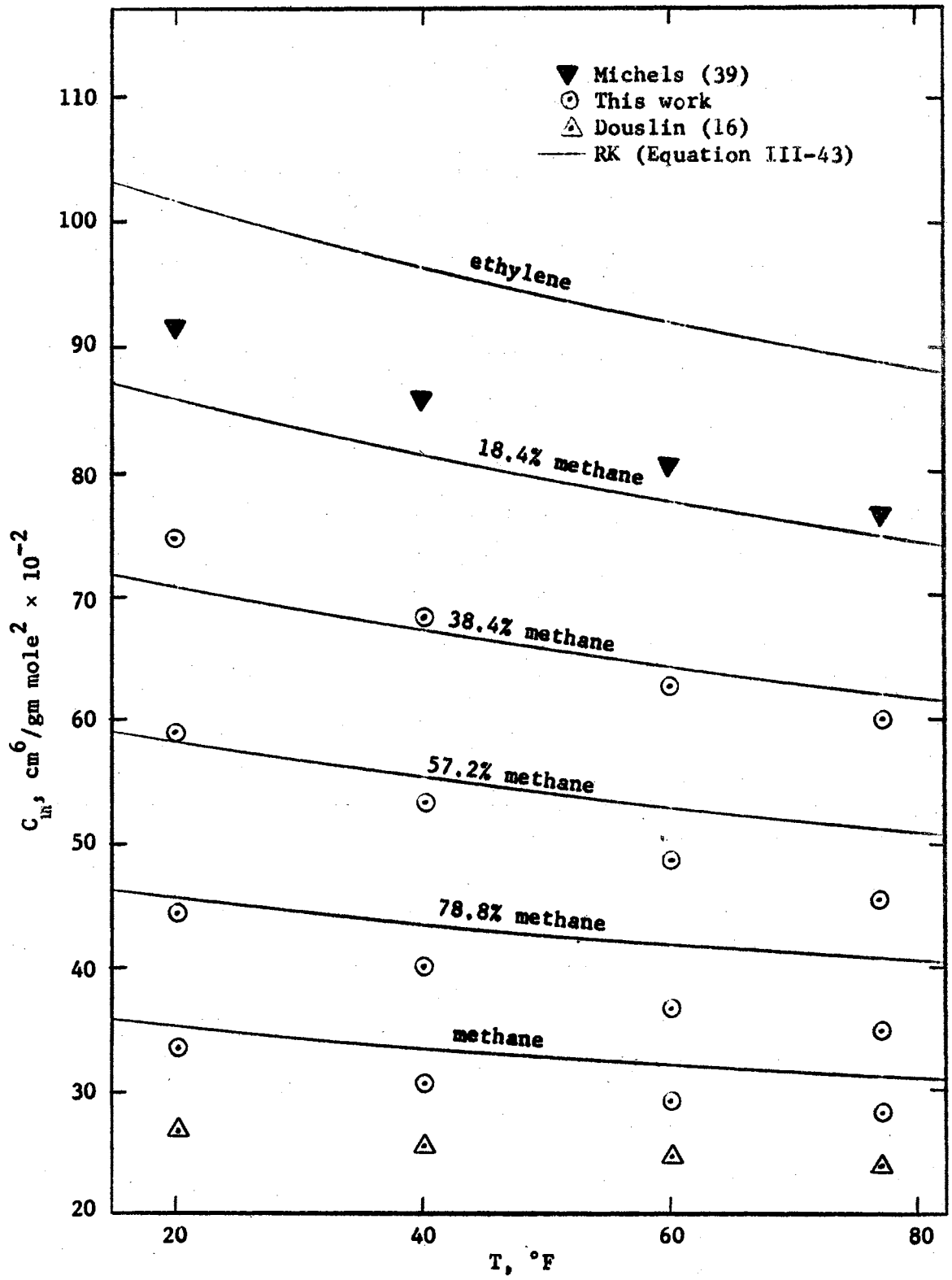

Figure 13

Third Virial Coefficients from RK Equation

General Remarks on Equation of State Comparisons

For the compressibility factor comparisons it was seen that the generalized BWR equation provides a better overall fit to the data than does the original BWR equation. For the pure component points the generalized equation provides the better fit to the methane data, while the original BWR equation provides a better fit to the ethylene data. The fact should be emphasized, however, that the above comparisons represent only one binary system over a fairly narrow temperature range. The generalized equation should be tested for other binary systems before additional conclusions can be reached.

The objective of the comparisons was to determine and emphasize the need for further work on methods of improving equations of state. One criteria for an equation of state is the accurate prediction of virial coefficients. For this reason, experimental virial coefficients were compared directly versus coefficients predicted by equations of state.

For the second virial coefficients (Table XVII) the original BWR equation provided the best fit to the pure component data. Considering pure component and mixture data together, however, the generalized BWR equation provided the best fit. This difference is due in large part to the form of the mixing rules (Equations III-27). Although based on theoretical considerations these rules are still somewhat empirical.

For the third virial coefficients (Table XVIII) the generalized BWR equation provided the best fit, both for the pure components and for the mixtures. For the pure component points the standard deviations were 3.04×10^2 $cm^6/gm\ mole^2$ (generalized BWR), 5.04×10^2 $cm^6/gm\ mole^2$

(original BWR), and 9.66×10^2 $cm^6/gm\ mole^2$ (RK). Considering all points together the standard deviations were also lowest for the generalized equation.

For both the second and the third virial coefficient comparisons, the fact should be pointed out that the constants for the original BWR equation were determined largely from compressibility factor data; the equation was then expanded into virial form. A small adjustment in the constants could produce a relatively large change in the calculated virial coefficient.

From the above comparisons several approaches were suggested for future equation of state improvements. These approaches are presented in the following.

Comments on Further Improvements of Equations of State

One criteria in the development of a closed-form equation of state is that it should accurately predict the second and third virial coefficients. Ideally the equation would accurately predict higher-ordered coefficients also, but these coefficients are seldom available for comparison. With this approach in mind several arguments may be given in favor of the BWR (generalized or original) form of equation rather than the RK form.

The second and third virial coefficients in the BWR equation have the form

$$B(T) = B_o - \frac{A_o}{RT} - \frac{C_o}{RT^3} \qquad \text{(III-30)}$$

$$C(T) = b - \frac{a}{RT} + \frac{c}{RT^3} \qquad \text{(III-31)}$$

It is important here that the constants B_o, A_o, and C_o appear in Equation III-30 whereas the different constants b, a, and c appear in Equation III-31. For this reason the constants B_o, A_o, and C_o may be adjusted to fit experimental second virial coefficients without any effect on the expression for the third virial coefficients, and conversely.

For the RK equation the second and third virial coefficients are given as

$$B(T) = b - \frac{a}{RT^{3/2}}$$

$$C(T) = b^2 + \frac{ab}{RT^{3/2}} \qquad \text{(III-43)}$$

The second virial coefficient contains only two constants, and appears to be an oversimplification, even if the expression were fit directly to second virial coefficient data. In addition, the third virial coefficient is uniquely dependent upon the constants chosen for the second coefficient.

It is of further importance that the BWR expressions for B(T) and C(T) do not contain the constants α and γ. It would be possible to determine the six constants in Equations III-30 and III-31 from virial coefficient data (either experimental or generalized values). The equation could then be recombined into the normal closed form, given below.

$$Z = 1 + (B_o - \frac{A_o}{RT} - \frac{C_o}{RT^3})d + (b - \frac{a}{RT})d^2 \qquad \text{(III-26)}$$

$$+ \frac{a\alpha}{RT} d^5 + \frac{cd^2}{RT^3} (1 + \gamma d^2) \exp (-\gamma d^2)$$

In this equation the remaining unknown constants α and γ could be determined by regression analysis so as to produce the best fit to a set of compressibility factor data.

In principle both the generalized form and the original form of the BWR equation could be evaluated in this manner. The primary goal, however, is the development of an improved equation that would be of value from an engineering standpoint, particularly for binary and multicomponent mixtures. For this purpose the generalized form would have greater application.

C. Error Analysis of Data

In this section the accuracy of the data and of the isochoric apparatus is examined from two different viewpoints. These are: 1) making mathematical estimates of the error of the isochoric apparatus from the estimated errors of each measured quantity (such as temperature and pressure), and 2) comparing the resultant data directly with corresponding values from the literature. These two approaches are discussed in this order.

Estimated Experimental Error

Estimates of the experimental error in the compressibility factors were made by the method of propagation of errors (60). This method enables the estimation of the error in a function of directly measured quantities, provided that individual errors may be established for each of the directly measured quantities. As described previously the isochoric compressibility factors Z_{BT} are determined from Equation N-21 after first determining the isochoric run constant D from Equation N-20. For this calculation estimates were made of the error in each of the measured quantities in these equations. The errors in these quantities were then combined to estimate the resultant error in the compressibility factors Z_{BT}.

Fractional errors were estimated for the measured quantities in the equations as is shown in Table XIX.

The most important remaining factors are the measured pressure and temperature of the sample inside the bomb, the determination of the isochoric run constant D, and the correction for the sample in the DPI cell and exposed capillary line. The correction for the sample in the capillary line and DPI cell is given by the terms 0.01263 D_D, 0.01537 D_5, etc., in the equations. Errors of 0.01% in the pressure measurements and 0.02°K in the temperature T_B of the sample inside the bomb were used in the calculations. The error in the run constant D is dependent upon the error in the compressibility factor from the reference isotherm. The run constant is also affected by errors due to the capillary line.

In order to make error calculations it is necessary to assume errors in the reference isotherm. Three different fractional errors

TABLE XIX

ESTIMATED FRACTIONAL ERRORS

Volume Ratios	Average Fractional Errors
V_D/V_B	0.012
V_5/V_B	0.021
V_4/V_B	0.021
V_3/V_B	0.028
V_1/V_B	0.028
V_a/V_B	0.028
Temperatures of Capillary Lines and DPI Cell	
T_D	0.00018 (0.10°F)
T_5	0.00018 (0.10°F)
T_4	0.00018 (0.10°F)
T_3	0.0021 (1.0°F)
T_2	0.0021 (1.0°F)
T_1	0.0021 (1.0°F)
Miscellaneous Constants	
R	2×10^{-6}
α [1/]	0.05

[1/] Coefficient of thermal expansion for the bomb, Equation H-5.

were assumed and the corresponding error in the isochoric compressibility factor was estimated. Results are given in Table XX for the ethylene sample at 698.690 psia and 60°F; similar results are obtained if other mixture compositions or temperatures on the isochor are used.

TABLE XX

RESULTS OF ERROR ANALYSIS

$(\frac{\Delta Z}{Z})_{77°F}$ [1]	$(\frac{\Delta D}{D})$ [2]	$(\frac{\Delta Z}{Z})_{60°F}$ [3]
(assumed)	(calculated)	(calculated)
0.0000	0.0005	0.0007
0.0010	0.0011	0.0013
0.0050	0.0050	0.0050

[1] Reference isotherm.

[2] Run constant.

[3] Isochoric compressibility factor.

As an estimate of the limiting accuracy of the isochoric apparatus an error of zero was assumed in the reference isotherm. The corresponding fractional error in the run constant was 0.0005, and the error in the isochoric compressibility factor was 0.0007. In this case essentially all of the error (both in the run constant determination and in the final compressibility factor) was shown to be due to errors contributed by the sample in the capillary line and DPI cell.

The assumption of a fractional error of 0.0010 in the reference isotherm produced an error of 0.0011 in the run constant, with a final fractional error of 0.0013 in the compressibility factor. The error in this case was attributed approximately equally to errors in the reference isotherm and errors caused by the capillary line. The assumed errors of 0.01% and 0.02°K in the pressure measurement and bomb temperature, respectively, have only a small effect here.

For the assumed fractional error of 0.0050 in the reference isotherm the error in the run constant and final compressibility factor was essentially all attributed to the reference isotherm error. These calculations illustrate the fact that the accuracy of the isochoric apparatus will never exceed the accuracy of the compressibility factor from the reference isotherm.

Comparisons with Published Methane Data

In Figure 14, the methane data of Table IV are compared with the published data of Mueller et al (50) and Matthews and Hurd (34)

The data of Mueller were taken over the interval -200 to +50°F, with pressures from 40 to 7000 psia. The compressibility data is stated to be accurate to 0.13%. By using a large sheet of graph

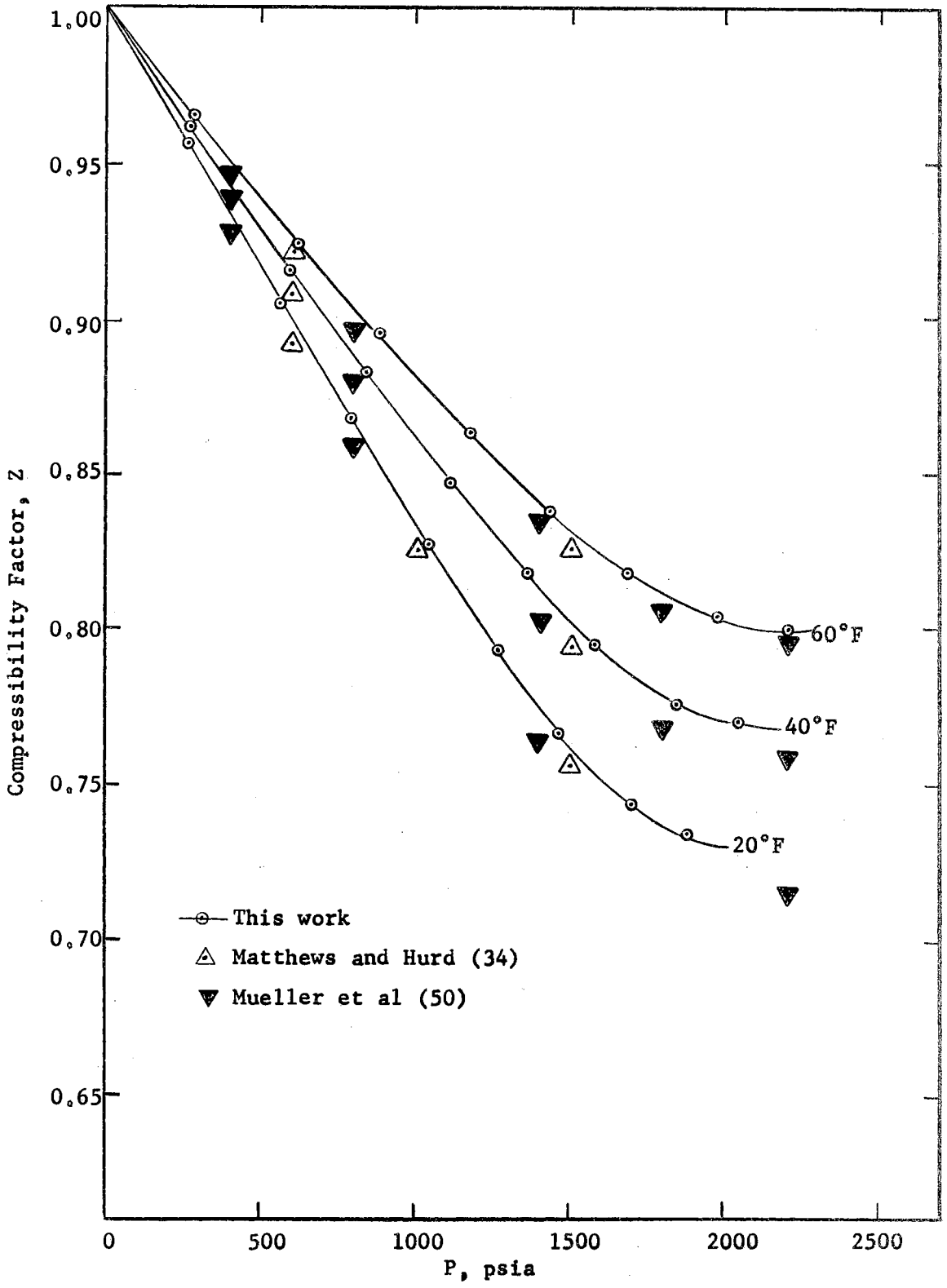

Figure 14

Compressibility Factor Comparisons for Methane

paper the data was interpolated to the temperatures 60, 40, and 20°F. The maximum error introduced by the interpolation procedure was estimated as 0.1%; the errors in the interpolated data points are thus 0.2% or less.

The superheated methane data of Matthews and Hurd cover the temperature range -260 to +500°F, with pressures from 10 to 1500 psia. These data represent a compilation of the data of Kvalnes and Gaddy (30) and of Olds, Reamer, Sage, and Lacey (51). The data of Kvalnes and Gaddy cover the temperature range -70 to +200°C, with pressures from 300 to 15,000 psia. The data are reported accurate to 0.2%. The temperatures of the Sage and Lacey data (+100 to +460°F) are higher than the temperatures of this investigation; the corresponding pressures are from 200 to 10,000 psia, with the reported accuracy of the data being 0.2%. From an examination of Figure 14 the data of Mueller et al and Matthews and Hurd are seen to be in agreement to within the stated accuracy (0.2%) from both sources.

From a large plot similar to Figure 14 the above literature values were compared at even values of pressure with the data of this investigation. For the Matthews and Hurd data 17 corresponding data points were compared at pressures up to 1500 psia (the limit of the Matthews and Hurd data). For each pair of points the data of this investigation were consistently higher than the literature values, with the average deviation being 0.7%.

For the comparison with the Mueller data, the 24 data points of this investigation were higher in each case than the literature values. The average deviation was approximately 0.7%.

Comparisons with Published Ethylene Data

In Figure 15 the vapor-phase ethylene data from Table IV are compared with the literature data of Walters et al (68) and York and White (69).

The data of Walters cover the range +20 to +100°F, with pressures from 50 to 600 psia. The data are presented in the form of an equation, which has an estimated accuracy of 0.25%. The data of York and White cover the range -140 to +500°F, with pressures from 14.7 to 4400 psia. These data represent an interpolation and extension of the data of Michels (38). An accuracy of 0.3% is claimed by York and White. From Figure 15 the literature values from the two sources are seen to agree within the accuracy (0.25 to 0.3%) claimed by both investigators.

Using a large plot similar to Figure 15 these literature values were compared at even values of pressure with the data of this investigation. In all cases the data of this investigation were higher than the literature data. The average difference between compressibility factors was approximately 0.6%. The York and White data above 600 psia were not used in this direct comparison, as these data below 77°F represent an extrapolation by York and White of the data of Michels.

The pronounced curvature of the 60°F isotherm in the region 700 to 1200 psia deserves some comment. The curvature arises since the points are in the neighborhood of the critical point (49.82°F, 742.1 psia).

Considering the accuracy of the published literature data and the differences between the literature data and the data of this investigation, the following conclusion can be made. The data of this investigation appear high by as much as 0.4 to 0.5% for methane, and are high by 0.3 to 0.4% for ethylene.

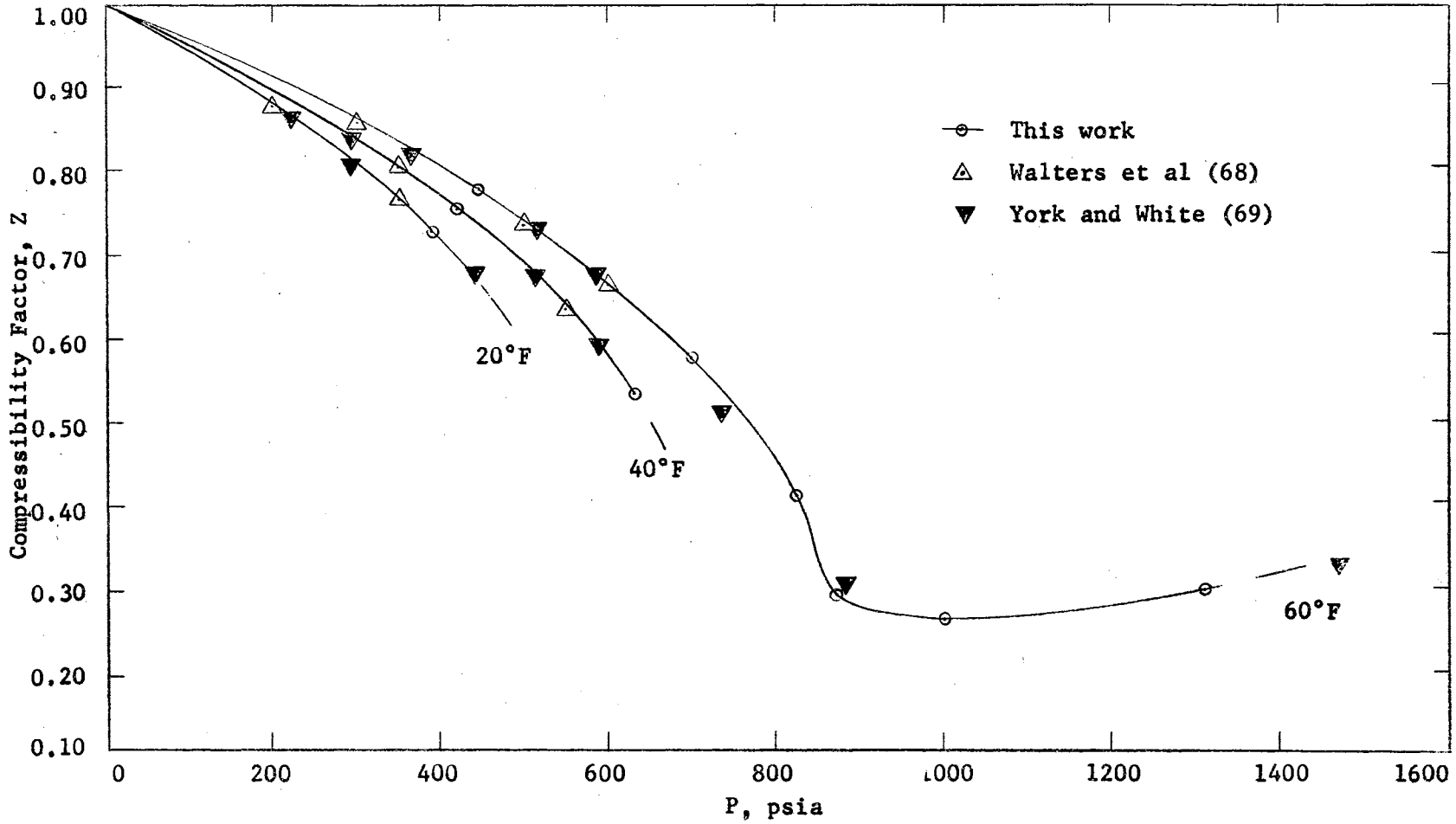

Figure 15

Vapor Phase Compressibility Factor Comparisons for Ethylene

CHAPTER VII

CONCLUSIONS AND RECOMMENDATIONS

The purposes of this investigation were:

1) to develop and operate an experimental PVT apparatus for the determination of precise volumetric data for a binary system,

2) to compare the resultant data with existing virial coefficients and equations of state in an effort to determine and emphasize the need for further work on methods of improving these equations.

Experimental data were taken for the methane-ethylene binary system, and virial coefficients were derived. The data were compared with equations of state and with theoretical virial coefficient relationships. Conclusions and recommendations from this investigation are summarized in the following.

A. Calculational

Conclusions

1. The experimental compressibility factors were compared versus the original BWR equation and the Edmister generalized BWR equation. The standard deviations from the experimental values were determined to be 0.015 for the generalized BWR equation and 0.022 for the original BWR equation.

2. Experimental second and third virial coefficients for the methane-ethylene system were compared with the BWR equation (6), the Edmister generalized form of the BWR equation (20), and the RK

equation (58). The Edmister generalized form fits this system better than do the other two equations tested. For second virial coefficients, standard deviations from the experimental data are summarized as BWR (5.99 cm^3/gm mole), generalized BWR (3.14 cm^3/gm mole), and RK (7.37 cm^3/gm mole). For third virial coefficients, the resultant standard deviations are BWR(3.7×10^2 $cm^6/gm\ mole^2$), generalized BWR(2.1×10^2 $cm^6/gm\ mole^2$), and RK(12.8×10^2 $cm^6/gm\ mole^2$).

3. For each of the six systems investigated the reference isotherm data from the Burnett apparatus (31) was used. The densities for the isochoric runs were determined directly from the reference isotherm. Indications are that this data is somewhat high; the data is subject to a later revision.

4. No accurate methods were found for the estimation of the interaction coefficient B_{12} from the pure component coefficients. The estimated values were used in Equation III-12 to recalculate values of B_m; the resulting B_m were compared versus the experimental B_m. Of the methods tested the square root method (Equation III-21) gives the lowest standard deviation (6.2 cm^3/gm mole) from the experimental B_m.

5. Least squares values of the interaction coefficient B_{12} were determined by fitting Equation III-12 to the experimental data. The values of B_m were then recalculated using the least squares B_{12}. The B_m so calculated agree with the experimental coefficients to within the estimated accuracy (1.5 cm^3/gm mole) of the coefficients. The standard deviation from the experimental data was 0.74 cm^3/gm mole over the entire range of temperature and composition. This method is quite useful in evaluating the internal consistency of the data.

6. The above conclusions indicate the need for further development of an equation of state. For practicality in calculations and for maximum utility in the application to mixtures, the equation should be generalized and in closed form. To conform with theoretical considerations, the equation should be expressable in "open-ended" form, and the resultant second and third virial coefficients should agree with experimental data.

7. The derivation of virial coefficients by the slope-intercept method was discussed in Chapter III. In this investigation a modification to the method was used in which the original approximation to the second coefficient was significantly improved upon in the derivation of third virial coefficients. This procedure has been used by previous investigators, but its use has not been extensive. The method is sufficiently useful to be re-emphasized at this point.

Recommendations

1. Additional calculational work should be undertaken toward the development of an improved equation of state. The developmental procedure outlined below should be tested on a preliminary basis, using only selected systems for which data is available over an extended range of conditions.

a) The second and third virial coefficients in the BWR equation (Equation III-30 and III-31) should be fitted to experimental pure component virial coefficients, thus evaluating the constants B_o, A_o, C_o, b, a, and c.

b) Using the above values of the constants, the remaining constants α and γ should then be determined by fitting the closed form BWR equation (Equation III-26) to the experimental compressibility factor data.

c) The resulting BWR constants should then be generalized by plotting versus ω, as was done by Edmister in the present generalized form of the BWR equation.

2. The new generalized equation should be tested against mixture compressibility factor data, using the standard mixing rules (Equation III-27). No attempt should be made to improve upon the mathematical form of these mixing rules, however, until definite values are established for the constants for pure components.

3. Programs undertaken to develop improved equations of state should be concentrated only on the generalized BWR equation mentioned above. The two-constant RK equation has the disadvantage that the second and third virial coefficients (Equations III-43) are not independent, as both equations contain both of the constants a and b.

B. Experimental

Conclusions

1. The isochoric method is satisfactory for the experimental determination of compressibility factors. The only significant requirement is that the reference isotherm be established from an independent source. The apparatus is suited to determinations in the gaseous or two-phase region; this particular apparatus was

satisfactorily operated over the temperature range 77 to 20°F, with pressures from 260 to 2400 psia.

2. The long time required to attain thermal equilibrium between successive experimental points is an inherent disadvantage of the procedure. During normal operation, data is taken at the rate of one point per 12 hour period; thus, in order to take a significant amount of data a period of several months is required.

Recommendations

1. For future use in equation of state and virial coefficient work, additional data should be taken with the apparatus. A binary hydrocarbon system is preferable for study, as the resultant data would be of greatest value for comparisons with equations of state.

2. If the data is to be used primarily in the derivation and analysis of virial coefficients, primary emphasis should be placed on the region 100 to 3000 psia. Experimental data taken outside this range has little effect on the determination of virial coefficients by the slope-intercept method. The reference isotherm temperature (77°F) is satisfactory for the upper limit of temperature. The lower temperature limit, however, should be extended. A lower temperature of -50°F is recommended; this temperature would provide a considerably larger temperature range, thus allowing a more thorough theoretical analysis of the resultant data.

3. For the pure components as well as the mixtures, samples of the highest purity should be obtained. Analyzed mixtures of "prep grade" gases are readily available from commercial suppliers.

For future use of the apparatus the following modifications are recommended.

4. Using the existing mechanical refrigeration system (containing Freon-12) the apparatus may be operated as low as 0 to 10°F. This operating range could be extended as low as -50°F or below by using a system containing a different refrigerant such as Freon 22 (B.P. -41.4°F) or possibly Freon 13 (B.P. -114.6°F). A closed loop system of this type has the advantage of both convenience and economy as compared to liquid nitrogen-cooled systems.

5. As a circulating liquid in the annular space containing the copper refrigeration coils, the use of the 60% ethylene glycol/40% water solution should be continued. The flammability characteristics of other frequently used liquids, such as iso-pentane or iso-octane, make their use undesirable.

6. If the attainment of temperatures significantly below -50°F is desired, the use of liquid nitrogen (B.P. -322°F) should be attempted. The direct use of acetone and dry ice (sublimation point -112°F) for long periods of time was found to give poor temperature control inside the cryostat. This was due to considerable thermal gradients that occurred in the acetone solution.

7. One source of experimental error was the DPI cell, which contained a small amount of gas and was located outside the low temperature cryostat (Figure 1, Chapter IV). This particular type DPI cell was designed for operating temperature no lower than +40°F. Consideration should be given to replacing this cell with a cryogenic type cell, which could be placed directly inside the cryostat. Such

cryogenic cells have recently been developed by Ruska, and are similar to the Ruska cell used in the present investigation. With the cryogenic cell situated inside the low-temperature cryostat it would still be necessary to separate the fluid in the upper portion of the DPI cell from the oil in the Ruska gage by means of a high pressure mercury u-tube. The fluid in the DPI cell must have a freezing point below the lowest temperature investigated. For this application methylcyclopentane (freezing point -224°F) is recommended.

8. In this investigation the DPI cell and the bomb were connected via 1/8 inch OD stainless steel tubing. As the inner volume of this tubing is significant, the tubing should be replaced by 1/16 inch OD tubing.

9. In the present apparatus the measuring thermometer and thermocouple were located in the controlled temperature air bath, immediately adjacent to the bomb. For increased accuracy in temperature measurements, it is recommended that a calibrated platinum thermometer be installed inside the bomb. The mounting of this thermometer inside the bomb (Figure 2, Chapter IV) could be accomplished by using special packing glands developed by the Conax Corporation, Buffalo, New York. The glands may be mounted through the wall with ordinary 1/4 inch NPT mounting threads, and will withstand temperatures as low as -300°F at working pressures up to 10,000 psi.

A metal-enclosed platinum thermometer is available from the Leeds and Northrup Company (Catalog No. 8160) that would likely serve for this application for temperatures as low as -40°F. For much wider ranges of application (-436° to +900°F) platinum resistance temperature sensors are available from the Sostman Company,

Cranford, New Jersey. These sensors have a reported temperature stability of 0.001°C and could easily be calibrated over the desired working range.

The entire platinum thermometer and packing gland assembly could thus be mounted into the bomb through its top part. This would require a modification to the upper part of the bomb due to the 7/64 inch drill and due also to the seat for the Ruska connector.

10. The bottom and center bearings on the steel blower shaft (Plate III, Chapter IV) should be replaced by bearings designed for continuous operation at lower temperatures.

11. As mentioned previously, the temperature control inside the cryostat was affected by rapid fluctuations in the laboratory air temperature. For future work the apparatus should be located so that temperature control of approximately $\pm$ 1°F could be attained in the immediate vicinity of the cryostat.

A SELECTED BIBLIOGRAPHY

1. Amagat, E. H., Ann. Chim. et Phys. 29, 68 (1893).

2. Amagat, E. H., Annales de Chimie (5), 22, 353, (1881).

3. Bean, H. S., J. Research, National Bureau of Standards, vol 4 (1930).

4. Beattie, J. A., Proc. Am. Acad. Arts Sci. 69, 389 (1934).

5. Benedict, M., G. B. Webb, and L. C. Rubin, Chem. Eng. Progress 47, 419 (1951).

6. Benedict, M., G. B. Webb, and L. C. Rubin, J. Chem. Phys. 8, 334 (1940).

7. Bloomer, O. T., Institute of Gas Technology Research Bulletin 13, Institute of Gas Technology, Chicago, Illinois (1952).

8. Bridgman, P. W., "The Physics of High Pressure", G. Bell and Sons, Ltd., London (1958).

9. Burnett, E. S., J. Appl. Mechanics 58, A-136 (1936).

10. Canfield, F. B., T. W. Leland, and R. Kobayashi, Advan. Cry. Eng. 8, 146, Plenum Press, New York (1963).

11. Cawood, W., and H. S. Patterson, J. Chem. Soc. (London), Part 1, 619 (1933).

12. Condon, E. U., and H. Odishaw, "Handbook of Physics", McGraw-Hill Book Company, New York (1958).

13. Connally, J. F., and G. A. Kandalic, Phys. Fluids 3, 463 (1960).

14. Dodge, B. F., "Chemical Engineering Thermodynamics", McGraw-Hill Book Co., Inc., New York (1944).

15. Doolittle, A. K., I. Simon, and R. M. Cornish, AIChE Journal 6, 150 (1960).

16. Douslin, D. R., "Progress in International Research on Thermodynamic and Transport Properties." Papers of the Symposium on Thermophysical Properties, 2nd, Princeton, N. J., (1962), 135.

17. Douslin, D. R., R. T. Moore, J. P. Dawson, and G. Waddington, J. Am. Chem. Soc. 80, 2031 (1958).

18. Eakin, B. E., and R. T. Ellington, Papers of the Symposium on Thermal Properties, Purdue University, Lafayette, Indiana, (1959), 195.

19. Edmister, W. C., "Applied Hydrocarbon Thermodynamics", Gulf Publishing Company, Houston, Texas (1961).

20. Edmister, W. C., Private Communication, May 11, 1966.

21. Freeth, F. A., and T. T. H. Verschoyle, Proc. Royal Soc. 130A, 453 (1931).

22. Goodwin, R. D., J. Research, National Bureau of Standards, vol 65C, 231 (1961).

23. Hirschfelder, J. O., C. F. Curtis, and R. B. Bird, "Molecular Theory of Gases and Liquids", John Wiley and Sons, Inc., New York (1964).

24. Holborn, L., and H. Schultze, Annalen der Physik 47, 1089 (1915).

25. Hsu, C. C., and J. J. McKetta, J. Chem. Eng. Data 9, 45 (1964).

26. International Congress of Pure and Applied Chemistry, 18th, Montreal, Quebec, 1961.

27. Johnson, D. P., J. L. Cross, J. D. Hill, and H. A. Bowman, Ind. Eng. Chem. 49, 2046 (1957).

28. Keyes, F. G., Proc. Am. Acad. Arts Sci. 68, 505 (1933).

29. Keyes, F. G., and H. G. Burks, J. Am. Chem. Soc. 49, 1403 (1927).

30. Kvalnes, H. M., and V. L. Gaddy, J. Am. Chem. Soc. 53, 394 (1931).

31. Lee, R. C., Private Communication, July 19, 1966.

32. Levelt, J. M. H., Doctorate Thesis, University of Amsterdam (1958).

33. Masson, I., and L. G. F. Dolley, Proc. Royal Soc. 103A, 524 (1923).

34. Matthews, C. J., and C. O. Hurd, Trans. AIChE 42, 55 (1946).

35. Mayer, J. E., J. Phys. Chem. 43, 71 (1939).

36. Michels, A., Annalen der Physik 73, 577 (1924).

37. Michels, A., B. Blaisse, and J. Hoogschagen, Physica 9, 565 (1942).

38. Michels, A., J. DeGruyter, and F. Niesen, Physica 3, 346 (1936).

39. Michels, A., and M. Geldermans, Physica 9, 967 (1942).

40. Michels, A., and R. O. Gibson, Annalen der Physik 87, 850 (1928).

41. Michels, A., J. M. Levelt, and W. DeGraaff, Physica 24, 659 (1958).

42. Michels, A., R. J. Lunbeck, and G. J. Wolkers, Physica 17, 801 (1951).

43. Michels, A., C. Michels, and H. Wouters, Proc. Royal Soc. 153A, 214 (1935).

44. Michels, A., and G. W. Nederbragt, Physica 2, 1001 (1935).

45. Michels, A., and G. W. Nederbragt, Physica 3, 569 (1936).

46. Michels, A., T. Wassenaar, J. M. Levelt, and W. DeGraaff, Appl. Sci. Res. 4A, 381 (1954).

47. Michels, A., T. Wassenaar, and Th. N. Zwietering, Physica 18, 67 (1952).

48. Miller, J. E., L. Stroud, and L. W. Brandt, J. Chem. Eng. Data 5, 6 (1961).

49. Mueller, W. H., Doctorate Thesis, The Rice Institute, Houston, Texas (1959).

50. Mueller, W. H., T. W. Leland, Jr., and R. Kobayashi, AIChE Journal 7, 267 (1961).

51. Olds, R. H., H. H. Reamer, B. H. Sage, and W. H. Lacey, Ind. Eng. Chem. 35, 922 (1943).

52. Pavlovich, N. V., and D. L. Timrot, Teploinergetika 5, 69 (1958).

53. Pfefferle, W. C., Jr., J. A. Goff, and J. G. Miller, J. Chem. Phys. 23, 509 (1955).

54. Pfennig, H. W., and J. J. McKetta, Pet. Ref. 36, No. 11, 309 (1957).

55. Pitzer, K. S., D. Z. Lippman, R. F. Curl, Jr., C. M. Huggins, and D. E. Patersen, J. Am. Chem. Soc. 77, 3427 (1955).

56. Prausnitz, J. M., AIChE Journal 5, 3 (1959).

57. Prausnitz, J. M., and R. D. Gunn, AIChE Journal 4, 430 (1958).

58. Redlich, O., and J. N. S. Kwong, Chem. Rev. 44, 233 (1949).

59. Rossinni, F. D., F. T. Gucker, Jr., H. L. Johnson, L. Pauling, and G. W. Vinal, J. Am. Chem. Soc. 74, 2699 (1952).

60. Scarborough, J. L., "Numerical Mathematical Analysis", 4th edition, The Johns Hopkins Press, Baltimore, Maryland (1958).

61. Schamp, H. W., Jr., E. A. Mason, A. C. B. Richardson, and A. Altman, Phys. Fluids 1, 329 (1958).

62. Schneider, W. G., Can. J. Research 27B, 339 (1949).

63. Silberberg, I. H., K. A. Kobe, and J. J. McKetta, J. Chem. Eng. Data 4, 314 (1959).

64. Solbrig, C. W., and R. T. Ellington, Chem. Eng. Progress Symp. Series 59, No. 44, 127 (1963).

65. Stimson, H. F., J. Research, National Bureau of Standards, vol 65A, No. 3 (1961).

66. Timoshenko, S., "Strength of Materials, Part II, Advanced Theory and Problems", 3rd edition, D. Van Nostrand Company, Princeton, New Jersey (1957).

67. Vennix, Alan J., Doctorate Thesis, Rice University, Houston, Texas (1966).

68. Walters, R. J., J. H. Tracht, E. B. Weinberger, and J. K. Rodgers, Chem. Eng. Progress 50, 511 (1954).

69. York, R., and E. F. White, Trans. AIChE 40, 227 (1944).

APPENDIX A

THERMOMETRY STANDARDS AND THERMOCOUPLE CALIBRATIONS

Calibration of Thermocouples

The copper-constantan thermocouple B2 was connected to the potentiometer through a double pole-double throw (DPDT) switch as is illustrated in Figure 4. The thermocouple and platinum resistance thermometer were situated in the cryostat (Figure 1), directly beside the bomb. To further insure thermal equilibrium between the thermocouple and thermometer, a small glass container was filled with liquid iso-octane, and the thermocouple and platinum thermometer were immersed into the liquid at a distance of separation of about one inch.

The thermocouple was calibrated at approximately 40°F increments over the temperature range -40 to +95°F. Twenty readings of thermocouple output (mv) versus thermometer resistance (absolute ohms) were made at each successive temperature level. The calibration is expressed over the above temperature range as

$$T°F = 29.382 + 45.938(POT) - 0.49224(POT)^2 + 0.59268(POT)^3 \qquad (A-1)$$

where POT = the thermocouple output, mv, with reference to an ice bath. The accuracy of the calibration is estimated as 0.01 to 0.02°K.

The DPI cell thermocouple was connected to the potentiometer as shown in Figure 4. For purposes of calibration, the thermocouple

and platinum thermometer were placed inside an insulated, high-temperature air thermostat. This thermostat was in use for phase equilibria determinations, and was located adjacent to the isochoric apparatus. Thermal equilibrium was insured by immersing both the thermocouple and thermometer in a beaker containing heavy hydrocarbon oil.

The thermocouple was calibrated at three temperature levels over the range 80 to 115°F, with twenty calibration points being taken at each temperature level. The calibration is expressed over the above temperature range as

$$T°F = 24.987 + 56.861(POT) - 4.8565(POT)^2 \qquad (A-2)$$

The accuracy of the calibration is estimated as 0.01 to 0.02°K.

Reference Junction

The reference junction thermocouples (Figure 4) were maintained inside a covered, one liter, vacuum type flask filled with an equilibrium solution of water and ice. Distilled water for preparing ice was obtained from a Barnstead still located in the laboratories of the School of Civil Engineering.

The vacuum flask was periodically cleaned with soap and water and then rinsed with ethyl ether to remove any traces of impurities.

Platinum Resistance Thermometer

The resistance thermometer is a Model 8163 Leeds and Northrup four lead instrument (Serial Number 1576919). The thermometer was calibrated by NBS on May 7, 1964, for the temperature range -190 to 445°C. The temperatures are given in degrees Celsius (centigrade) on the

International Practical Temperature Scale of 1948 (65). The calibration points are the triple point of water, the steam point, the sulfur point, and the oxygen point. These points are measured with a continuous current of 2.0 milliamperes through the platinum element. The thermometer was certified by NBS to be a satisfactory defining standard for temperature in accordance with the text of the International Practical Temperature Scale. The calibration is defined by the following formula,

$$t = \frac{R_t - R_o}{\alpha R_o} + \delta\left(\frac{t}{100} - 1\right)\frac{t}{100} + \beta\left(\frac{t}{100} - 1\right)\left(\frac{t}{100}\right)^3 \qquad \text{(A-3)}$$

where t is the temperature, at the outside surface of the tube protecting the platinum resistor, in degrees Celsius; and R_t and R_o are the resistances of the platinum resistor at t° and 0°C, respectively.

The following values are given for the four constants.

α	0.003925284	
δ	1.49164	
β	0.11033	t below 0°C
	0	t above 0°C
R_o	25.5168	absolute ohms

Temperature Bridge

The temperature bridge is a Leeds and Northrup Mueller temperature bridge (Cat. No. 8069-B). The operating range of the bridge is from zero to 111.111 ohms, the bridge balance being obtained by six step-by-step dial switches to within 0.0001 absolute ohms. The null detector for the bridge is a Leeds and Northrup high sensitivity ballistic galvanometer (Cat. No. 2284-d), used with a Leeds and Northrup lamp

and scale reading device (Cat. No. 2170). The galvanometer was located atop a concrete vibration-free pedestal which was sunk into the earth.

APPENDIX B

SAMPLE CALCULATION OF PRESSURE

The pressure to be calculated is the absolute pressure, psia, in the lower chamber of the DPI cell.

The masses are listed by Ruska as "Apparent Mass versus Brass," or the mass M_A which they appear to have when compared in air under normal conditions against normal brass standards (no correction being made for the buoyant effect of the air).

The approximate relationship

$$W = \frac{g}{g_c}\left(1 - \frac{\rho_{AH}}{\rho_B}\right)M_A \qquad \text{(B-1)}$$

is recommended by Ruska as being accurate to within one part per million. Here W = the actual weight load on the piston, lb

ρ_{AH} = the density of air at Houston = 0.0012 gm/cc

ρ_B = the density of brass = 8.4 gm/cc

g = the acceleration due to gravity at Stillwater[1/] = 979.777 cm/sec^2

g_c = the standard acceleration due to gravity = 980.665 cm/sec^2

[1/] See Appendix L.

The calibration data for the Ruska masses, M_A, is tabulated in Appendix J.

The pressure P at the reference mark on the Ruska gage is given by

$$P = \frac{W}{A_E} \tag{B-2}$$

where P = pressure, psig

A_E = the effective area of the piston at P psig and t°C.

The area of the piston must be corrected for thermal expansion and for pressure distortion. The following equations are recommended by Ruska.

$$A_{o_t} = A_o[1 + C(t - 25)]$$

$$A_E = A_{o_t}(1 + bP) \tag{B-3}$$

Here A_o = area of piston at 25°C and zero psig

C = coefficient of thermal expansion for the piston

t = Ruska temperature, °C

A_{o_t} = area of piston at zero pressure and t°C

b = coefficient of pressure distortion.

The oil head correction HCORR between the reference mark on the Ruska gage and the diaphragm of the DPI cell is given by

$$HCORR = h\rho \tag{B-4}$$

where h = height, inches, between the reference mark and level of diaphragm,

ρ = .031 psi/vertical inch of oil height, as recommended by Ruska.

From Figure N-1, h = -(13.819 - 2.0) inches; thus HCORR = -(13.819 -2.0) (0.031) = -.366 psi.

The zero shift of the DPI cell with pressure was determined by Ruska. The results may be expressed by the linear relationship

$$P_L = P + 2.08 \times 10^{-6} P = (1 + 2.08 \times 10^{-6})P \qquad \text{(B-5)}$$

where P = the pressure, psi, of the upper chamber of the DPI cell, and

P_L = the pressure, psi, of the lower chamber of the DPI cell.

Combining the above corrections with Equation B-2 gives

$$P_L = (W/A_E - 0.366)(1 + 2.08 \times 10^{-6}) \text{ psig, or} \qquad \text{(B-6)}$$

$$P_L = (W/A_E - 0.366)(1 + 2.08 \times 10^{-6}) + \text{ATM} \quad \text{psia} \qquad \text{(B-7)}$$

where ATM = the barometric pressure, as determined by the Texas Instruments barometer.

A sample calculation is given below. The required data is listed in Table B-I.

For the low range cylinder

$$A_o = 0.130219 \text{ in}^2$$
$$C = 1.7 \times 10^{-5}/°C$$
$$b = -5.4 \times 10^{-8}/\text{psi}$$

From Equation B-1

$$W = \frac{979.777}{980.665}\left(1 - \frac{0.0012}{8.4}\right) M_A$$

$$= (0.99895176)(231.22625) = 230.98387 \text{ lb.}$$

From Equation B-3

$$A_E = 0.130219\ [1 + 1.7 \times 10^{-5}(25.9 - 25.0)][1 - 5.4 \times 10^{-8}(1788)]$$

$$= 0.1302084\ in^2.$$

From Equation B-7

$$P_L = (\frac{230.98387}{0.1302084} - 0.366)(1 + 2.08 \times 10^{-6}) + 14.172$$

$$P_L = 1787.765\ psia.$$

TABLE B-I

DATA FOR PRESSURE CALCULATION

Run No. 9A — Cylinder: Low Range

Masses	Apparent Mass Versus Brass (M_A) pounds
A	26.03509
B	26.03537
C	26.03571
D	26.03570
E	26.03536
F	26.03592
G	26.03603
H	26.03558
L	13.01794
M	5.20714
O	2.60359
P	1.30181
W	0.02604
B Bar	0.00260
C Bar	0.00130
Low Tare	0.78107
	M_A = 231.22625

t = 25.9°C

ATM = 14.172 psia

APPENDIX C

OPERATING CHARACTERISTICS OF THE TEXAS INSTRUMENTS BAROMETER

A Texas Instruments servo-nulling precision pressure gage (Model No. 141A) was used for determining barometric pressure.

This gage consists of a zero to 100 cm-Hg range fused (low hysteresis) quartz bourdon tube contained within a capsule. A small mirror is suspended from the lower portion of the bourdon tube. An optical transducer is mounted on a gear which travels concentrically around the suspended mirror. Light reflected from the mirror falls on a pair of balanced photocells which are connected to a microammeter readout scale. A closed-loop motor-driven servo system continuously accomplishes the nulling by automatically positioning the gear so that the microammeter reading is zero.

The tube has full scale rotation of 100 degrees, and the corresponding position of the gear is digitally presented on a counter readout. The null position is constantly maintained for minute variations in the pressure being measured. The counter reading may then be multiplied by a scale factor (determined by calibration) to determine the gage pressure. As this instrument is used exclusively for the measurement of absolute pressure, the capsule surrounding the bourdon tube is permanently evacuated.

To determine the barometric pressure only two readings are necessary; 1) the counter reading, and 2) the temperature of the instrument (for making a small correction for very precise readings).

The instrument has been calibrated over the entire range (zero to 100 cm-Hg) versus a Texas Instruments dead weight gage. The dead weight gage has an accuracy of 0.015%, with a calibration that is directly traceable to NBS. As recommended by Texas Instruments, the calibration data was fitted to an empirical equation. The equation is

$$P = 0.019336842\ [1 + 1.3 \times 10^{-4}(\frac{T - 32.0}{1.8} - 24.0)] \cdot$$

(C-1)

$$[0.03167 + 9.9358826\ R - 0.8743147 \times 10^{-3}R^2 - 0.16175319 \times 10^{-5}R^3]$$

where P = psia

R = scale reading (approximate) cm-Hg

T = temperature at gage, °F.

APPENDIX D

CALIBRATION OF BOURDON GAGES

TABLE D-I

CALIBRATION OF REFERENCE BOURDON GAGES

Ruska Pressure[1/] psia	Acco Helicoid Bourdon Gage psia	XFO Maxisafe Bourdon Gage psia
610	790	705
1140	1310	1225
1950	2155	2045

[1/] All units psia. Barometric pressure determined by Texas Instruments barometer.

TABLE D-II

CALIBRATION OF CROSBY BOURDON GAGE

Ruska Pressure psia	Crosby AIH Bourdon Gage psia
165	200
280	305
365	390
465	495
1010	1005
1515	1500
2010	1985

APPENDIX E

SAMPLE CALCULATION OF VOLUME RATIO V_D/V_B

The determination of the ratio of the volume V_D of the DPI cell to the volume V_B of the bomb was discussed in Chapter IV. A sample calculation of this ratio is given as follows.

Before the expansion the temperature at each section of the apparatus was determined, and the pressure P_D' at the diaphragm of the DPI cell was measured. Pressures for each section of the apparatus were corrected for heads of gas using Equations N-14 through N-16, and the corresponding compressibility factors for the nitrogen were determined from the literature values of Michels (42). Airco prepurified nitrogen[1/] was used. The results are tabulated as follows.

[1/] The prepurified nitrogen was obtained from a local supplier. The maximum oxygen content was given as 0.001%, and the moisture content was 0.0012% with a trace of argon. The remainder was nitrogen.

TABLE E-I

DATA, BEFORE EXPANSION, FOR DETERMINATION OF VOLUME RATIO

Run #4

T'_D(°F)	T'_5	T'_4	T'_3	T'_2	T'_1	T'_B
93.875	72.7	72.7	79.73	83.24	86.76	93.799
P'_D(psia)	P'_5	P'_4	P'_3	P'_2	P'_1	P'_B
2052.353	2052.387	0.00151	0.00151	0.00151	0.00151	0.00151
Z'_D	Z'_5	Z'_4	Z'_3	Z'_2	Z'_1	Z'_B
1.0328	1.0243	1.0	1.0	1.0	1.0	1.0

After the expansion the results are given as follows.

TABLE E-II

DATA, AFTER EXPANSION, FOR DETERMINATION OF VOLUME RATIO

Run #4

T_D(°F)	T_5	T_4	T_3	T_2	T_1	T_B
93.967	73.2	73.2	80.07	83.51	86.95	93.828
P_D(psia)	P_5	P_4	P_3	P_2	P_1	P_B
54.11103	54.11195	54.11195	54.11331	54.11427	54.11514	54.11686
Z_D	Z_5	Z_4	Z_3	Z_2	Z_1	Z_B
1.0057	1.0053	1.0053	1.0055	1.0055	1.0056	1.0057

Equation N-10 was used to determine the volume ratio.

$$\frac{V_D}{V_B} = -\Bigg\{ \frac{[F(T_B-95) + 0.003868]\left[\frac{P}{ZT} - \left(\frac{P}{ZT}\right)'\right]_{BT} + 0.01537\left[\left(\frac{P}{ZT}\right) - \left(\frac{P}{ZT}\right)'\right]_5}{\left[\left(\frac{P}{ZT}\right) - \left(\frac{P}{ZT}\right)'\right]_D} + \frac{0.01511\left[\left(\frac{P}{ZT}\right) - \left(\frac{P}{ZT}\right)'\right]_4 + 0.003794\left\{\left[\left(\frac{P}{ZT}\right)-\left(\frac{P'}{ZT}\right)\right]_3 + \left[\left(\frac{P}{ZT}\right)-\left(\frac{P}{ZT}\right)'\right]_2\right\}}{\left[\left(\frac{P}{ZT}\right) - \left(\frac{P}{ZT}\right)'\right]_D} + \frac{0.003273\left[\left(\frac{P}{ZT}\right) - \left(\frac{P}{ZT}\right)'\right]_1}{\left[\left(\frac{P}{ZT}\right) - \left(\frac{P}{ZT}\right)'\right]_D} \Bigg\} \qquad \text{(N-10)}$$

where $F(T_B - 95)$ is given by Equation N-9.

$$F(T_B - 95) = \frac{V_{BT}}{V_B} = [1 + 9.5 \times 10^{-6}(T_B - 95)]^3 \qquad \text{(N-9)}$$

Substituting the data from Tables E-I and E-II in Equation N-10,

$$[F(T_B - 95) + 0.003868] \times$$

$$\left[\frac{54.11686}{(1.0057)(93.828 + 459.670)} - \frac{0.00151}{1.0(93.799 + 459.670)}\right] = 0.098822$$

$$0.01537\left[\frac{54.11195}{(1.0053)(73.2 + 459.670)} - \frac{2052.387}{1.0243(72.7 + 459.670)}\right] = -0.056296$$

$$0.01511\left[\frac{54.11195}{1.0053(73.2 + 459.670)} - \frac{0.00151}{1.0(72.7 + 459.670)}\right] = +0.001526$$

$$0.003794\left\{\left[\frac{54.11331}{1.0055(80.07 + 459.670)} - \frac{0.00151}{1.0(79.73 + 459.670)}\right] + \left[\frac{54.11427}{1.0055(83.51 + 459.670)} - \frac{0.00151}{1.0055(83.51 + 459.670)}\right]\right\} = 0.000754$$

$$0.003273\left[\frac{54.11514}{1.0056(86.95 + 459.670)} - \frac{0.00151}{1.0(86.76 + 459.670)}\right] = 0.000322$$

$$\left[\frac{54.11103}{1.0057(93.967 + 459.670)} - \frac{2052.353}{1.0328(93.875 + 459.670)}\right] = -3.492721$$

$$V_D/V_B = -\left[\frac{0.098822 - 0.056296 + 0.001526 + 0.000754 + 0.000322}{-3.492721}\right]$$

$$V_D/V_B = 0.01292$$

The corresponding results for additional determinations are given as follows.

TABLE E-III

TABULATION OF VOLUME RATIOS

Run No.	V_D/V_B	
3	0.01267	
4	0.01292	
5	0.01225	$(\frac{V_D}{V_B})_{avg} = 0.01263$

The average value, 0.01263, was used in all determinations in this thesis.

APPENDIX F

SAMPLE CALCULATION OF A COMPRESSIBILITY FACTOR

In Appendix N, Equations N-20 and N-21 are derived for calculating the final compressibility factors from experimental data. A sample calculation is presented below for the 57.2% methane system.

For different temperature levels along the isochor, pressures and temperatures corresponding to each section of the apparatus are given in Table F-I.

TABLE F-I

DATA FOR COMPRESSIBILITY FACTOR CALCULATION--FIRST ITERATION

Isochor number 36 Sample: 57.2% methane

T_B = 77°F (P_B = 675.035 psia) Z_B(REF) = 0.8609

T, °F	T_1	T_2	T_3	T_4	T_5	T_D
	88.74	61.53	64.81	76.4	76.4	95.696
P, psia	P_1	P_2	P_3	P_4	P_5	P_D
	675.009	675.000	674.991	674.978	674.978	674.969
	Z_1	Z_2	Z_3	Z_4	Z_5	Z_D
	1.0	1.0	1.0	1.0	1.0	1.0

$T_B = 60°F$ ($P_B = 647.201$ psia)

T, °F	T_1	T_2	T_3	T_4	T_5	T_D
	80.49	58.64	64.00	74.2	74.2	95.242
P, psia	P_1	P_2	P_3	P_4	P_5	P_D
	647.175	647.167	647.158	647.145	647.145	647.137
	Z_1	Z_2	Z_3	Z_4	Z_5	Z_D
	1.0	1.0	1.0	1.0	1.0	1.0

$T_B = 40°F$ ($P_B = 613.305$ psia)

T, °F	T_1	T_2	T_3	T_4	T_5	T_D
	71.20	57.23	64.90	74.8	74.8	95.385
P, psia	P_1	P_2	P_3	P_4	P_5	P_D
	613.279	613.272	613.263	613.251	613.251	613.243
	Z_1	Z_2	Z_3	Z_4	Z_5	Z_D
	1.0	1.0	1.0	1.0	1.0	1.0

$T_B = 20°F$ ($P_B = 577.547$ psia)

T, °F	T_1	T_2	T_3	T_4	T_5	T_D
	61.53	55.24	65.74	74.3	74.3	95.182
P, psia	P_1	P_2	P_3	P_4	P_5	T_D
	577.522	577.515	577.507	577.495	577.495	577.488
	Z_1	Z_2	Z_3	Z_4	Z_5	Z_D
	1.0	1.0	1.0	1.0	1.0	1.0

Here the value of $Z_B(REF) = 0.8609$ (77°F and 675.035 psia) was taken from the reference isotherm data from the Burnett apparatus (31). All temperatures given above were determined from the thermocouple calibrations given in Appendix A; a sample calculation of a pressure point is given in Appendix B. For the first iteration the values of Z_1, Z_2, Z_3, Z_4, Z_5, and Z_D were assumed to be unity, as shown.

Equation N-20 was determined to be

$$D = [F(T_B - 95) + 0.003868]D_{BT} + 0.01263\ D_D + 0.01537\ D_5 + 0.01511\ D_4 + 0.003794(D_3 + D_2) + 0.003273\ D_1 \qquad \text{(N-20)}$$

where D_{BT}, D_D, D_5, D_4, D_3, D_2, and D_1 are densities. In a similar manner Equation N-21 is given as

$$Z_{BT} = \left(\frac{P}{RT}\right)_{BT}\left[\frac{F(T_B - 95) + 0.003868}{DEN}\right] \qquad \text{(N-21)}$$

where

$$DEN = D - 0.01263\ D_D - 0.01537\ D_5 - 0.01511\ D_4 - 0.003794\ (D_3 + D_2) - 0.003273\ D_1 \qquad \text{(N-22)}$$

The first step in the calculation is the determination of the run constant, D. This determination is made at 77°F. The values of T_B(77°F), P_B(675.035 psia) and Z_B(REF), from above and all corresponding values of T, P, and Z are substituted in Equation N-20. The resulting value of the run constant is

$$D = 0.14390 \qquad \text{(F-1)}$$

Using this value of D, the compressibility factors on this same isochor are calculated at the lower temperature levels 60, 40, and 20°F by substituting the above values of temperature and pressure into Equation N-21. The results are summarized in Table F-II.

TABLE F-II

CALCULATED COMPRESSIBILITY FACTORS--RESULTS OF FIRST ITERATION

Isochor number 36 Sample: 57.2% methane

T, °F	P_B, psia	Z
77	675.035	0.8609 (REF)
60	647.201	0.85035
40	613.305	0.83478
20	577.547	0.81638

This procedure was repeated for all other isochors for the 57.2% methane system, and the results were used to interpolate improved values of Z_1, Z_2, Z_3, Z_4, Z_5, and Z_D for use in the next iteration. The interpolation was performed by cross-plotting the data, and the results are given in Table F-III.

TABLE F-III

DATA FOR COMPRESSIBILITY FACTOR CALCULATION--SECOND ITERATION

Isochor number 36 Sample: 57.2% methane

T_B = 77°F (P_B = 675.035 psia) Z_B(REF) = 0.8609

T, °F	T_1	T_2	T_3	T_4	T_5	T_D
	88.84	61.53	64.81	76.4	76.4	95.696
P, psia	P_1	P_2	P_3	P_4	P_5	P_D
	675.016	675.006	674.995	674.979	674.979	674.969
	Z_1	Z_2	Z_3	Z_4	Z_5	Z_D
	0.8692	0.8450	0.8489	0.8602	0.8602	0.8730

T_B = 60°F (P_B = 647.201 psia)

T, °F	T_1	T_2	T_3	T_4	T_5	T_D
	80.49	58.64	64.00	74.2	74.2	95.242
P, psia	P_1	P_2	P_3	P_4	P_5	P_D
	647.182	647.172	647.162	647.147	647.147	647.137
	Z_1	Z_2	Z_3	Z_4	Z_5	Z_D
	0.8692	0.8450	0.8489	0.8602	0.8602	0.8730

T_B = 40°F (P_B = 613.305 psia)

T, °F	T_1	T_2	T_3	T_4	T_5	T_D
	71.20	57.23	64.90	74.8	74.8	95.385
P, psia	P_1	P_2	P_3	P_4	P_5	P_D
	613.285	613.276	613.266	613.252	613.252	613.243
	Z_1	Z_2	Z_3	Z_4	Z_5	Z_D
	0.8702	0.8466	0.8646	0.8973	0.8732	0.8867

T_B = 20°F (P_B = 577.547 psia)

T, °F	T_1	T_2	T_3	T_4	T_5	T_D
	61.53	55.24	65.74	74.3	74.3	95.182
P, psia	P_1	P_2	P_3	P_4	P_5	P_D
	577.529	577.520	577.510	577.497	577.497	577.488
	Z_1	Z_2	Z_3	Z_4	Z_5	Z_D
	0.8700	0.8633	0.8740	0.8808	0.8808	0.8932

Using these improved values of compressibility factor, all above calculations were repeated. From Equation N-20 the value of D was determined to be

$$D = 0.14390 \qquad (F\text{-}2)$$

This value agrees to five significant figures with the original calculation of D (Equation F-1).

Using this value of D the compressibility factors at lower temperatures on the isochor were recalculated, using Equation N-21. The results are given in Table F-IV, below.

TABLE F-IV

CALCULATED COMPRESSIBILITY FACTOR--RESULTS OF SECOND ITERATION

Isochor number 36 Sample: 57.2% methane

T, °F	P_B, psia	Z	Z (rounded)
77	675.034	0.8609 (REF)	0.8609 (REF)
60	647.201	0.85037	0.8504
40	613.304	0.83481	0.8348
20	577.547	0.81637	0.8164

In this case the maximum change in Z was three units in the fifth significant digit, which is negligible. Also, very small changes in P_B arise since the pressure correction due to the difference in head is dependent on the compressibility factors. Generally the rounded compressibility factors after the second iteration agreed to four significant figures with the results of the first iteration. In a few cases the calculations were taken through the third iteration in order to obtain results consistent to four significant figures. In the fourth column the final compressibility factors are shown rounded to four significant figures. All compressibility factors given in Table IV (Chapter VI) were determined in this manner.

APPENDIX G

FUNDAMENTAL CONSTANTS AND MIXTURE COMPOSITIONS

The latest defined value of the universal gas constant R is given (59) as 82.0567 cm^3 -atm/deg K-mole. Converting this value to engineering units, R = 10.731496 (psia - ft^3)/(lb mole °R).

The most recent (65) definition of absolute temperature is expressed as T(°K) = t(°C) + 273.150. Converting this expression directly to the absolute Rankine scale gives T(°R) = t(°F) + 459.670.

The six gas samples used in this investigation were blended and analyzed by the donor, Phillips Petroleum Company, Bartlesville, Oklahoma. The samples were Phillips "pure grade." The Phillips' analyses were performed by mass spectrometry and were reported to the nearest 0.1 mole per cent. The 99.9% ethylene sample and the 99.0% methane sample were independently analyzed by gas chromatography in the laboratories of the School of Chemical Engineering. For each of the components in the two samples the results of these independent analyses differed by less than 0.1%. Results of the entire analysis are given in Table G-I below; all molecular weights were based on the Carbon 12 International Scale of Atomic Weights (26).

TABLE G-I

COMPOSITION ANALYSIS OF MIXTURES

Phillips Petroleum Company Sample Transmittals
No. 44043 through 44048

Components	Mole %	(Methane % - Ethylene %)	Average Molecular Weight	Phillips Cylinder No.
Methane	Trace	0 - 100	28.054	MG-3943
Ethylene	99.9+			
Ethane	Trace			
Total	100.0			
Methane	18.4	20 - 80	25.844	MG-4174
Ethylene	81.6			
Ethane	Trace			
Propane	Trace			
Total	100.0			
Methane	38.4	40 - 60	23.474	MG-1605
Ethylene	61.4			
Propane	0.2			
Ethane	Trace			
Propylene	Trace			
Total	100.0			
Methane	57.2	60 - 40	21.234	MG-576
Ethylene	42.4			
Propane	0.3			
Ethane	0.1			
Propylene	Trace			
Total	100.0			

TABLE G-I (CONTINUED)

Components	Mole %	(Methane % - Ethylene %)	Average Molecular Weight	Phillips Cylinder No.
Methane	78.8	80 - 20	18.656	MG-4083
Ethylene	20.7			
Propane	0.4			
Ethane	0.1			
Propylene	Trace			
Total	100.0			
Methane	99.0	100 - 0	16.213	MG-265
Nitrogen	0.6			
Propane	0.1			
Ethane	0.1			
Isobutane	Trace			
Carbon Dioxide	0.2			
Total	100.0			

APPENDIX H

CALCULATION OF EFFECT OF TEMPERATURE ON THE BOMB VOLUME

The effect of temperature on the bomb volume is determined by assuming the inner volume of the bomb (Figure 2) to be a cylinder of circumference C_{BT} and length L_{BT} at temperature T_B(°F).

The volume V_{BT} at temperature T_B is thus given by

$$V_{BT} = \frac{C_{BT}^2 L_{BT}}{4\pi} \tag{H-1}$$

and the volume V_B at 95°F is

$$V_B = \frac{C_B^2 L_B}{4\pi} \tag{H-2}$$

where C_B and L_B represent the circumference and length, respectively, at 95°F.

The effect of temperature on the circumference and length of the inner volume is expressed by

$$C_{BT} = C_B[1 + \alpha(T_B - 95)]$$

$$L_{BT} = L_B[1 + \alpha(T_B - 95)] \tag{H-3}$$

Here α is the coefficient of thermal expansion, $(°F)^{-1}$.

The expressions for C_{BT} and L_{BT} may be substituted into Equation H-1 to give

$$V_{BT} = \frac{C_B^2 L_B}{4\pi} [1 + \alpha(T_B - 95)]^3 \qquad \text{(H-4)}$$

Dividing Equation H-4 by Equation H-2 gives

$$\frac{V_{BT}}{V_B} = [1 + \alpha(T_B - 95)]^3 \qquad \text{(H-5)}$$

The value of α for type 303 austenitic steel (0 to 600°F) is 9.5×10^{-6} $(°F)^{-1}$. Substituting this value into Equation H-5 gives

$$\frac{V_{BT}}{V_B} = [1 + 9.5 \times 10^{-6}(T_B - 95)]^3 = F(T_B - 95) \qquad \text{(N-9)}$$

APPENDIX J

RUSKA PISTON GAGE CALIBRATION DATA

The Ruska piston gage is a dual range instrument (model 2400HL). The instrument uses two piston-cylinder combinations (low range 6 - 2428 psi; high range 30 - 12,140 psi). Ruska calibrated the gage versus a Ruska laboratory master dead weight gage (No. 7544) which was itself calibrated to an accuracy of one part in 10,000 parts versus an NBS controlled-clearance piston. The NBS identification numbers for the calibration are P6694A/2.6/161365 and P6694B/2.6/161365.

The instrument uses a total of 32 type-303 stainless steel loading weights, their masses being determined by Ruska. The final mass calibration data is given in Table J-I. The calibration is reported to a precision of one part in 50,000 for masses greater than 0.1 pound, one part in 20,000 for masses 0.01 to 0.1 pound, and one part in 10,000 for masses 0.001 to 0.01 pound. Additional gage specifications are given in Table J-II, and a sample pressure calculation is given in Appendix B.

TABLE J-I

RUSKA MASS CALIBRATION DATA

Calibration--Pressure Gage Masses
Calibration date 3-22-63
Ruska Serial No. 10381
Job No. A3567/C2630

Designation			Apparent Mass versus Brass (M_A) pounds
Low Tare		6 psi	0.78107
High Tare	30 psi		0.78107
A	1000	200	26.03509
B	1000	200	26.03537
C	1000	200	26.03571
D	1000	200	26.03570
E	1000	200	26.03536
F	1000	200	26.03592
G	1000	200	26.03603
H	1000	200	26.03558
I	1000	200	26.03563
J	1000	200	26.03608
K	1000	200	26.03568
L	500	100	13.01794
M	200	40	5.20714
N	200	40	5.20715
O	100	20	2.60359
P	50	10	1.30181
Q	20	4	0.52072
R	20	4	0.52074
S	10	2	0.26035
T	5	1	0.13020
U	2	0.4	0.05208
V	2	0.4	0.05209
W	1	0.2	0.02604
X	0.5	0.1	0.01302
A	0.2	0.04	0.005203
A	0.2	0.04	0 005202
B	0.1	0.02	0.002601
C	0.05	0.01	0.001301
D	0.02	0.004	0.000520
D	0.02	0.004	0.000521
E	0.01	0.002	0.000260
F	0.005	0.001	0.000130

TABLE J-II

RUSKA GAGE SPECIFICATIONS

Absolute accuracy		1:10,000
Resolution		5:1,000,000
	Low Range Piston-cyl	High Range Piston-cyl
Piston area 25°C; 0 psig	0.130219 in^2	0.0260440 in^2
Coefficient of thermal expansion	1.7×10^{-5}/°C	1.7×10^{-5}/°C
Coefficient of pressure distortion	-5.4×10^{-8}/psi	-3.6×10^{-8}/psi
Cylinder No.	LC-142	HC-133

APPENDIX K

DETERMINATION OF BOMB JACKET PRESSURE REQUIRED

FOR ELIMINATION OF PRESSURE DISTORTION

The inner chamber of the bomb is assumed to be a cylinder with inner radius a containing a gas at pressure P_i psia. The bomb is

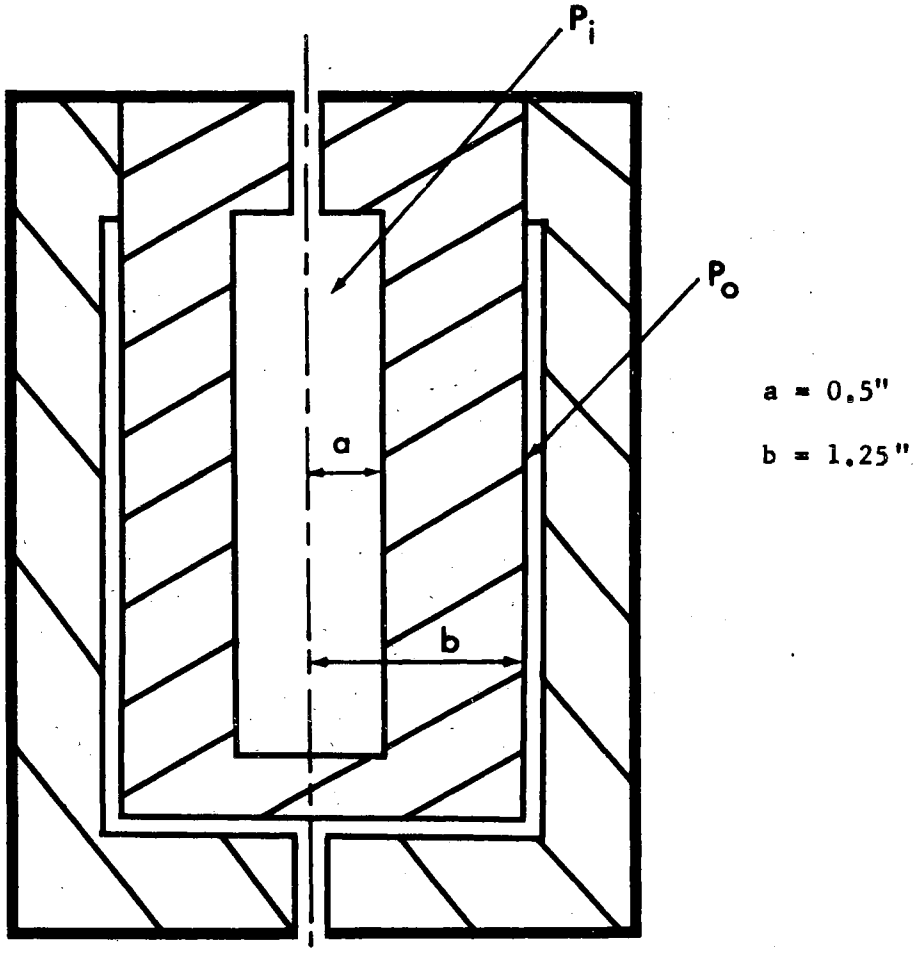

Figure K-1

Drawing of Bomb and Surrounding Jacket

surrounded by a thin cylindrically shaped jacket with inner radius $\underline{b}$, and confining a gas at pressure P_o psia. (See Figure K-1).

Making a free-body diagram across a horizontal section of the bomb (See Figure K-2, below) and summing up the forces on an element in the radial direction gives

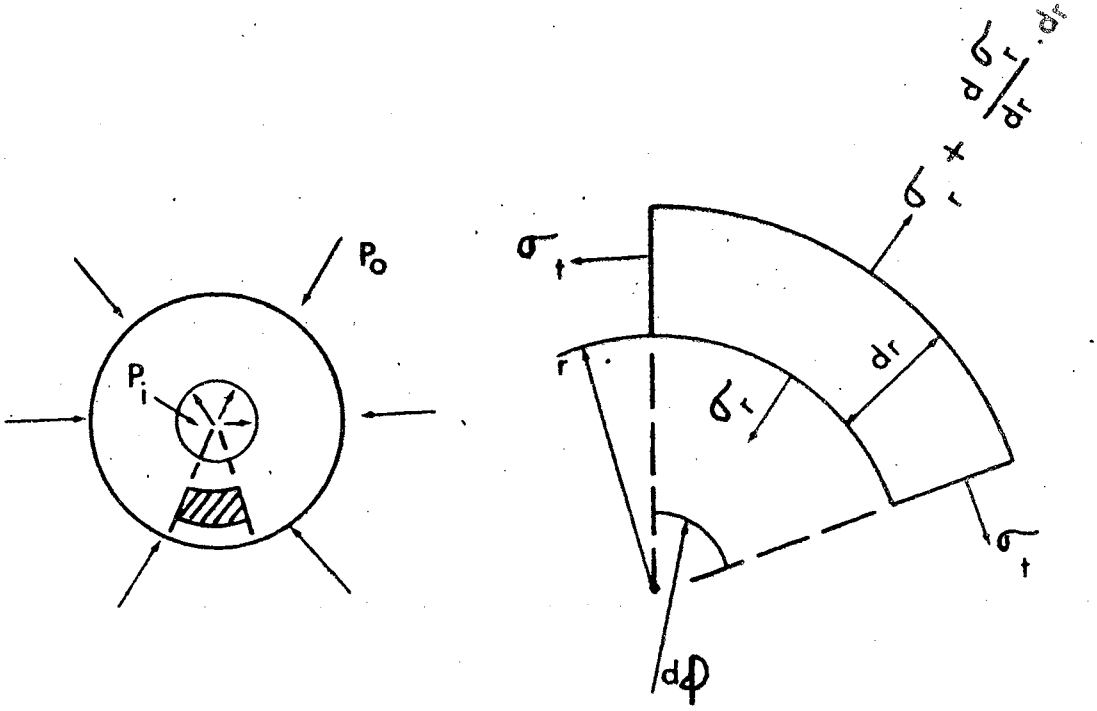

Figure K-2

Free Body Diagram Across Section of Bomb

$$\sigma_r r d\phi + \sigma_t dr d\phi - (\sigma_r + \frac{d\sigma_r}{dr} dr)(r + dr)d\phi = 0 \qquad \text{(K-1)}$$

where

σ_r = normal radial stress acting on the differential element

σ_t = normal hoop stress acting on the differential element

r = radius of the differential element

ϕ = angle between sides of the differential element

The weight of the element is neglected here.

Neglecting small quantities of higher order,

$$\sigma_t - \sigma_r - r \frac{d\sigma_r}{dr} = 0 \qquad \text{(K-2)}$$

Let u be the deformation of the cylinder in the radial direction at radius r. The deformation of the cylinder in the radial direction at r + dr is thus $u + \frac{du}{dr} dr$, and the total elongation on the element is $\frac{du}{dr} dr$.

The strain in the radial direction is thus $\varepsilon_r = \frac{du}{dr}$, and the strain ε_t in the circumferential direction is

$$\varepsilon_t = \frac{u}{r} \qquad \text{(K-3)}$$

The stresses in terms of strains are given (66) by the relations

$$\sigma_r = \frac{E}{1 - \mu^2} (\frac{du}{dr} + \mu \frac{u}{r}) \qquad \text{(K-4)}$$

$$\sigma_t = \frac{E}{1 - \mu^2} (\frac{u}{r} + \mu \frac{du}{dr}) \qquad \text{(K-5)}$$

where

E = modulus of elasticity in tension and compression

μ = Poisson's ratio.

Substituting Equations K-4 and K-5 into Equation K-2, the following equation results

$$\frac{d^2u}{dr^2} + \frac{1}{r}\frac{du}{dr} - \frac{u}{r^2} = 0 \qquad \text{(K-6)}$$

which may be solved to give

$$u = C_1 r + \frac{C_2}{r} \qquad \text{(K-7)}$$

Here C_1 and C_2 are constants to be determined from the following conditions on the inner and outer surfaces of the bomb.

$$\sigma_r = \frac{E}{1-\mu^2}\left[C_1(1+\mu) - C_2\frac{1-\mu}{r^2}\right]$$

$$\sigma_t = \frac{E}{1-\mu^2}\left[C_1(1+\mu) + C_2\frac{1-\mu}{r^2}\right] \qquad \text{(K-8)}$$

$$(\sigma_r)_{r=b} = -P_o \qquad (\sigma_r)_{r=a} = -P_i$$

Solving for C_1 and C_2 gives

$$C_1 = \left(\frac{1-\mu}{E}\right)\frac{a^2P_i - b^2P_o}{b^2 - a^2} \qquad \text{(K-9)}$$

$$C_2 = \left(\frac{1+\mu}{E}\right)\frac{a^2b^2(P_i - P_o)}{b^2 - a^2} \qquad \text{(K-10)}$$

Substituting Equations K-9 and K-10 into Equation K-7 gives the deformation of the cylinder as

$$u = \left(\frac{1-\mu}{E}\right)\left(\frac{a^2P_i - b^2P_o}{b^2 - a^2}\right)r + \left(\frac{1+\mu}{E}\right)\frac{a^2b^2(P_i - P_o)}{b^2 - a^2}\cdot\left(\frac{1}{r}\right) \qquad \text{(K-11)}$$

The deformation u_L due to the axial stresses σ_L must be added to the deformation given by Equation K-11

$$\sigma_L = \frac{P_i a^2 - P_o b^2}{b^2 - a^2}$$

$$\varepsilon_u = -\frac{\mu}{E}\sigma_L \tag{K-12}$$

$$u_L = -\left(\frac{\mu}{E}\right)\frac{P_i a^2 - P_o b^2}{(b^2 - a^2)}\, r \tag{K-13}$$

Here ε_u is the axial strain. u_L is of opposite sign to u in Equation K-11 above, as it is in opposite direction to the deformation u. The total deformation from both Equations K-11 and K-13 is

$$u = \frac{1-\mu}{E}\frac{a^2P_i - b^2P_o}{(b^2 - a^2)}\, r + \left(\frac{1+\mu}{E}\right)\frac{a^2b^2(P_i - P_o)}{(b^2 - a^2)} \cdot \frac{1}{r} - \frac{\mu}{E}\frac{(P_i a^2 - P_o b^2)}{(b^2 - a^2)}\, r \tag{K-14}$$

At the inner radius r = a this deformation must be zero.

$$u = 0 \text{ at } r = a \tag{K-15}$$

This gives

$$0 = (1-\mu)(a^2P_i - b^2P_o) + (1+\mu)b^2(P_i - P_o) - \mu(P_i a^2 - P_o b^2) \tag{K-16}$$

which may be rearranged to

$$P_o = \frac{a^2(1-2\mu) + b^2(1+\mu)}{b^2(2-\mu)} \cdot P_i \tag{K-17}$$

For a = 1/2", b = 1 1/4", and μ = 0.3 (for type 303 stainless steel), Equation K-17 becomes

$$P_o = 0.8024\ P_i \qquad \text{(K-18)}$$

APPENDIX L

ACCELERATION DUE TO GRAVITY AT STILLWATER, OKLAHOMA

The local acceleration due to gravity is given by Condon and Odishaw (12) as

$$g = 978.0524[1 + 0.005297 \sin^2 \psi - 0.0000059 \sin^2 (2\psi) + 0.0000276 \cos^2 \psi \cos 2(\lambda + 25°)] - 0.000060 h \qquad (L-1)$$

where

ψ = latitude

λ = longitude (positive east of Greewich)

h = feet above sea level

At Stillwater, ψ = 36°7' N., λ = 97°4' W., and h = 930 ft. This gives a value for g of

$$g = 979.777 \text{ cm/sec}^2$$

APPENDIX M

ESTIMATION OF INTERACTION SECOND VIRIAL COEFFICIENTS

In correcting the experimental second virial coefficients for impurities (Chapter VI) it was necessary to estimate interaction second virial coefficients B_{12} for the following molecular pairs: 1) methane-nitrogen, 2) ethylene-ethane, and 3) ethylene-propane. The estimations were made using the method proposed by Prausnitz (56, 57). Sample calculations are given below.

Sample Calculation of Methane-Nitrogen Coefficient

The following equation was presented in Chapter III.

$$\frac{B_{ij}}{V_{c_{ij}}} = \theta_B\left(\frac{T}{T_{c_{ij}}}, \omega_{ij}\right) \qquad \text{(III-18)}$$

The combining rules for estimating the interaction parameters $V_{c_{ij}}$, $T_{c_{ij}}$, and ω_{ij} were given by Prausnitz as

$$\begin{aligned} V_{c_{ij}} &= \frac{1}{2}\left(V_{c_i} + V_{c_j}\right) \\ \omega_{ij} &= \frac{1}{2}\left(\omega_i + \omega_j\right) \qquad \text{(M-1)} \\ T_{c_{ij}} &= k_{ij}\sqrt{T_{c_i} T_{c_j}} \end{aligned}$$

where the temperature correction factor k_{ij} is presented graphically as a function of the critical volume ratio V_{c_i}/V_{c_j}.

Denoting methane by subscript i and nitrogen by subscript j, there results

$$V_{c_i} = 1.578^{1/}$$

$$V_{c_j} = 1.443$$

$$V_{c_{ij}} = \frac{1}{2}(1.578 + 1.443) = 1.5105$$

$$V_{c_i}/V_{c_j} = 1.578/1.443 = 1.09$$

$$\omega_i = 0.013$$

$$\omega_j = 0.04$$

$$\omega_{ij} = \frac{1}{2}(0.013 + 0.04) = 0.0265$$

From Figure 1 of reference (56), using a value of V_{c_i}/V_{c_j} of 1.09,

$$k_{ij} = 0.99$$

$$T_{c_i} = 343.89 \qquad T_{c_j} = 226.71$$

$$T_{c_{ij}} = 0.99\sqrt{(343.89)(226.71)} = 276.0$$

1/ In the following calculations all units will be ft^3/lb mole, psia, and °R unless otherwise stated.

The generalized function $(-\theta_B)$ is given in tabular form (56) as a function of $T/T_{c_{ij}}$ and ω_{ij}.

At T = 536.670 (77°F), $T/T_{c_{ij}} = \frac{536.670}{276.0} = 1.95$; and $\omega_{ij} = 0.0265$.

From graphs of the tabular values of $(-\theta_B)$, $\theta_B = -0.202$.

Substituting into Equation III-18,

$$B_{ij} = \theta_B V_{c_{ij}} = (-0.202)(1.5105) = -0.305$$

Converting to cgs units,

$$B_{ij} = (62.428)(-0.305) = -19.1 \text{ cm}^3/\text{gm mole}$$

Results for all temperatures are summarized as follows.

TABLE M-I

Methane-Nitrogen Interaction Coefficients

T°F	B_{12} $\text{cm}^3/\text{gm mole}$
77	-19.1
60	-22.0
40	-25.3
20	-29.0

For the ethylene-ethane and the ethylene-propane coefficients the same calculational procedure was used. The results are summarized below.

TABLE M-II

Ethylene-Ethane Interaction Coefficients

T°F	B_{12} cm^3/gm mole
77	-150.
60	-162.
40	-175.
20	-191.

TABLE M-III

Ethylene-Propane Interaction Coefficients

T°F	B_{12} cm^3/gm mole
77	-200.
60	-216.
40	-234.
20	-254.

The results for the ethylene-ethane and ethylene-propane coefficients are markedly lower (algebraically) than the results for the methane-nitrogen coefficients. This difference is to be expected, however, and is largely due to the fact that the critical temperatures of ethylene, ethane, and propane are considerably higher than those for methane and nitrogen.

APPENDIX N

DERIVATION OF CHARACTERIZING EQUATIONS FOR THE APPARATUS

Determination of the Volume Ratio V_D/V_B

The determination of the volume ratio was discussed in Chapter IV. The equation for this ratio is developed in the following.

Basically, the bomb and DPI cell are allowed to reach equilibrium, the interconnecting valve between the two cells is closed, and the bomb is rinsed with nitrogen and evacuated. The DPI cell is rinsed and is then filled to about 2500 psia with the nitrogen.

The temperatures and pressures of all portions of the system are measured and the interconnecting valve is then opened. After the gas is allowed to equilibrate throughout the system, the temperatures and pressures of all portions of the system are again measured. This information is sufficient to determine the volume ratio as is discussed below.

The dimensioned schematic diagram of the cryostat and DPI cell is shown in Figure N-1; the following quantities are defined with reference to this figure.

V_{BT} = volume of bomb at T°F

V_B = volume of bomb at 95°F

V_D = volume of DPI cell and capillary tubing contained within the DPI cell thermostat at 95°F.

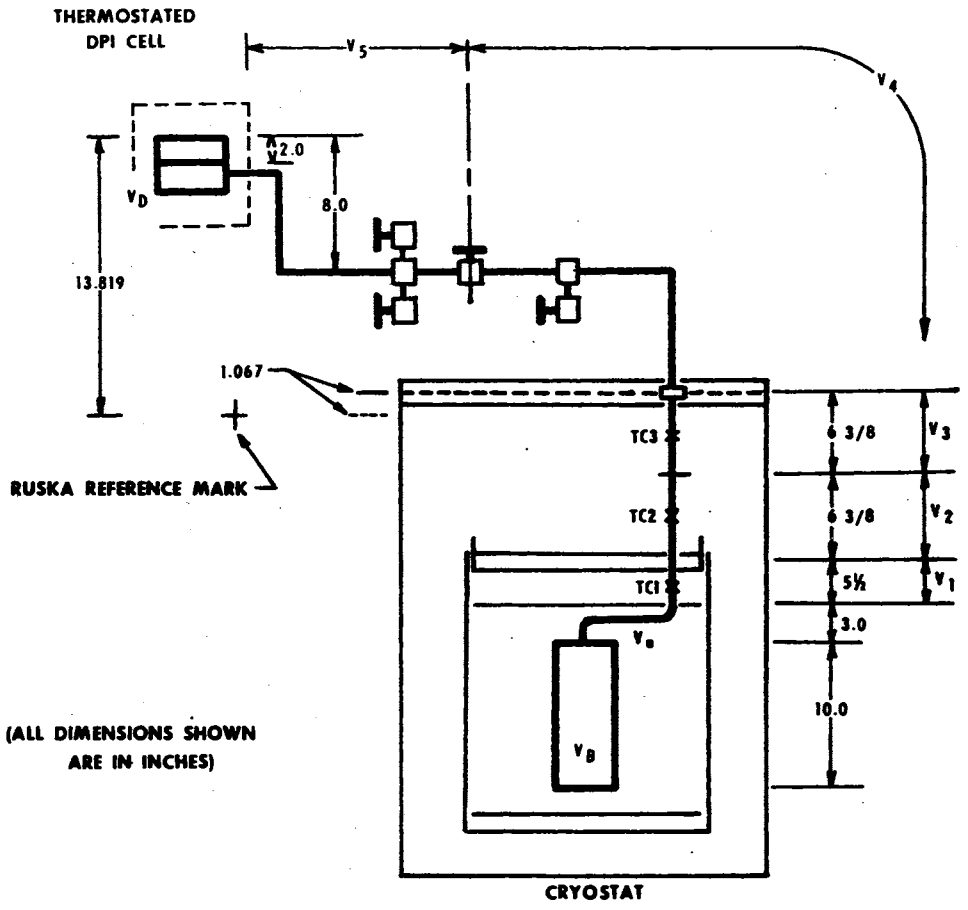

Figure N-1

Schematic Diagram of Cryostat and DPI Cell

V_5 = volume of capillary and fittings extending from the outside of the DPI cell thermostat to the interconnecting valve, as shown

V_4 = volume of capillary and fittings extending from the interconnecting valve to the bottom of the connecting union, as shown

V_3, V_2, and V_1 = volumes, respectively, of the sections of the capillary extending from the bottom of the connecting union to the baffle immediately above the bomb

V_a = volume of capillary between the baffle and the bomb

Before opening the expansion valve,

P_i' = pressure, psia, of gas in volume V_i

T_i' = temperature of gas in volume V_i

Z_i' = compressibility factor (PV/RT) at T_i' and P_i'

n_i' = moles of gas in volume V_i

n' = total moles of gas in system, = $\sum n_i'$

Before the valve is opened, a material balance gives

$$n' = \sum n_i' = n_{BT}' + n_D' + n_5' + n_4' + n_3' + n_2' + n_1' + n_a' \qquad \text{(N-1)}$$

Making the substitution $n_i' = \frac{P_i'V_i'}{Z_i'RT_i} = \left(\frac{PV}{ZRT_i}\right)'$, we have

$$n' = \left(\frac{PV}{ZRT}\right)'_{BT} + \left(\frac{PV}{ZRT}\right)'_{D} + \left(\frac{PV}{ZRT}\right)'_{5} + \left(\frac{PV}{ZRT}\right)'_{4} + \left(\frac{PV}{ZRT}\right)'_{3} + \left(\frac{PV}{ZRT}\right)'_{2} + \left(\frac{PV}{ZRT}\right)'_{1} + \left(\frac{PV}{ZRT}\right)'_{a} \qquad \text{(N-2)}$$

After opening the valve, a material balance gives

$$n = \sum n_i = n_{BT} + n_D + n_5 + n_4 + n_3 + n_2 + n_1 + n_a \qquad \text{(N-3)}$$

where n_i = moles of gas in volume V_i after opening the valve,

n = total moles of gas in system after opening the valve, = $\sum n_i$.

Making the substitution $n_i = \frac{P_i V_i}{Z_i R T_i} = (\frac{PV}{ZRT})_i$, we have

$$n = (\frac{PV}{ZRT})_{BT} + (\frac{PV}{ZRT})_D + (\frac{PV}{ZRT})_5 + (\frac{PV}{ZRT})_4 + (\frac{PV}{ZRT})_3 + (\frac{PV}{ZRT})_2 + (\frac{PV}{ZRT})_1 + (\frac{PV}{ZRT})_a \quad \text{(N-4)}$$

Since the total amount of gas in the system is constant, both before and after opening the expansion valve, we may write $n' = n$. Thus the right-hand sides of Equations N-2 and N-4 may be equated.

$$(\frac{PV}{ZRT})'_{BT} + (\frac{PV}{ZRT})'_D + (\frac{PV}{ZRT})'_5 + (\frac{PV}{ZRT})'_4 + (\frac{PV}{ZRT})'_3 + (\frac{PV}{ZRT})'_2 + (\frac{PV}{ZRT})'_1 + (\frac{PV}{ZRT})'_a =$$

$$(\frac{PV}{ZRT})_{BT} + (\frac{PV}{ZRT})_D + (\frac{PV}{ZRT})_5 + (\frac{PV}{ZRT})_4 + (\frac{PV}{ZRT})_3 + (\frac{PV}{ZRT})_2 + (\frac{PV}{ZRT})_1 + (\frac{PV}{ZRT})_a \quad \text{(N-5)}$$

Multiplying both sides of Equation N-5 by R/V_B, we have

$$(\frac{P}{ZT})'_{BT}\frac{V_{BT}}{V_B} + (\frac{P}{ZT})'_D\frac{V_D}{V_B} + (\frac{P}{ZT})'_5\frac{V_5}{V_B} + (\frac{P}{ZT})'_4\frac{V_4}{V_B} + (\frac{P}{ZT})'_3\frac{V_3}{V_B} + (\frac{P}{ZT})'_2\frac{V_2}{V_B} + (\frac{P}{ZT})'_1\frac{V_1}{V_B} +$$

$$(\frac{P}{ZT})'_a\frac{V_a}{V_B} = (\frac{P}{ZT})_{BT}\frac{V_{BT}}{V_B} + (\frac{P}{ZT})_D\frac{V_D}{V_B} + (\frac{P}{ZT})_5\frac{V_5}{V_B} + (\frac{P}{ZT})_4\frac{V_4}{V_B} + (\frac{P}{ZT})_3\frac{V_3}{V_B} + (\frac{P}{ZT})_2\frac{V_2}{V_B} +$$

$$(\frac{P}{ZT})_1\frac{V_1}{V_B} + (\frac{P}{ZT})_a\frac{V_a}{V_B} \quad \text{(N-6)}$$

Equation N-6 may be rearranged to the form

$$\frac{V_D}{V_B} = -\left\{\frac{\left[\left(\frac{P}{ZT}\right)'\right]_{BT}\cdot\frac{V_{BT}}{V_B} + \left[\left(\frac{P}{ZT}\right) - \left(\frac{P}{ZT}\right)'\right]_5\cdot\frac{V_5}{V_B} + \left[\left(\frac{P}{ZT}\right) - \left(\frac{P}{ZT}\right)'\right]_4\cdot\frac{V_4}{V_B}}{\left[\left(\frac{P}{ZT}\right) - \left(\frac{P}{ZT}\right)'\right]_D}\right.$$

$$+\frac{\left[\left(\frac{P}{ZT}\right) - \left(\frac{P}{ZT}\right)'\right]_3\cdot\frac{V_3}{V_B} + \left[\left(\frac{P}{ZT}\right) - \left(\frac{P}{ZT}\right)'\right]_2\cdot\frac{V_2}{V_B} + \left[\left(\frac{P}{ZT}\right) - \left(\frac{P}{ZT}\right)'\right]_1}{\left[\left(\frac{P}{ZT}\right) - \left(\frac{P}{ZT}\right)'\right]_D}$$

$$\left.+\frac{\left[\left(\frac{P}{ZT}\right) - \left(\frac{P}{ZT}\right)'\right]_a\cdot\frac{V_a}{V_B}}{\left[\left(\frac{P}{ZT}\right) - \left(\frac{P}{ZT}\right)'\right]_D}\right\} \qquad \text{(N-7)}$$

The pressure and temperature of the capillary volume V_a is assumed to be the same as the pressure and temperature of the bomb both before and after the expansion valve is opened. Also, $V_3 = V_2$ (Figure N-1). This allows Equation N-7 to be written as

$$\frac{V_D}{V_B} = -\left\{\frac{\left[\frac{P}{ZT} - \left(\frac{P}{ZT}\right)'\right]_{BT}\left(\frac{V_{BT}}{V_B} + \frac{V_a}{V_B}\right) + \left[\frac{P}{ZT} - \left(\frac{P}{ZT}\right)'\right]_5\cdot\frac{V_5}{V_B} + \left[\frac{P}{ZT} - \left(\frac{P}{ZT}\right)'\right]_4\cdot\frac{V_4}{V_B}}{\left[\frac{P}{ZT} - \left(\frac{P}{ZT}\right)'\right]_D}\right.$$

$$\left.+\frac{\left\{\left[\frac{P}{ZT} - \left(\frac{P}{ZT}\right)'\right]_3 + \left[\frac{P}{ZT} - \left(\frac{P}{ZT}\right)'\right]_2\right\}\cdot\frac{V_3}{V_B} + \left[\frac{P}{ZT} - \left(\frac{P}{ZT}\right)'\right]_1\cdot\frac{V_1}{V_B}}{\left[\frac{P}{ZT} - \left(\frac{P}{ZT}\right)'\right]_D}\right\} \qquad \text{(N-8)}$$

In order to calculate the required ratio from Equation N-8, the volume ratios V_{BT}/V_B, V_a/V_B, V_5/V_B, V_4/V_B, V_3/V_B, and V_1/V_B must be known. As these ratios are relatively small the accuracy of their determination does not have to be as great as with other directly measured quantities such as pressure and temperature.

The volume ratio V_{BT}/V_B is by definition the effect of temperature on the volume of the bomb. It is shown in Appendix H that

$$\frac{V_{BT}}{V_B} = [1 + 9.5 \times 10^{-6}(T_B - 95)]^3 = F(T_B - 95) \qquad \text{(N-9)}$$

The volumes V_a, V_5, V_4, V_3, and V_1 were determined by direct measuring of the length of capillary tubing between the DPI cell and the bomb. The inner volume V_B was determined from the scale drawing (Figure 2) of the bomb. The results are given in Table N-I. Using these ratios the final form of Equation N-8 is thus

$$\frac{V_D}{V_B} = -\left\{\frac{[F(T_B - 95) + 0.003868][\frac{P}{RT} - (\frac{P}{RT})']_{BT} + 0.01537[\frac{P}{ZT} - (\frac{P}{ZT})']_5}{[\frac{P}{ZT} - (\frac{P}{ZT})']_D} + \right.$$

$$\frac{0.01511[\frac{P}{ZT} - (\frac{P}{RT})']_4 + 0.003794\{[\frac{P}{ZT} - (\frac{P}{ZT})']_3 + [\frac{P}{ZT} - (\frac{P}{ZT})']_2\}}{[\frac{P}{ZT} - (\frac{P}{ZT})']_D} +$$

$$\left.\frac{0.003273[\frac{P}{ZT} - (\frac{P}{ZT})']_1}{[\frac{P}{ZT} - (\frac{P}{ZT})']_D}\right\} \qquad \text{(N-10)}$$

TABLE N-I

VOLUMES AND VOLUME RATIOS FOR CAPILLARY CORRECTIONS

Volumes	V_B	V_a	V_5	V_4	V_3	V_2	V_1
cubic inches	5.1542	0.01994	0.07923	0.07794	0.01956	0.01956	0.01687
Volume ratios		V_a/V_B 0.003868	V_5/V_B 0.01537	V_4/V_B 0.01511	V_3/V_B 0.003794	V_2/V_B 0.003794	V_1/V_B 0.003273

Equation N-10 was used in this work to determine the volume ratio. A sample calculation is given in Appendix E.

The smaller terms in the expression such as $0.01511[\frac{P}{ZT} - (\frac{P}{ZT})']_4$, represent the correction for the quantity of gas in the interconnecting capillary. In order to evaluate these terms it is necessary that the compressibility factors Z_5, Z_4, Z_3, Z_2, and Z_1 be known. For the volume ratio calibration these compressibility factors are also determined from the known volumetric properties of nitrogen.

It is worthwhile to point out that the ratio V_D/V_B is a constant for the apparatus and does not change with temperature or with each particular sample as different isochors are being run.

After the volume ratio determination has been completed, the interconnecting valve is allowed to remain open for all further compressibility determinations with the apparatus.

Pressure Corrections for Differences in Vertical Height

The pressure as determined at the reference mark of the Ruska piston gage (Figure N-1) is corrected by the factor -0.366 psi (discussed in Appendix B) to yield the pressure at the level of the diaphragm of the DPI cell. The pressure correction for the head of gas between the diaphragm level and each separate section of the high pressure gas system is discussed as follows.

The pressure correction ΔP between any two points 1 and 2, separated by a vertical displacement h, is given by

$$\Delta P = \frac{g}{g_c} \int_{h_1}^{h_2} \rho dh = \frac{g}{g_c} \int_{o}^{h} \rho dh \qquad \text{(N-11)}$$

where ρ = the density of the gas between points 1 and 2, and

g/g_c = the correction to local acceleration due to gravity.

If the density is assumed to be constant over the interval h, Equation N-11 may be written as

$$\Delta P = \frac{g}{g_c}\rho h \qquad \text{(N-12)}$$

The density of a gas is given by $\rho = \frac{P(MW)}{ZRT}$. Combining this expression with Equation N-12, it is seen that

$$\Delta P = \frac{hP(MW)}{(12)^3 ZRT}\ \frac{g}{g_c} \qquad \text{(N-13)}$$

where ΔP = the pressure correction, psi

h = the vertical displacement between the two points, inches

P = pressure, psia

MW = the molecular weight of the gas

T = temperature, °R

With reference to Figure N-1, it is seen that the pressure P_5 of the gas in the capillary volume V_5 may be calculated from a knowledge of the pressure P_D at the diaphragm, and the expression

$$P_5 = P_D + \frac{6.0\ P_D(MW)}{1728\ Z_5RT_5}\frac{g}{g_c}$$

$$= P_D\left[1 + \frac{6.0(MW)}{1728\ Z_5RT_5}\frac{g}{g_c}\right] \qquad \text{(N-14)}$$

Similar expressions for the pressures at volumes V_4, V_3, V_2, and V_1 of the capillary are given by

$$P_4 = P_5$$

$$P_3 = P_4\left[1 + \frac{9.002(MW)}{1728\ Z_3RT_3}\frac{g}{g_c}\right] \qquad \text{(N-15)}$$

$$P_2 = P_3\left[1 + \frac{6.375(MW)}{1728\ Z_2RT_2}\frac{g}{g_c}\right]$$

$$P_1 = P_2\left[1 + \frac{5.832(MW)}{1728\ Z_1RT_1}\frac{g}{g_c}\right]$$

In each case the vertical distance to the centroid of each particular section is used.

Finally the pressure P_B at the centroid of the bomb is given by

$$P_B = P_1\left[1 + \frac{11.500(MW)}{1728\ Z_BRT_B}\frac{g}{g_c}\right] \qquad \text{(N-16)}$$

In the application of the above equations (Equations N-14 through N-16) for the calculation of pressure corrections, it is seen that these corrections are very small. In the application of Equations N-10, N-20, and N-21, the above equations are utilized.

Development of Equations for the Compressibility Factors

As was discussed in Chapter IV, the volumetric properties of the sample along each isochoric path are determined by utilizing the known volumetric properties of the sample at the reference temperature.

The cryostat is maintained at 77°F, the system is rinsed and evacuated, and is then charged to the desired density with the sample. After equilibrium has been attained the temperatures and pressures of all portions of the system are measured.

Since the interconnecting valve of the system is open, Equation N-4, derived previously, applies:

$$n = \left(\frac{PV}{ZRT}\right)_{BT} + \left(\frac{PV}{ZRT}\right)_{D} + \left(\frac{PV}{ZRT}\right)_{5} + \left(\frac{PV}{ZRT}\right)_{4} + \left(\frac{PV}{ZRT}\right)_{3} + \left(\frac{PV}{ZRT}\right)_{2} + \left(\frac{PV}{ZRT}\right)_{1} + \left(\frac{PV}{ZRT}\right)_{a} \tag{N-4}$$

Dividing both sides of Equation N-4 by V_B gives

$$\frac{n}{V_B} = \left(\frac{P}{ZRT}\right)_{BT}\frac{V_{BT}}{V_B} + \left(\frac{P}{ZRT}\right)_{D}\frac{V_D}{V_B} + \left(\frac{P}{ZRT}\right)_{5}\frac{V_5}{V_B} + \left(\frac{P}{ZRT}\right)_{4}\frac{V_4}{V_B} + \left(\frac{P}{ZRT}\right)_{3}\frac{V_3}{V_B} + \left(\frac{P}{ZRT}\right)_{2}\frac{V_2}{V_B} + \left(\frac{P}{ZRT}\right)_{1}\frac{V_1}{V_B} + \left(\frac{P}{ZRT}\right)_{a}\frac{V_a}{V_B} \tag{N-17}$$

The expression for V_{BT}/V_B has been given in Equation N-9. The value for V_D/V_B is known from calibration, using Equation N-10. Values of the volume ratios $\frac{V_5}{V_B}$, $\frac{V_4}{V_B}$, $\frac{V_3}{V_B}$, $\frac{V_2}{V_B}$, $\frac{V_1}{V_B}$, and $\frac{V_a}{V_B}$ are given in Table N-I. Equation N-17 may thus be written as

$$D \equiv \frac{n}{V_B} = \left(\frac{P}{ZRT}\right)_{BT}[F(T_B - 95) + 0.003868] + \left(\frac{P}{ZRT}\right)_{D}\frac{V_D}{V_B} + 0.01537\left(\frac{P}{ZRT}\right)_{5} + 0.01511\left(\frac{P}{ZRT}\right)_{4} + 0.003794\left[\left(\frac{P}{ZT}\right)_{3} + \left(\frac{P}{ZT}\right)_{2}\right] + 0.003273\left(\frac{P}{ZRT}\right)_{1} \tag{N-18}$$

The quantity D (defined as n/V_B) was mentioned in Chapter IV. D is not a true density, but a run constant, since the number of moles n applies to the entire system, including the DPI cell, whereas V_B

represents the volume of the bomb only. Although D is not a true density it does have a constant value along an isochor since the total number of moles n of the system and the volume V_B remain constant. In the equations that follow, the overall density for the entire system (including the DPI cell) is not required.

A more convenient form of Equation N-18 is obtained by making the substitutions

$$\left(\frac{P}{ZRT}\right)_{BT} = D_{BT}$$

$$\left(\frac{P}{ZRT}\right)_{D} = D_{D}$$

$$\left(\frac{P}{ZRT}\right)_{5} = D_{5}$$

$$\left(\frac{P}{ZRT}\right)_{4} = D_{4} \qquad \text{(N-19)}$$

$$\left(\frac{P}{ZRT}\right)_{3} = D_{3}$$

$$\left(\frac{P}{ZRT}\right)_{2} = D_{2}$$

$$\left(\frac{P}{ZRT}\right)_{1} = D_{1}$$

The quantities D_{BT}, D_D, D_5, D_4, D_3, D_2, and D_1 are true densities by definition, and are not to be confused with the quantity D. With these substitutions, Equation N-18 thus becomes

$$D = [F(T_B - 95) + 0.003868]D_{BT} + 0.01263\ D_D + 0.01537\ D_5 + 0.01511\ D_4 + 0.003794\ (D_3 + D_2) + 0.003273\ D_1 \qquad \text{(N-20)}$$

Equation N-20 was the form used in this work for the determination of the quantity D from the reference isotherm.

For the determination of compressibility factors along the isochor at lower temperatures, it is convenient to rearrange Equation N-20 to the form

$$Z_{BT} = \left(\frac{P}{RT}\right)_{BT} \left[\frac{F(T_B - 95) + 0.003868}{DEN}\right] \qquad \text{(N-21)}$$

Here DEN represents the denominator of the expression in brackets and is given by

$$DEN = D - 0.01263\ D_D - 0.01537\ D_5 - 0.01511\ D_4 - 0.003794\ (D_3 + D_2) - 0.003273\ D_1 \qquad \text{(N-22)}$$

The quantity D appears in the denominator of Equation N-21. Thus corresponding values of P_{BT} and T_{BT} (the pressure and temperature in the bomb) are sufficient to calculate the compressibility factor Z_{BT} for any point on the isochor. Equation N-21 was the form used in this work for the experimental determination of compressibility factors.

NOMENCLATURE

a, A_o, a', A'_o	= constants in empirical equations of state
A_{o_t}	= area of piston at t°C and zero psig
A_E	= effective area of piston
ATM	= barometric pressure
b, B_o, b', B'_o	
$B(T)$	= Leiden second virial coefficient
$B'(T)$	= Berlin second virial coefficient
$B_{ij}(T)$	= interaction second virial coefficient
b	= coefficient of pressure distortion
	= reduced second virial coefficient
c, C_o, c', C'_o	= constants in empirical equations of state
$C(T)$	= Leiden third virial coefficient
$C'(T)$	= Berlin third virial coefficient
$C_{ijk}(T)$	= interaction third virial coefficient
C	= coefficient of thermal expansion for Ruska piston
d	= density, = 1/V
$D(T)$	= Leiden fourth virial coefficient
$D'(T)$	= Berlin fourth virial coefficient
D_{BT}	= true density as defined by Equation N-19
D_D	= true density as defined by Equation N-19
D_5	= true density as defined by Equation N-19

D_4 = true density as defined by Equation N-19

D_3 = true density as defined by Equation N-19

D_2 = true density as defined by Equation N-19

D_1 = true density as defined by Equation N-19

D = isochoric run constant, n/V_B, defined by Equation N-18

E = modulus of elasticity in Equation K-4

F = volume correction of bomb, defined by Equation N-9

g = local acceleration due to gravity

g_c = standard acceleration due to gravity

h = parameter in RK equation, = BP/Z

= vertical displacement in Equation N-11

HCORR = oil head correction, Equation B-4

k_{ij} = temperature correction factor, Equation M-1

M_A = Ruska masses as "apparent mass versus mass"

MW = molecular weight

n = number of moles

N = number of components

p_o = initial value of pressure for Burnett apparatus (Equation II-1)

p_r = r-th value of pressure for Burnett apparatus

P = pressure

P_i = inner pressure of constant volume bomb in Equation K-18

P_o = jacket pressure of constant volume bomb in Equation K-18

P_R^o = reduced vapor pressure

P_L = pressure of lower chamber of DPI cell, Equation B-5

POT	= potentiometer reading
R	= universal gas constant
	= scale reading of Texas Instruments barometer
R_t	= resistance of platinum resistor at temperature t
R_o	= resistance of platinum resistor at 0°C
T	= temperature
u	= cylinder deformation in Equation K-3
V	= molar volume
V_a	= volume of capillary as shown in Figure N-1
V_B	= total volume of bomb at 95°F
V_{BT}	= total volume of bomb at T°F
V_D	= volume of DPI cell and capillary tubing
V_I, V_{II}	= total volumes, respectively, of the Burnett apparatus bombs
V_1	= volume of capillary tubing as shown in Figure N-1
V_2	= volume of capillary tubing as shown in Figure N-1
V_3	= volume of capillary tubing as shown in Figure N-1
V_4	= volume of capillary tubing as shown in Figure N-1
V_5	= volume of capillary tubing as shown in Figure N-1
W	= actual weight load on Ruska piston
x	= composition
Z	= compressibility factor, PV/RT
Z_o	= compressibility factor at pressure p_o for Burnett apparatus
Z^o	= compressibility factor for a simple fluid in Equation III-15
Z'	= compressibility factor correction in Equation III-15

Greek Letters

α	= constant in BWR equation of state
	= coefficient of thermal expansion in Equation H-5
	= constant in platinum thermometer calibratopm
α'	= constant in generalized BWR equation of state
β	= constant in platinum thermometer calibration
γ	= constant in BWR equation of state
γ'	= constant in generalized BWR equation of state
δ	= constant in platinum thermometer calibration
Δ	= finite change in a quantity
θ	= reduced temperature, T/T_c
θ_B	= function in Equation III-17
λ	= longitude in Equation L-1
μ	= Poisson's ratio
ρ	= density
σ_r	= normal radial stress in Equation K-1
σ_t	= normal hoop stress in Equation K-1
$\sum$	= summation
ψ	= latitude in Equation L-1
ω	= accentric factor

Subscripts

avg	= average value
B,BT	= bomb
c	= critical property
D	= DPI cell

E	= effective
i, j, k	= components of a mixture
m	= mixture
r	= number of expansion for Burnett apparatus (Equation II-1)
R	= reduced property
5, 4, 3, 2, 1	= properties of exposed apparatus sections 5, 4, 3, 2 and 1, respectively (Figure N-1)

Superscripts

'	= property of apparatus before opening expansion value

VITA

Henry Grady McMath, Jr.

Candidate for the Degree of

Doctor of Philosophy

Thesis: VOLUMETRIC PROPERTIES AND VIRIAL COEFFICIENTS OF THE METHANE-ETHYLENE SYSTEM, USING THE TECHNIQUE OF ISOCHORIC CHANGES OF PRESSURE WITH TEMPERATURE

Major Field: Chemical Engineering

Biographical:

Personal Data: Born in El Dorado, Arkansas, January 29, 1939, the son of Henry Grady and Fannie Lou McMath. Married to Sara F. Adcox of El Dorado, Arkansas, on July 2, 1960.

Education: Attended elementary school in Strong, Arkansas; attended high school in Strong, Arkansas and El Dorado, Arkansas, graduating from El Dorado High School in 1956; received the Bachelor of Science degree in Chemical Engineering from Louisiana Polytechnic Institute in January, 1961; received the Master of Science degree in Chemical Engineering from Louisiana Polytechnic Institute in June, 1962; completed the requirements for the Doctor of Philosophy degree at Oklahoma State University in May, 1967.

Professional Experience: Employed in the Technical Service Department of Monsanto Chemical Company the summers of 1960 and 1961. Currently on active duty with the United States Air Force, serving as Project Officer, Ultra-Energy Concepts, Air Force Rocket Propulsion Laboratory, Edwards AFB, California.